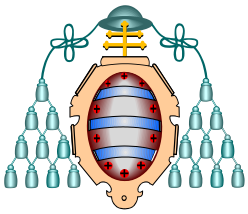

UNIVERSIDAD DE OVIEDO

PROGRAMA DOCTORADO

MORFOLOGÍA Y BIOLOGÍA CELULAR

CHARACTERIZATION OF HEPATIC DAMAGE CAUSED BY OBESITY LEPTIN DEFICIENCY. POSSIBLE ATTENUATION BY MELATONIN

.....

AUTOR: **Beatriz de Luxán Delgado**

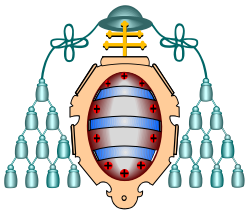

UNIVERSIDAD DE OVIEDO

PROGRAMA DOCTORADO

MORFOLOGÍA Y BIOLOGÍA CELULAR

CHARACTERIZATION OF HEPATIC DAMAGE CAUSED BY OBESITY LEPTIN DEFICIENCY. POSSIBLE ATTENUATION BY MELATONIN

.....

AUTOR: **Beatriz de Luxán Delgado**

RESUMEN DEL CONTENIDO DE TESIS DOCTORAL

1.- Título de la Tesis Doctoral	
Español CARACTERIZACIÓN DEL DAÑO HEPÁTICO CAUSADO POR LA OBESIDAD INDUCIDA POR DEFICIENCIA EN LEPTINA. POSIBLE ATENUACIÓN POR LA MELATONINA	Inglés: CHARACTERIZATION OF HEPATIC DAMAGE CAUSED BY OBESITY LEPTIN DEFICIENCY. POSSIBLE ATTENUATION BY MELATONIN

2.- Autor	
Nombre: Beatriz de Luxán Delgado	DNI -
Programa de Doctorado: MORFOLOGIA Y BIOLOGIA CELULAR	
Órgano responsable: DPTO.MORFOLOGIA Y BIOLOGIA CELULAR	

RESUMEN (en español)

La obesidad es un problema de salud mundial que afecta a millones de personas en todo el mundo. El estilo de vida sedentario de la sociedad moderna, junto con el aumento de la ingesta de alimentos cada vez más energéticos ha convertido a la obesidad en un problema de salud mundial.

A pesar de los grandes esfuerzos destinados al estudio de la obesidad y sus enfermedades asociadas, todavía no se conocen bien los mecanismos que subyacen al desarrollo de estas patologías. Una de las razones que complican el estudio de la obesidad es la gran cantidad de causas que la inducen. Sin embargo, la resistencia a la señalización de leptina mediada por deficiencias en su receptor, o la ausencia de leptina son las principales causas de la obesidad mórbida. Por ello, nuestro estudio con el modelo de obesidad deficiente en leptina nos permite identificar nuevas estrategias para frenar la progresión de estas patologías asociadas con la obesidad.

La implicación de la melatonina en muchas funciones fisiológicas como la regulación estacional del peso corporal, la ingesta de glucosa o la adiposidad, así como su papel como antioxidante la ha convertido en el centro de numerosos estudios contra la obesidad. De hecho, tanto la leptina como la melatonina muestran una secreción circadiana, con picos nocturnos que juegan un papel importante en la regulación del peso corporal y el equilibrio energético.

En primer lugar, llevamos a cabo un estudio preliminar para investigar el efecto

de un tratamiento de melatonina durante 2 semanas sobre la situación oxidativa, la respuesta autofagia y la adiposidad en el hígado de los ratones deficientes en leptina. Así, vimos que el tratamiento con melatonina redujo la adiposidad en el hígado de los ratones ob/ob mediante el bloqueo de la actividad autofágica probablemente mediada por una acción señalizada por la disminución de los niveles de estrés oxidativo.

Estos resultados preliminares fueron la base para un estudio en profundidad sobre el impacto de la deficiencia de insulina en las funciones celulares claves para el mantenimiento celular y la supervivencia de los ratones ob/ob, y el efecto que inyecciones diarias de melatonina intraperitoneal durante cuatro semanas ejerce sobre las alteraciones relacionadas con la deficiencia en leptina.

El hígado de estos ratones fue usado para evaluar el metabolismo de la glucosa, de lípidos y oxidativo, el estado inflamatorio, y los sistemas de control de calidad celular, tales como la respuesta a proteínas mal plegadas y la actividad autofágica. Además, también llevamos a cabo un estudio sobre la función mitocondrial mediante ensayos de consumo de oxígeno, y medidas de la expresión de los complejos de la cadena de transporte de electrones y contenido de ATP mitocondrial.

La obesidad asociada con la deficiencia en leptina causa una pérdida de función celular en el hígado, asociada con el incremento del peso corporal y del contenido de tejido adiposo blanco como resultado de un apetito excesivo. El tratamiento con melatonina redujo el estrés del retículo en los ratones deficientes en leptina y mejoro algunos de los síntomas característicos de la obesidad como la resistencia a insulina, el estrés oxidativo, la inflamación o la disfunción mitocondrial. Además, es digno de mención el papel de la administración de melatonina en el aumento de la ingesta de alimentos en ratones deficientes de leptina, sin incrementar el peso corporal y disminuyendo el tejido adiposo blanco.

Este estudio señala diferentes dianas celulares para el desarrollo de nuevas estrategias para contrarrestar las patologías celulares relacionadas con la obesidad, y apoya el potencial de la melatonina como tratamiento terapéutico para el tipo más común de la obesidad y sus trastornos hepáticos asociados.

RESUMEN (en Inglés)

Obesity is a global health problem that affects millions of people worldwide. The sedentary lifestyle of modern society along with the high intake of energetic food has made obesity a current worldwide health problem.

Despite great efforts to study obesity and its related diseases, the mechanisms underlying the development of these diseases are not well understood, being one of the main reasons, the wide variability of causes that induce obesity. However, resistance of leptin receptors and leptin absence, comprise the most reported causes of severe obesity including morbid obesity. Therefore, in the present thesis leptin-deficient animals (ob/ob) were used to identify the most relevant alterations produced in specific cellular pathways and involved in cellular decline or dysfunction. This is paramount to finally find novel strategies to slow or counteract the progression of obesity-related diseases.

The involvement of melatonin in many physiological functions, such as the regulation of seasonal body weight variation, glucose intake, or adiposity, and the role of this hormone as an essential antioxidant, have become the focus of numerous anti-obesity studies. In fact, leptin and melatonin show a circadian rhythm with peaks at night playing an important role in the regulation of body mass and energy balance.

We firstly conducted a preliminary study to investigate the effect that a 2-weeks melatonin treatment causes on oxidative status, autophagic response and adiposity in the liver of leptin-deficient mice. Thus, we found that melatonin administration reduced adiposity in the liver of ob/ob mice by decreasing autophagy activity through an action probably signalized by lower oxidative stress levels.

These preliminary findings formed the basis for an in-depth study about the impact of leptin deficiency on key cellular functions relevant for cell maintenance and survival of ob/ob mice, and the effects of 4-weeks intraperitoneal daily injections of melatonin on these alterations associated with leptin deficiency.

The liver of these mice were used to evaluate lipid, glucose and redox metabolism, inflammatory status, and cellular quality control systems, as unfolded protein response and autophagy. Besides, we also studied mitochondrial function by

measuring oxygen consumption, the expression of electron transport chain complexes and ATP content.

Obesity associated with leptin deficiency causes a loss of cell function in the liver, associated with increased body and white adipose tissue weight, as a result of excessive appetite. Melatonin treatment could significantly reduce reticulum stress in leptin-deficient mice and ameliorate several symptoms that characterize obesity as insulin resistance, oxidative stress, inflammation or mitochondrial dysfunction. Besides, is noteworthy the role of melatonin administration enhancing food intake in leptin-deficient mice, without increasing body weight and reducing white adipose tissue.

This study points out different cellular targets for the development of new strategies to counteract cell pathology of obesity-related diseases and supports the potential use of melatonin as a therapeutic adjuvant for the most common type of obesity and its liver-associated disorders.

SR. COORDINADOR DEL PROGRAMA DE DOCTORADO MORFOLOGIA Y BIOLOGIA CELULAR

This work has been supported with the projects of the Red temática de investigación cooperativa en envejecimiento y fragilidad, Ministerio de Sanidad-ISCIII (FISS-06-RD06/0013/0011), (FISS-06-RD06/0013/0028) and (FISS-13-RD12/0043/0030).

The author of the doctoral thesis has benefited from Severo Ochoa predoctoral fellowship from Principado de Asturias (BP11-135).

Thanks to the University of Oviedo for give its facilities and services.

Index

SUMMARY/RESUMEN

SUMMARY

Obesity is a global health problem that affects millions of people worldwide. The sedentary lifestyle of modern society along with the high intake of energetic food has made obesity a current worldwide health problem.

Despite great efforts to study obesity and its related diseases, the mechanisms underlying the development of these diseases are not well understood, being one of the main reasons, the wide variability of causes that induce obesity. However, resistance of leptin receptors and leptin absence, comprise the most reported causes of severe obesity including morbid obesity. Therefore, in the present thesis leptin-deficient animals (ob/ob) were used to identify the most relevant alterations produced in specific cellular pathways and involved in cellular decline or dysfunction. This is paramount to finally find novel strategies to slow or counteract the progression of obesity-related diseases.

The involvement of melatonin in many physiological functions, such as the regulation of seasonal body weight variation, glucose intake, or adiposity, and the role of this hormone as an essential antioxidant, have become the focus of numerous anti-obesity studies. In fact, leptin and melatonin show a circadian rhythm with peaks at night playing an important role in the regulation of body mass and energy balance.

We firstly conducted a preliminary study to investigate the effect that a 2-weeks melatonin treatment causes on oxidative status, autophagic response and adiposity in the liver of leptin-deficient mice. Thus, we found that melatonin administration reduced adiposity in the

liver of ob/ob mice by decreasing autophagy activity through an action probably signalized by lower oxidative stress levels.

These preliminary findings formed the basis for an in-depth study about the impact of leptin deficiency on key cellular functions relevant for cell maintenance and survival of ob/ob mice, and the effects of 4-weeks intraperitoneal daily injections of melatonin on these alterations associated with leptin deficiency.

The liver of these mice were used to evaluate lipid, glucose and redox metabolism, inflammatory status, and cellular quality control systems, as unfolded protein response and autophagy. Besides, we also studied mitochondrial function by measuring oxygen consumption, the expression of electron transport chain complexes and ATP content.

Obesity associated with leptin deficiency causes a loss of cell function in the liver, associated with increased body and white adipose tissue weight, as a result of excessive appetite. Melatonin treatment could significantly reduce reticulum stress in leptin-deficient mice and ameliorate several symptoms that characterize obesity as insulin resistance, oxidative stress, inflammation or mitochondrial dysfunction. Besides, is noteworthy the role of melatonin administration enhancing food intake in leptin-deficient mice, without increasing body weight and reducing white adipose tissue.

This study points out different cellular targets for the development of new strategies to counteract cell pathology of obesity-related diseases and supports the potential use of melatonin as a therapeutic adjuvant for the most common type of obesity and its liver-associated disorders.

RESUMEN

La obesidad es un problema de salud mundial que afecta a millones de personas en todo el mundo. El estilo de vida sedentario de la sociedad moderna, junto con el aumento de la ingesta de alimentos cada vez más energéticos ha convertido a la obesidad en un problema de salud mundial.

A pesar de los grandes esfuerzos destinados al estudio de la obesidad y sus enfermedades asociadas, todavía no se conocen bien los mecanismos que subyacen al desarrollo de estas patologías. Una de las razones que complican el estudio de la obesidad es la gran cantidad de causas que la inducen. Sin embargo, la resistencia a la señalización de leptina mediada por deficiencias en su receptor, o la ausencia de leptina son las principales causas de la obesidad mórbida. Por ello, nuestro estudio con el modelo de obesidad deficiente en leptina nos permite identificar nuevas estrategias para frenar la progresión de estas patologías asociadas con la obesidad.

La implicación de la melatonina en muchas funciones fisiológicas como la regulación estacional del peso corporal, la ingesta de glucosa o la adiposidad, así como su papel como antioxidante la ha convertido en el centro de numerosos estudios contra la obesidad. De hecho, tanto la leptina como la melatonina muestran una secreción circadiana, con picos nocturnos que juegan un papel importante en la regulación del peso corporal y el equilibrio energético.

En primer lugar, llevamos a cabo un estudio preliminar para investigar el efecto de un tratamiento de melatonina durante 2 semanas sobre la situación oxidativa, la respuesta autofagia y la adiposidad en el

hígado de los ratones deficientes en leptina. Así, vimos que el tratamiento con melatonina redujo la adiposidad en el hígado de los ratones ob/ob mediante el bloqueo de la actividad autofágica probablemente mediada por una acción señalizada por la disminución de los niveles de estrés oxidativo.

Estos resultados preliminares fueron la base para un estudio en profundidad sobre el impacto de la deficiencia de insulina en las funciones celulares claves para el mantenimiento celular y la supervivencia de los ratones ob/ob, y el efecto que inyecciones diarias de melatonina intraperitoneal durante cuatro semanas ejerce sobre las alteraciones relacionadas con la deficiencia en leptina.

El hígado de estos ratones fue usado para evaluar el metabolismo de la glucosa, de lípidos y oxidativo, el estado inflamatorio, y los sistemas de control de calidad celular, tales como la respuesta a proteínas mal plegadas y la actividad autofágica. Además, también llevamos a cabo un estudio sobre la función mitocondrial mediante ensayos de consumo de oxígeno, y medidas de la expresión de los complejos de la cadena de transporte de electrones y contenido de ATP mitocondrial.

La obesidad asociada con la deficiencia en leptina causa una pérdida de función celular en el hígado, asociada con el incremento del peso corporal y del contenido de tejido adiposo blanco como resultado de un apetito excesivo. El tratamiento con melatonina redujo el estrés del retículo en los ratones deficientes en leptina y mejoro algunos de los síntomas característicos de la obesidad como la resistencia a insulina, el estrés oxidativo, la inflamación o la disfunción mitocondrial. Además, es digno de mención el papel de la administración de melatonina en el aumento de la

ingesta de alimentos en ratones deficientes de leptina, sin incrementar el peso corporal y disminuyendo el tejido adiposo blanco.

Este estudio señala diferentes dianas celulares para el desarrollo de nuevas estrategias para contrarrestar las patologías celulares relacionadas con la obesidad, y apoya el potencial de la melatonina como tratamiento terapéutico para el tipo más común de la obesidad y sus trastornos hepáticos asociados.

ABBREVIATIONS

4-HNE: 4-hydroxy-2 (E)-nonenal

8-OHG: 8-Hydroxyguanosine

ABTS: 2,2'-azino-bis(3-ethylbenzothiazoline-6-sulphonic acid

AdipoR1: adiponectin receptor 1

AdipoR2: adiponectin receptor 2

Akt: also called protein kinase B

AMP: adenosine monophosphate

AMPK: adenosine monophosphate-activated protein kinase

ANT: adenine nucleotide translocase

ATF6α: activating transcription factor-6-α

Atg: autophagy related

ATP: adenosine triphosphate

Bax: Bcl2 associated X protein

Bcl-2: B-cell lymphoma 2

CAT: catalase

C/EBP: CCAAT enhancer binding protein

cDNA: complementary DNA

CHOP: C/EBP homologous protein

CMA: chaperone-mediated autophagy

Drp1: dynamin related protein 1

EGTA: Ethylene-bis (oxyethylenenitrilo) tetraacetic acid

eIF2α: α-subunit of eukaryotic initiation factor

ER: endoplasmic reticulum

ERAD: endoplasmic reticulum-associated degradation

Erk: extracellular signal-regulated kinases

FAD: flavin adenine dinucleotide

FCCP: carbonyl cyanide-4-(trifluoromethoxy) phenylhydrazone

FMN: flavin mononucleotide

FoxO: class O of forkhead box transcription factors

GLUT: glucose transporter

GPx: glutathione peroxidase

GR: glutathione reductase

GSH: reduced glutathione

GSSG: oxidized glutathione

HEPES: 4-(2-Hydroxyethyl) piperazine-1-ethanesulfonic acid

HRP: horseradish peroxidase

HSC-70: heat shock cognate protein 70

IL-6: Interleukin 6

Ire1α: Inositolrequiring enzyme-1

IRS-1/2: insulin receptor substrate 1 or 2

IκB: NF-κB inhibitor

Ικκ: IκB kinase

JNK: c-Jun N-terminal kinase

Keap1: Kelch-like ECH-associated protein 1

LAL: lysosomal acid lipase

LAMP2A: lysosome-associated membrane protein type 2A

LC3: microtubule-associated protein 1 light chain 3

LDL: low-density lipoprotein

LIB: liver isolation buffer

LRB: liver resuspension buffer

MAP: mitogen-activated protein

MAPK: mitogen-activated protein kinases

MDA: malondialdehyde

Mfn1/2: mitofusin 1 and 2

MIM: mitochondrial inner membrane

MOM: mitochondrial outer membrane

MOMP: mitochondrial outer membrane permeabilization

mPTP: mitochondrial permeability transition pore

mRNA: messenger RNA

MT1/2: melatonin receptor 1 or 2

mTOR: mammalian target of rapamycin

NADPH: nicotinamide adenine dinucleotide phosphate

NAFLD: non-alcoholic fatty liver disease

NF-κB: nuclear factor kappa-light-chain enhancer of activated B cells

Nrf2: nuclear factor (erythroid-derived 2)-like 2

Opa1: optic atrophy-1

p62: sequestosome-1

PCD: programmed cell death

PERK: double-stranded RNA-activated protein kinase–like endoplasmic reticulum kinase

PCD: programmed cell death

PCR: polymerase chain reaction

PDK1: phosphoinositide-dependent kinase 1

PGC-1α: peroxisome proliferator-activated receptor gamma co-activator-1 alpha

PI3K: phosphatidylinositol 3-kinase

PI (3,4)P_2: phosphatidylinositol 3,4-bisphosphate

PI (3,4,5)P_3: phosphatidylinositol 3,4,5-triphosphate

PI (4,5)P_2: phosphatidylinositol 4,5-biphosphate

PKC: protein kinase c

PTEN: phosphatase and tensin homolog

PPARα: peroxisome proliferator-activated receptor alpha

PPARγ: peroxisome proliferator-activated receptor gamma

PUFA: polyunsaturated fatty acid

ROS: reactive oxygen species

ROR: orphan receptor

RNS: reactive nitrogen species

RZR: retinoid Z receptor

SDS: sodium dodecyl sulfate

SHIP2: SH2-containing inositol phosphatase

SOD: superoxide dismutase

TAA: total antioxidant activity

TFAM: mitochondrial transcription factor A

TNF-α: tumor necrosis factor α

TSC1/2: tuberous sclerosis complex 1/2

TRAF2: TNF-α receptor-associated factor 2

Tx: trolox

UPR: unfolded protein response

VDAC: voltage-dependent anion channel

XBP1: X-box binding protein 1

INTRODUCTION

OBESITY

Obesity is a global health problem that affects millions of people worldwide. Constant access to highly energetic food has become usual, which along with the sedentary lifestyle of modern society causes an imbalance between caloric intake and energy expenditure, and as a result, obesity is an inevitable consequence. The overabundance of nutrients caused by an enhanced food intake leads to the dysregulation of adipocytokines, lipid and glucose metabolism (Couillard, Mauriege et al. 2000; Fu, Watkins et al. 2012; Lin, Wu et al. 2014). Obesity is characterized by abnormal increase in adipose tissue mass with increased fat cell size and number, as well as the accumulation of ectopic lipid accumulation in non-adipose tissues.

Despite the efforts and resources spent on prevention and treatment of obesity and its comorbidities, the number of obese people has not stopped for the last thirty years. According to the World Health Organization, in 2014, the percentage of the worldwide adult population that suffered from obesity had already reached 13%, the 39% had overweight, and its incidence also continues rising in children (2013), so finding strategies to curb and/or treat this disease and its medical complications is becoming a pressing need.

Among the multiple causes of obesity are: the lack of balance between intake and energy expenditure, sedentary lifestyle, genetic factors, health problems such as hypothyroidism, drugs, smoking and age. Besides, lack of sleep that is one of the factors inherent in industrialized countries has been related to long-term weight gain and the pathogenesis of obesity (Cizza, Requena et al. 2011). Cizza and colleagues have reviewed several mechanisms by which the sleep deprivation affects body weight, and they suggested that this relationship is based on the combined effect

of several factors, rather than been exclusively due to increased appetite and food intake. Seasonality and hibernation have great implications in the energy balance, and melatonin through the regulation of brown adipose tissue metabolism and circadian rhythms, works as a link between these processes and the control of body weight (Cizza, Requena et al. 2011).

Obesity leads to adverse metabolic abnormalities such as dyslipidemia, hypertension, or glucose intolerance. These alterations are grouped into metabolic syndrome that is a risk factor of several diseases such as cardiovascular disease, neurodegenerative disorders and diabetes (Wree, Kahraman et al. 2011; Lavallard and Gual 2014). Among them, the most important alterations in obesity include insulin resistance, mitochondrial dysfunction, systemic inflammation, increased oxidative stress and dysregulation of cellular quality control systems like autophagy and the unfolded protein response.

Obesity-associated liver disease

Besides being the main organ of detoxification of the body, the liver plays a fundamental role in regulating metabolic homeostasis (Rui 2014). Food is digested in the gastrointestinal tract, and glucose, fatty acids, and amino acids are carried to the liver through the bloodstream via the portal vein circulation system (Rui 2014). The liver is a central organ for synthesis, metabolism, storage and redistribution of carbohydrates, proteins and lipids, so it is closely linked to metabolic disorders (Bechmann, Hannivoort et al. 2012).

The liver is the main source of body glucose production through two different pathways:

- Glycogenolysis or the breakdown of glycogen in short-term fasting conditions.
- Gluconeogenesis which is *de novo* synthesis of glucose in medium to long-term fasting conditions, depends on enzymatic activities and hormonal regulation (insulin, glucagon and glucocorticoids). Lactate, pyruvate, glycerol and alanine are the main glucose precursors (Puigserver and Spiegelman 2003).

The liver is involved in lipid metabolism in three different aspects (Wree, Kahraman et al. 2011): *de novo* synthesis and active uptake of free fatty acids, *de novo* synthesis and oxidation of triglycerides, and export of free fatty acids as triglycerides and very low-density lipoproteins. The rapid increase of obesity and metabolic syndrome in western countries comes with alterations in hepatic lipid and glucose that lead to high prevalence of liver diseases. One of the most common liver diseases that occur in obese people is the nonalcoholic fatty liver disease (NAFLD), whose prevalence reaches 70-90% in obese or diabetic patients (Vernon, Baranova et al. 2011). This is a cluster of hepatic disorders that occur in the absence of excessive alcohol consumption, and predisposes to acute liver injury, cirrhosis and liver cancer (Bechmann, Hannivoort et al. 2012; Baratta, Pastori et al. 2015).

The expanded adipose tissue characteristic of obesity is accompanied by an increase in the migration of free fatty acids from adipose tissue to the liver, leading to fatty liver or hepatic steatosis. Other factors contributing to the development of hepatic steatosis in NAFLD are the upregulation of lipogenic pathways, a defective mitochondrial fatty acid oxidation or the inhibition of triglyceride secretion (Carr and Ahima 2015).

The liver responds to the massive presence of lipids by upregulating the biogenesis of lipid droplets (and thus avoid fatty acid lipotoxicity) (Singh and Cuervo 2012), but hepatic steatosis also can be due to the conversion of hepatocytes into fat storage cells, or adipocytes, which is known as adipogenic steatosis (Yu, Matsusue et al. 2003).

Leptin role in obesity

A tremendous effort has been made in the last decades to elucidate the molecular mechanisms underlying the pathology of obesity. However, the factors involved in its regulation are not yet fully understood. Using animal models to understand the regulation of food intake and energy expenditure is critical for the development of obesity treatments. Several different animal models have been employed to study the environmental, physiological and genetic basis of obesity (Speakman, Hambly et al. 2007). There are several types of genetic animal models employed, which include obesity models with spontaneous mutations, and random and target induced mutations (Speakman, Hambly et al. 2007). In addition to genetic models, the literature includes numerous studies on diet-induced obesity, including high-calorie diets rich in fat or fructose (Kasim-Karakas, Vriend et al. 1996; Pfluger, Herranz et al. 2008).

Among the spontaneous genetic models of obesity highlight the ob/ob and db/db mice and the Zucker obese rat (Speakman, Hambly et al. 2007). These three models have in common the involvement of the lack of leptin signaling in the development of obesity, either by absence of this molecule or its receptor.

Leptin was discovered in 1994 and is a 16 kDa polypeptide that presents a helical cytokine-like structure (Szewczyk-Golec, Wozniak et al. 2015). It is a pleiotropic hormone and is one of the most important

adipokines secreted by white adipose tissue together with adiponectin (Tan, Sun et al. 2012). However, a variety of other tissues such as stomach, skeletal muscle and hypothalamus also synthesize and secrete leptin (Zieba, Szczesna et al. 2008).

Leptin is commonly known as the "satiety hormone" as it works as a reporter of nutritional status, decreasing appetite and inhibiting food intake. It modulates feeding behavior mainly at level of the hypothalamus (Zieba, Szczesna et al. 2008), to inhibit orexigenic (appetite-stimulatory) neuropeptides and enhance anorectic peptides secretion (Malik, Marino et al. 2011). Leptin also stimulates energy expenditure. Thus, it regulates whole-body energy homeostasis through the reduction of lipid content by fatty acid oxidation in the liver and other peripheral tissues (Tan, Sun et al. 2012); and thermogenesis (Jo and Buettner 2014) through central and peripheral signaling (Holmstrom, Tom et al. 2013). Besides, leptin modulates insulin sensitivity via crosstalk with the insulin signaling pathway (Holmstrom, Tom et al. 2013).

Under normal conditions, leptin is produced and secreted in proportional amounts to the mass of body fat (Malik, Marino et al. 2011), being greater in subcutaneous white adipose tissue than in visceral white adipose tissue (Szewczyk-Golec, Wozniak et al. 2015). Thus, leptin levels correlate with the body mass index (BMI) promoting a negative energy balance and the repletion of body energy stores, thereby decreasing feeding and promoting activity. However, obesity leads to a leptin insensitivity state or resistance. In this case, obese individuals exhibit high leptin circulating levels but without reducing neither appetite nor body weight because the hypothalamic signaling does not take place (Zieba, Szczesna et al. 2008).

Hormones involved in energy homeostasis such as leptin, ghrelin, orexin, insulin and glucagon oscillate in circadian rhythms and, in the case of seasonal animals, they also oscillate in circannual rhythms (Kirsz, Szczesna et al. 2014). Circadian rhythms in serum leptin concentrations have also been proposed to be related to the daily changes in appetite and sleep/wake cycle (Mantele, Otway et al. 2012), having its maxim secretion overnight (Alonso-Vale, Andreotti et al. 2006).

Leptin-deficient (ob/ob) mice are infertile and exhibit hyperphagy, obesity, diabetes, and fatty liver, so lipid hepatic homeostasis is significantly affected (Zieba, Szczesna et al. 2008; Malik, Marino et al. 2011; Tan, Sun et al. 2012). For all these reasons, leptin-deficient mouse is considered as a good model to study the effects of obesity and its liver-related complications.

INSULIN RESISTANCE

Insulin is a peptide hormone produced in the islets of Langerhans from pancreatic beta cells in response to postprandial blood glucose increases (Carr and Correnti 2015). It is the anabolic hormone for excellence, since it is responsible for promoting the synthesis and storage of carbohydrates, lipids and proteins, as well as to prevent their degradation (Saltiel and Pessin 2002). Insulin avoids hyperglycemia by inducing glucose uptake by skeletal muscle and adipose tissue, and inhibits liver glucose production and glycogenolysis, so it regulates blood glucose levels (Ye 2013; Carr and Correnti 2015).

In the same way, insulin also stimulates conversion and accumulation of glucose in the liver as glycogen and triglycerides (Carr and Correnti 2015). In normal physiology, insulin exerts its effects via specific binding of the hormone to its membrane receptor (Fig. 1). When insulin

binds to the insulin receptor, it stimulates receptor autophosphorylation and internalization activating its intrinsic tyrosine kinase. This event leads to phosphorylation on tyrosine residues of a variety of docking proteins including insulin receptor substrate (IRS) proteins. When IRS-1/2 is activated through Tyr-phosphorylation, it can activate phosphatidylinositol 3 (PI3)-kinase, which converts phosphatidylinositol 4,5-bisphosphate to phosphatidylinositol (3,4,5)-trisphosphate. Akt (also known as protein kinase B) is phosphorylated and activated after PIP_3 binding, stimulating the translocation of glucose transporters to membrane to allow glucose uptake from the blood to the tissue involved (Carr and Correnti 2015). Akt activation also induces phosphorylation of a number of substrates and is critically involved in promoting the anabolic effects of insulin on glucose and lipid metabolism (Ozcan, Cristina de Souza et al. 2013).

Obesity-associated insulin resistance

Frequently, in obesity, insulin signaling is defective so that the tissue cannot respond efficiently to insulin, which leads us to speak of a state of insulin resistance. In theory, defective insulin signaling could occur at the level of IRS-1, through an alternatively phosphorylation of IRS-1, such that insulin-induced glucose uptake is damaged and insulin-sensitive tissues loss their ability to respond to insulin (Ozcan, Cao et al. 2004). Insulin resistance in adipose tissue results in an increased free fatty acid flux to the liver, leading to hepatic insulin resistance, steatosis (Lavallard, Meijer et al. 2012), enhanced hepatic gluconeogenesis and reduction of glycogen synthesis (Ye 2013; Zhang, Cao et al. 2015). Insulin resistance is the primary cause of type 2 diabetes. There are several factors that may contribute to developing insulin resistance and they include: obesity,

inflammation, mitochondrial dysfunction, endoplasmic reticulum (ER) stress, aging and oxidative stress (Ye 2013).

Sirtuins are NAD^+-dependent class III histone deacetylases member of the silent information regulator 2 (Sir2) like family proteins (Lim, Kim et al. 2012). The best-studied of these enzymes, sirtuin 1 (Sirt1), was originally described as a factor regulating of longevity, that acts as an aging suppressor working as an accessory clock protein (Hardeland 2013).

However, Sirt1 is also known to be fundamental in regulation of metabolism and glucose and fat homeostasis (Chen, Lai et al. 2013). Numerous evidences point to that Sirt1 plays a protective role against glucotoxicity and lipotoxicity (Picard, Kurtev et al. 2004; Rodgers, Lerin et al. 2005; Liang, Kume et al. 2009), and in this context, several reports have proved that its deficiency is involved in the development of hepatic insulin resistance (Lagouge, Argmann et al. 2006; Wang, Kim et al. 2011; Chen, Lai et al. 2013), specifically through decreasing Akt phosphorylation at Ser473 (Wang, Kim et al. 2011).

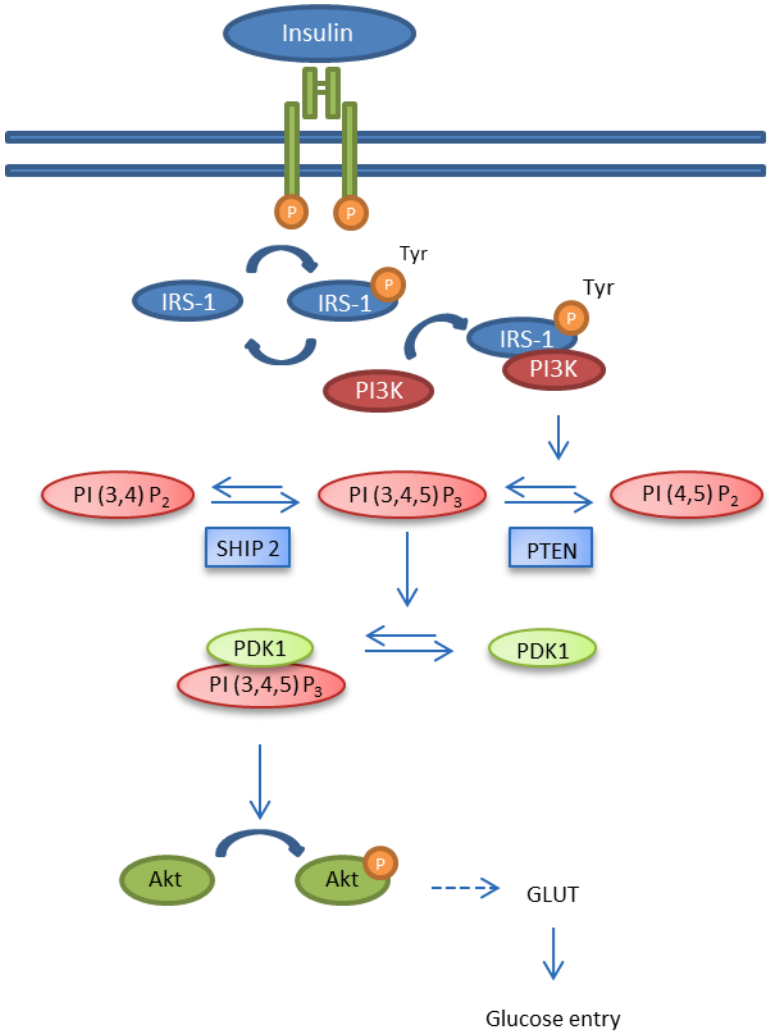

Figure 1. Insulin signaling cascade. When insulin binds to its receptor, a signaling cascade is triggered. In this cascade are involved, among other proteins, Tyr phosphorylated IRS-1, PI3K and phosphorylated Akt, which eventually lead to the entry of glucose into the cell. IRS-1- insulin receptor substrate , PI3K- phosphatidylinositol 3-kinase, PI(3,4) P_2- phosphatidylinositol 3,4-bisphosphate, PI(3,4,5)P_3- phosphatidylinositol 3,4,5-triphosphate, PI(4,5)P_2- phosphatidylinositol 4,5-bisphosphate, PTEN- phosphatase and tensin homolog, SHIP2- SH2 containing inositol phosphatase, PDK1- phosphoinositoside dependent kinase 1, Akt- or protein kinase B, GLUT- glucose transporter.

MITOCHONDRIAL FUNCTION AND DYSFUNCTION

Mitochondrion, from the Greek "*mitos*" (thread) and "*chondrion*" (granule) is an essential cellular organelle of eukaryotic cells, whose main role is to provide the energy needed (Craigen 2010). These organelles are specialized in consumption of oxygen to produce ATP through the process of oxidative phosphorylation.

Mitochondrial structure and dynamics

The number of mitochondria, and its size and shape may vary, however, the ultrastructure of mitochondria always responds to the same scheme. Mitochondria are composed by two lipid bilayer membranes separating three spaces: the cytosol, the intermembrane space, and the mitochondrial matrix (Fig. 2).

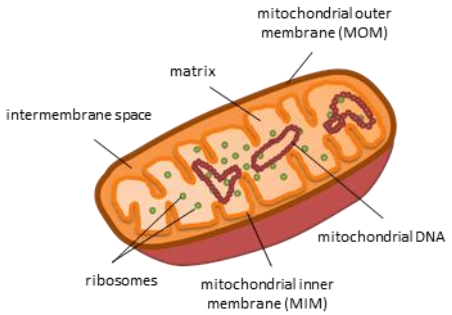

Figure 2. Typical pattern of mitochondrial structure. MOM- mitochondrial outer membrane, MIM- mitochondrial inner membrane.

- The mitochondrial outer membrane (MOM) is structurally similar to other cell membranes and delineates the organelle. It is rich in cholesterol, highly permeable to most molecules, and contains a non-selective channel named voltage-dependent anion channel (VDAC).
- The mitochondrial inner membrane (MIM), which delimits the central cavity called matrix, is rich in cardiolipin, virtually lack cholesterol and is impermeable to ions (Scatena, Bottoni et al. 2007), so that all exchanges are performed by specific

transporters for metabolites. Because of MIM impermeability, mitochondria generate an electrochemical gradient responsible for delivering the proton-motive force to produce ATP. Thus, the maintenance of MIM integrity is critical for the maintenance of mitochondrial functions (Scatena, Bottoni et al. 2007). This membrane is folded numerous times, resulting in the cristae, which greatly increase MIM surface and contain the four electron transport chain complexes and the ATP synthase.

- The mitochondrial matrix contains Krebs cycle and β-oxidation of fatty acids enzymes, ribosomes and the mitochondrial genome.

The morphology of mitochondria is variable in different cell types and tissues, and even changes within the same cell depending on physiological conditions. It is a very dynamic organelle that continuously divides and fuses with other mitochondrial bodies, so it can acquire from a small rounder shape to an extended filamentous mitochondrial network (Putti, Sica et al. 2015). This dynamism of the mitochondrial compartment is determined by fusion and fission processes involving MOM and MIM.

Westermann reviewed that mitochondria can experience these changes in according to its different functions and in response to different requirements, such as ATP production by oxidative phosphorylation, calcium homeostasis, reactive oxygen species (ROS) production, mitochondrial distribution, remodeling of mitochondria during developmental processes and coordination of cell death programs (Westermann 2012; Wai and Langer 2016).

The balance between the fusion and fission machineries is strictly associated with mitochondrial bioenergetics. Fusion of mitochondria

enables them to mix their contents, such as mitochondrial DNA and metabolic intermediates, and thus they can recover the activity of damaged or depolarized membranes (Montgomery and Turner 2015). Thus, unopposed fusion results into a hyperfused mitochondrial network and counteracts metabolic insults preserving cellular integrity and protecting against autophagy, so this process is usually associated with the optimization of mitochondrial function (Wai and Langer 2016). On the other hand, the process of mitochondrial fission increases the number of mitochondria, and prepares the cell for division and meiosis (Montgomery and Turner 2015). Unopposed fission causes mitochondrial fragmentation, that is commonly related to the autophagic removal of damaged mitochondria (Westermann 2012). Thus, the fission process is usually associated with metabolic dysfunction and disease (Wai and Langer 2016).

The main proteins involved in the regulation of mitochondrial dynamics are (Fig. 3):

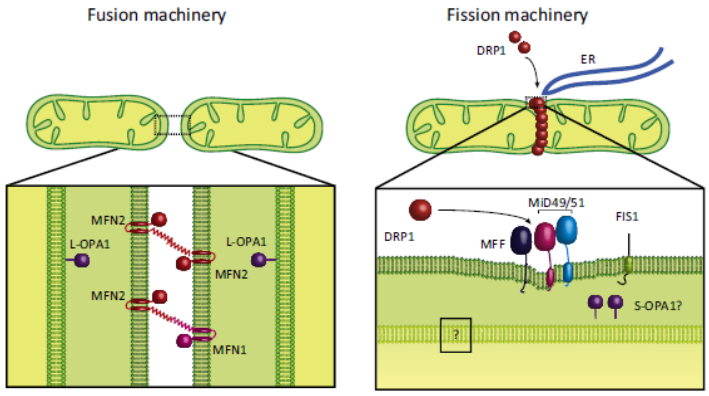

Figure 3. Regulation of mitochondrial fusion and fission. The mains proteins involved in mitochondrial fusion are mitofusin 1/2 (Mfn1 and Mfn2, in red) at the outer mitochondrial membrane and autosomal dominant optic atrophy-1 (L-OPA1, in purple) at the inner mitochondrial membrane. Dynamin-related protein 1 (Drp1, in red) and fission protein 1 (Fis1) are the main proteins involved in mitochondrial fission. This figure was taken form (Wai and Langer 2016).

- Mitofusin 1 and 2 (Mfn1 and 2) which are located on the MOM and take part in outer fusion process. Mfn2 is also implicated in the connection between mitochondria and ER, and its depletion may play a role in ER stress development in metabolic stress conditions (de Brito and Scorrano 2008).
- The optic atrophy-1 (Opa1), which is present in the MIM, participates in the inner membranes fusion and cristae remodeling, and it protects from apoptosis (Frezza, Cipolat et al. 2006)
- Dynamin related protein 1 (Drp1), which found in the cytosol and is involved in mitochondrial fission and apoptosis.
- Fission protein 1 (Fis1) is inserted on the MOM, and recruits Drp1 on this membrane (Putti, Sica et al. 2015).

Mitochondrial electron transport chain and oxidative phosphorylation

The electron transport chain consists of five multiprotein complexes located in the MIM. Electrons flow from NADH (oxidized in complex I) or succinate (complex II) to generate a proton gradient that will be used by the fifth complex to produce ATP (Fig. 4).

Each complex contains several co-factors and prosthetic groups (Silva and Oliveira 2012):

- Complex I (EC: 1.6.5.3, NADH dehydrogenase, or NADH:ubiquinone oxidoreductase) contains flavin mononucleotide (FMN) and 22–24 iron–sulfur (Fe–S) proteins in 5–7 clusters. It catalyzes the reduction of ubiquinone through NADH oxidation.
- Complex II (EC: 1.3.5.1, succinate dehydrogenase or II succinate:ubiquinone oxidoreductase) contains flavin adenine dinucleotide (FAD), 7–8 Fe–S proteins in three clusters and cytochrome b_{560}. It catalyzes the oxidation of succinate to give the fumarate, which results in $FADH_2$ turning in FAD.
- Complex III (EC: 1.10.2.2, cytochrome bc1 complex or Ubiquinol:cytochrome-c oxidoreductase) contains cytochrome b (the ultimate electron acceptor in this complex), cytochrome c1, and one Fe–S protein. It allows electron transfer to a mobile second carrier located in the intermembrane space (cytochrome c), which transports the electrons to the complex IV.

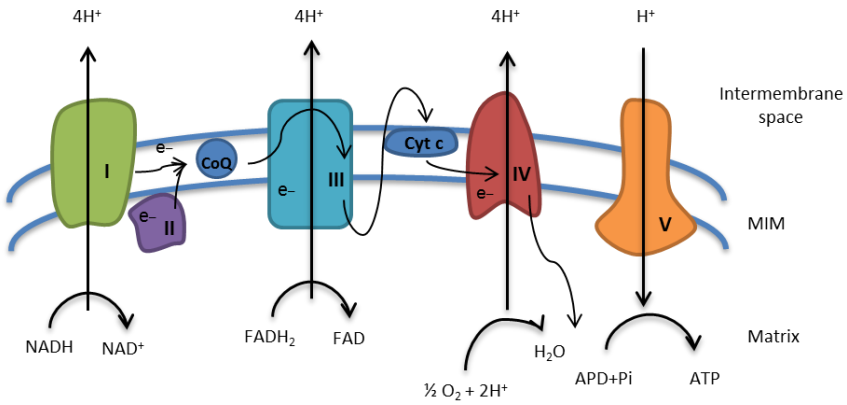

Figure 4**.** Schematic view of the electron transport chain complexes and ATP synthesis. Electrons flow through the respiratory complexes, creating a proton gradient that will be used by the ATP synthase to produce ATP. NADPH- nicotinamide adenine dinucleotide phosphate, FADH2- flavin adenine dinucleotide, CoQ-Coenzyme Q or ubiquinone, Cyt c- cytochrome c, ADP- adenine dinucleotide phosphate, ATP- adenine trinucleotide phospate, MIM- mitochondrial inner membrane. Adapted from (Silva and Oliveira 2012).

- Complex IV (EC: 1.9.3.1, cytochrome-c oxidase or cytochrome-c:oxygen oxidoreductase) contains cytochrome a, cytochrome a_3, and two copper ions. This complex oxidizes cytochrome c and electrons are transferred to O_2, which it is the final electronacceptor of the respiratory chain.
- Complex V (EC: 3.6.3.14, ATP phosphohydrolase (H^+-transporting), F_0F_1-ATPase, or ATP synthase) is usually not considered part of the electron transport chain, but forms part of oxidative phosphorylation.

Respiratory parameters

State 3 of mitochondrial respiration reflects the maximal ATP synthesis, or maximum O_2 consumption rate (respiration), in the presence of ADP (Fig. 5). The increase in respiration denotes the use of the proton-

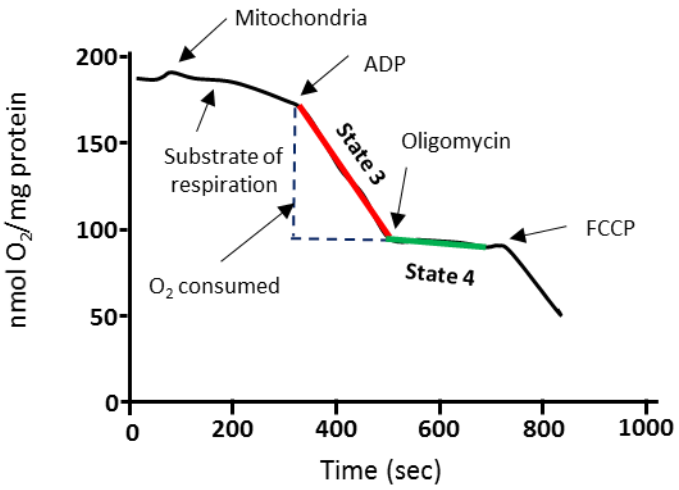

Figure 5. Representative plot of oxygen consumption assay in isolated mitochondria. In the presence of substrate of the respiratory complexes, mitochondria begin to consume oxygen. By adding ADP (state 3, in red), mitochondria consume more oxygen reflecting the maximal ATP synthesis in presence of ADP. When mitochondria have consumed all the ADP, or an ATP synthase inhibitor (oligomycin) is added, the respiration takes place in an inefficient manner due to proton leakage (state 4, in green). Finally, by adding a mitochondrial uncoupler like carbonyl cyanide-4-(trifluoromethoxy) phenylhydrazone (FCCP), oxygen consumption is increased to the maximum. This figure was adapted from (Garcia-Cazarin, Snider et al. 2011).

motive force for the synthesis of ATP, being restored by the augmented proton pumping activity of the respiratory chain. When all ADP is phosphorylated into ATP by the action of the ATP-synthase, the respiration returns to or close to the initial pre-ADP addition values."(Silva and Oliveira 2012).

State 4 represents mitochondrial respiration in absence of ADP or without ATP synthesis, and therefore due to proton leakage or passive entry from the cytosol into the mitochondrial matrix.

The respiratory control ratio (RCR) represents the ratio between state 3 respiration and the state 4. It is a parameter that determines the

coupling between substrate oxidation and phosphorylation, so it is indication of how coupled mitochondria are (Silva and Oliveira 2012).

Oxidative phosphorylation efficiency is determined by the ADP/O ratio. It represents the amount of oxygen reduced to water the respiratory chain per ADP phosphorylated (Silva and Oliveira 2012).

Mitochondrial dysfunction in obesity

Mitochondrial dysfunction is defined as a reduction in mitochondrial number, density or function (Ye 2013). It is well known that mitochondrial dysfunction plays an important role in obesity-related diseases and, particularly, in the liver for the development of insulin resistance (Agil, El-Hammadi et al. 2015). Ye and colleagues have described several lines of evidence that highlight the relevance of mitochondria during the development of insulin resistance and the associated type 2 diabetes, either because the mitochondrial dysfunction causes insulin resistance or because mitochondrial dysfunction is the consequence of the insulin signaling impairment (Ye 2013). Mitochondrial dysfunction, and specifically a decreased electron transport chain activity, has also been related with the development of hepatic steatosis (Perez-Carreras, Del Hoyo et al. 2003; Paradies, Paradies et al. 2014).

OXIDATIVE STRESS

Free radicals are molecules or molecular fragments highly unstable and reactive because of they contain one or more unpaired electron in atomic or molecular orbitals. Free radicals are products of normal cellular metabolism that can be generated by enzymatic and non-enzymatic process. However, mitochondria are considered the main

source of free radicals. Mitochondria consume around 90% of a cell's oxygen to produce ATP, so the production of potentially harmful reactive oxygen species (ROS) is an inevitable consequence. It has been described that approximately between 0.2 and 2% of the oxygen taken up by the cell is converted to ROS in the mitochondria, mainly in complexes I and III (Paradies, Paradies et al. 2014).

Among the main free radicals, the most important ROS are superoxide anion ($O_2^{\bullet-}$), peroxide radical ($ROO^{\bullet-}$) and hydroxyl radical ($^{\bullet}OH$). The production of $O_2^{\bullet-}$ occurs mostly within the electron transport chain. This ROS quickly dismutases to hydrogen peroxide (H_2O_2), whose detrimental role is the enormous capacity to diffuse across cell membranes, and quickly spread throughout the body. Besides, when H_2O_2 reacts with transition metals such as Fe^{2+} via the Fenton reaction, or with $O_2^{\bullet-}$ by the Haber-Weiss reaction, $^{\bullet}OH$ is formed. Despite its short half-life, $^{\bullet}OH$ is the most reactive and dangerous ROS due to its ability to speedily react close to its site of formation (Fig. 6).

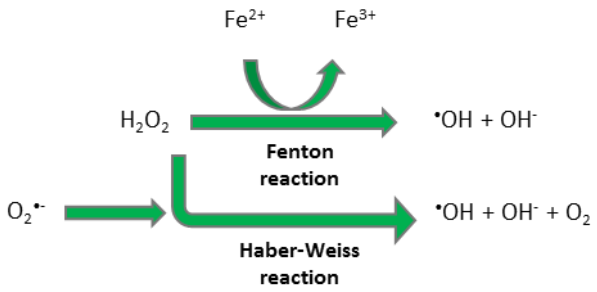

Figure 6. Free radical formation by the Fenton and Haber-Weiss reactions.

On the other hand, mitochondrial nitric oxide (NO) can react with ROS produced in the mitochondria, resulting in the generation of reactive nitrogen species (RNS), which in turn can be harmful to the electron

transport chain function disturbing electron transfer to oxygen (Paradies, Paradies et al. 2014) and producing higher amounts of free radicals.

However, besides mitochondrial respiratory chain there are many other cellular sources of significant amounts of free radicals, such as the ER, peroxisomes, cytosolic NO synthase and lipoxygenases from the cytosol and the plasmatic membrane among many others.

At low or moderated concentrations, ROS have physiological functions and beneficial effects related with their actions as secondary messengers in many signaling systems and as defense agents against certain pathogens (Valko, Leibfritz et al. 2007). However, when the antioxidant defense is not able to alleviate ROS and RNS overproduction disturbing the redox balance or homeostasis, we face oxidative stress. This situation of oxidative stress will detonate a cascade of deleterious effects on macromolecules termed oxidative damage. Oxidative stress and damage are implicated in several pathological conditions, like cardiovascular disease, cancer, neurological disorders, diabetes, ischemia/reperfusion and ageing (Valko, Leibfritz et al. 2007). In addition, ROS production is closely associated with an impairment of the mitochondrial respiratory chain (Paradies, Paradies et al. 2014), and with the MOM permeabilization (MOMP), an important factor in mediating intrinsic apoptosis (Loureiro, Magalhaes-Novais et al. 2015).

Antioxidant defense

An antioxidant is a molecule that delays or inhibits the oxidation of a substrate, even when it is found at low concentrations in comparison with the substrate, without losing its own stability. Evolutionarily, the organisms developed efficient systems to combat free radical-induced

oxidative stress. Among these protective mechanisms are enzymatic and no enzymatic antioxidant defenses.

Enzymatic antioxidant defense

Enzymatic antioxidant defense include, among others, the enzymes superoxide dismutase (SOD; EC 1.15.1.1), catalase (CAT; EC 1.11.1.6), glutathione peroxidase (GPx; EC 1.11.1.9) and glutathione reductase (GR; EC 1.6.4.2) (Fig. 7).

SOD, which catalyzes the dismutation of $O_2^{\bullet-}$ to H_2O_2, is distributed in all cells with anaerobic respiration. This is the first line of enzymatic antioxidant defense, and it is necessary that SOD works coupled with the enzymes responsible for removing H_2O_2. In mammals there are three SOD

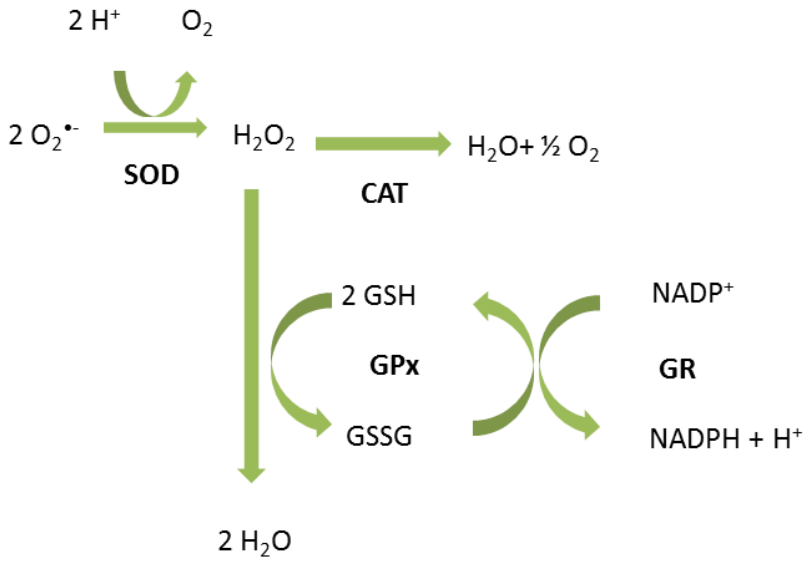

Figure 7. Enzymatic antioxidant defense. SOD- superoxide dismutase; CAT- catalase, GPx- glutathione peroxidase; GR- glutathione reductase ; $O_2^{\cdot-}$superoxide anion; H_2O_2- hydrogen peroxide; GSH- reduced glutathione; GSSG- oxidized glutathione; NADPH- nicotinamide adenine dinucleotide phosphate. Figure adapted from the doctoral thesis of Zapico, 2005 (Tomás-Zapico 2005)

isoforms, which differ in their cellular localization and in the cofactors necessary for their function: cytosolic SOD also named SOD1 (with Cu/Zn in its active center), mitochondrial SOD or SOD2 (with Mn in its active center) and extracellular SOD or SOD3 (with Cu/Zn in its active center) (Loschen, Azzi et al. 1974).

CAT catalyzes the conversion from 2 H_2O_2 to H_2O and O_2. This enzyme is mainly located in the peroxisome, but it is also found in the mitochondria (Salvi, Battaglia et al. 2007). CAT has low affinity for its substrate, so it is more efficient removing H_2O_2 when found at high concentrations.

The GPx-GR system includes the enzymes GPx and GR, and glutathione and nicotinamide adenine dinucleotide phosphate (NADPH) as cofactors. GPx scavenges H_2O_2 using reduced glutathione (GSH) and releasing oxidized glutathione (GSSG) and H_2O. Unlike CAT, GPx has high affinity for its substrate, so it works better at low concentrations of H_2O_2. GPx acts in tandem with GR, which catalyzes the reduction of GSSG to GSH taking a H^+ from NADPH and allowing its reuse by GPx.

Non-enzymatic antioxidant defense

The non-enzymatic antioxidant defense is composed by molecules that present the ability to donate an electron to reactive species neutralizing free radical toxicity, without becoming toxic by itself. In turn, the non-enzymatic antioxidant defense can be obtained from the diet (ascorbic acid, tocopherol, carotenoids, flavonoids, etc.) or be synthesized by the body (glutathione, uric acid, bilirubin, albumin, melatonin, etc.).

Oxidative damage

Despite all the mechanisms existing to fight against free radicals, the antioxidant defense is sometimes inefficient and/or inadequate leading to a situation of oxidative damage that affects proteins, lipids and DNA.

Oxidative damage to proteins

Proteins can be damaged in the peptide backbone and side chains, in particular cysteine and methionine residues are susceptible to oxidation by the action of ROS/RNS (Stadtman 2004). There are several types of oxidative damage to proteins, including: nitration, formation of protein-protein bonds, breakdown of peptide bonds, glutathionylation, S-nitrosylation, but the most studied is protein carbonylation. In most cases, post-translational modifications suffered by proteins when they are subjected to oxidative stress, are reversible. However, accumulation of oxidized forms of damaged proteins has been associated with aging and age-associated diseases, such as Alzheimer's disease.

Oxidative damage to lipids

Lipids are the most susceptible macromolecules to oxidative stress. Oxidative damage to lipids, or lipid peroxidation (LPO) is an uncontrolled auto-oxidative destruction process that affects mainly polyunsaturated fatty acid (PUFA) residues of phospholipids, which are extremely sensitive to oxidation. It occurs through an attack of free radicals to the hydrophobic chains of membrane phospholipids, removing one hydrogen atom, and thus generating the radical $ROO^{\bullet -}$, that leads to a series of chain redox reactions. Consequently, potentially toxic aldehydes are formed, including malondialdehyde (MDA) and 4-hydroxy-2 (E) -

nonenal (4-HNE) that are considered the main peroxidation products (Esterbauer, Schaur et al. 1991). Therefore this toxic aldehydes are considered as good markers of lipid peroxidation and their accumulation has been related to diabetes (Valko, Leibfritz et al. 2007).

Oxidative damage to DNA

DNA can be damaged in both the purine and pyrimidine bases and also in the deoxyribose backbone. It usually occurs by the action of ($^{\bullet}$OH) radicals and epoxides on nitrogenous bases. The most studied DNA lesion is the formation of 8-hydroxyguanosine (8-OHdG), as the first step involved in mutagenesis, carcinogenesis and aging (Valko, Leibfritz et al. 2007).

Obesity-induced oxidative stress

In obesity, free radical production and oxidative stress occur in mitochondria mainly due to oversupply of fatty acids and glucose, and leading to overload the electron transport chain (Ye 2013). Besides, the literature includes different mechanisms by which oxidative stress is induced by obesity and its related diseases. Vincent and Taylor reviewed several potential contributors to oxidative stress in obesity (Vincent and Taylor 2006), such as hyperglycaemia (Aronson and Rayfield 2002), increased muscle activity to carry excessive weight (Vincent, Morgan et al. 2004), elevated tissue lipid levels (Beltowski, Wojcicka et al. 2000; Vincent, Powers et al. 2001), inadequate antioxidant defense (Ohrvall, Tengblad et al. 1993; Vincent, Powers et al. 2001; Wallstrom, Wirfalt et al. 2001), chronic inflammation, (Davi, Guagnano et al. 2002; Fernandez-Real, Broch et al. 2003; Saito, Yonemasu et al. 2003) endothelial ROS production (Egan, Greene et al. 2001; Wheatcroft, Williams et al. 2003) and hyperleptinemia

(Bouloumie, Marumo et al. 1999). In each of these cases, free radical production is directly increased or there is an insufficient antioxidant capacity to attenuate the damage inflicted by the free radicals (Vincent, Innes et al. 2007; Sainz, Rodriguez et al. 2010).

INFLAMMATION

Inflammation is a physiological protective response that is part of the innate immune defense. Inflammation is characterized by an elevated number of white blood cells and increased levels of pro-inflammatory cytokines in the circulation or tissue (Ye 2013). The inflammatory response is triggered to isolate and remove pathogens and/or exogenous harmful materials as well as during tissue repair, organ remodeling and wound healing (Ye 2013). Although inflammation is a protective response, the inflammatory process can be potentially damaging and associated with the pathogenesis of many acute and chronic disorders such as: allergy, cardiovascular and autoimmune diseases, type 2 diabetes, cancer, etc. Thus, inflammation can be beneficial or harmful to the liver, depending on factors such as the duration and intensity of the inflammatory process and the type of damage that seeks redress. For instance, mild inflammatory responses have been shown to have hepatoprotective effects, repairing and restoring hepatic homeostasis (Brenner, Galluzzi et al. 2013). However, when inflammation is uncontrolled and exacerbated, it can causes massive loss of hepatocytes, worsening metabolic disorders such as obesity, diabetes, and non-alcoholic fatty liver disease (NAFLD) (Brenner, Galluzzi et al. 2013).

Over recent decades, numerous studies have established a link between obesity, obesity related diseases and inflammation, particularly through ER stress activation (Boden, Duan et al. 2008; Manley, Williams et

al. 2013; Park, Kim et al. 2014). In obesity, there is a chronic and low grade inflammation which begins with elevated macrophage infiltration and pro-inflammatory cytokines expression in adipose tissue and liver. These inflammatory mediators enter the blood stream to cause systemic inflammation (Ye 2013).

One of the key signaling pathways in the control of inflammatory and immune state is the nuclear factor kappa-light-chain-enhancer of activated B cells (NF-κB) pathway (Fig. 8). NF-κB is a family of transcription factors highly conserved across species and widely expressed in many tissues and cells. In mammals, this family is also known as Rel family, and is composed by five members (p50, p52, p65 or RelA, c-Rel, and RelB) that work as dimers, and whose subunits can homodimerize or heterodimerize (Muriach, Flores-Bellver et al. 2014).Under basal conditions, NF-kB dimers are in a latent cytoplasmic form, inhibited by IkB (NF-κB inhibitor), until the arrival of an appropriated stimulus. When it takes place, IκB is phosphorylated by the kinase complex known as IKK (IκB kinase) that leads to IκB ubiquitination and proteasomal degradation. Thereby, NF-kB dimmers are liberated, their DNA-binding domain exposed, and can be translocated into the cell nucleus stimulating the transcription of its target genes (Shoelson, Lee et al. 2003; Muriach, Flores-Bellver et al. 2014).

NF-kB is involved in the response to stimuli such as oxidative stress and inflammation, and a wide variety of extracellular stimuli such as toxic metals, UV radiation, asbestos and alcohol promote its activation (Valko, Leibfritz et al. 2007). This pathway takes part in cell survival, differentiation and growth, and its activation has been closely related to carcinogenesis (Valko, Leibfritz et al. 2007).

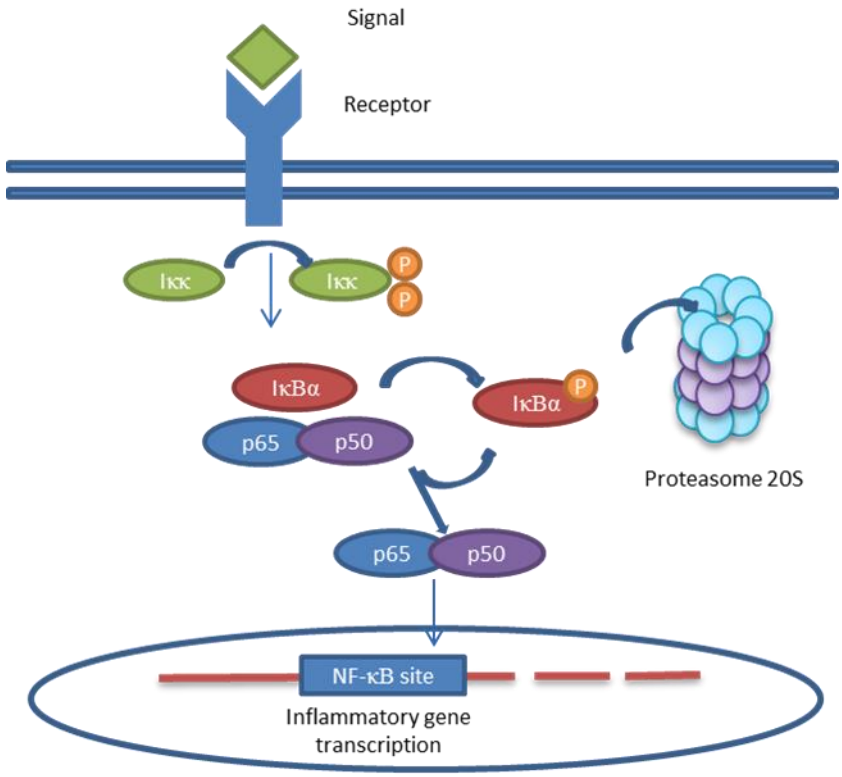

Figure 8. Activation of the NF-κB (nuclear factor k-light-chain enhancer of activated B cells) pathway. The IKK phosphorylate the inhibitor IκB, targeting to its proteasome degradation. Then, the NF-κB dimers (p65 / p50) can enter into the nucleus to induce the transcription of specific genes involved in proliferation, inflammation and survival. IκB- NF-κB inhibitor; Ikκ- IκB kinase.

Other factor involved in the regulation of the inflammatory response is Sirt1, that has been recently implicated in the repression of inflammation in metabolic tissues such as liver, where overexpression of Sirt1 decreases TNF-α (tumor necrosis factor α) and IL-6 (interleukin 6) expression (Pfluger, Herranz et al. 2008) and Sirt1 deletion increases NF-κB activity (Purushotham, Schug et al. 2009).

CELLULAR QUALITY CONTROL SYSTEMS

The cell has multiple mechanisms for monitoring the state of its structures to maintain cellular homeostasis and preserve the integrity of the cell. The ubiquitin-proteasome system is responsible for removing short half-life proteins; the unfolded protein response (UPR) is triggered against misfolded or unfolded proteins and check the correct maturation of proteins; autophagy degrades protein aggregates or even whole unnecessary or non-functional organelles; and when these systems fail or are insufficient, programed cell death (PCD) or apoptosis takes place in a controlled manner to remove damaged or unnecessary cells, to try to preserve tissue integrity.

Ubiquitin-proteasome system

Eukaryotic cells contain a major intracellular proteolytic structure known as the proteasome. The proteasome is multi-subunit enzyme complex that is mainly located in the cytoplasm, whose function is to catalyze the selective degradation of short-lived and damaged proteins to maintain cellular homeostasis (Cuervo 2004; Groll and Potts 2011). To be degraded by the proteasome system, the protein has to be flagged for destruction by the ubiquitin conjugation system, whereby a polyubiquitin chain is attached on the target protein (Adams 2003).

The characteristic mammalian proteasome is the 26S (Fig. 9), which is formed by the association of the barrel-shaped 20S proteasome subunit and two 19S regulatory cap subunits. The 19S proteasome binds the polyubiquitin chain, denatures the protein, and internalize the protein into the 20S proteolytic core. The 20S proteasome is the catalytic core of the proteasome complex and the responsible for the breakdown of key

proteins. This core consist of four stacked heptameric ring structures that are themselves composed by two different types of subunits: two inner β catalytic rings and two outer α structural rings (Adams 2003).

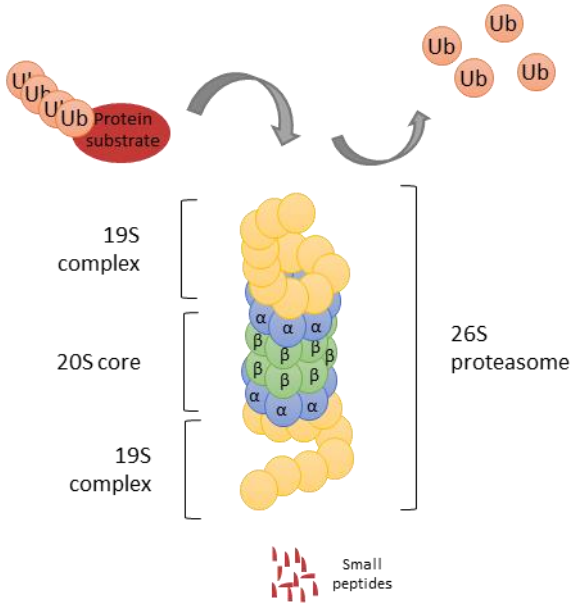

Figure 9. Diagram of the ubiquitin proteasome pathway. The 26S proteasome is formed by the 20S core capped with the 19S regulatory complexes, which recognize polyubiquitinated proteins. Ub- ubiquitin. This figure was adapted from (Bardag-Gorce 2010).

Unfolded protein response

The ER is an organelle in eukaryotic cells that is formed by an interconnected network of membranes called cisternae. This organelle has the ability to adapt and respond to periodic cycles associated with feeding, fasting, and other metabolic demands of limited duration. Thus, it has a vital role in maintaining cellular and organismic metabolic homeostasis (Fu, Watkins et al. 2012). The ER is mainly responsible for: providing a Ca^{2+} reservoir (Hoyer-Hansen and Jaattela 2007), synthesizing up to 75% of

proteins, specially transmembrane proteins and proteins destined for secretion and regulating the maturation and proper folding of proteins (Schroder and Kaufman 2005). To execute these functions, it performs post-translational modifications such as cleavage, glycosylation, and the formation of intra- and inter-molecular disulfide bonds, to take proteins to its mature conformation. The liver is a highly synthetic organ, so hepatocytes contain abundant ER to processes millions of molecules in seconds (Ji and Kaplowitz 2006; Fu, Watkins et al. 2012).

Disruption of any of the processes in which ER is involved goes along with the accumulation of unfolded and/or misfolded proteins in the lumen of the ER leading to a condition termed ER stress. These alterations in the ER function are usually associated with the presence of cellular stressors, like nutrient deprivation, hypoxia and changes in glycosylation status (Fan, Sun et al. 2013). To deal with this stress, cells trigger an evolutionarily conserved response known as unfolded protein response or UPR (Ozcan, Cao et al. 2004; Schroder and Kaufman 2005). The UPR occurs through activation of three main signaling membrane proteins of ER that are activated depending on the folding requirements of the ER:Inositolrequiring enzyme–1 (Ire1α), double-stranded RNA-activated protein kinase–like endoplasmic reticulum kinase (PERK),activating transcriptionfactor-6-α (ATF6α) (Yoshida, Matsui et al. 2003; Yoo 2013).

Under non-stress conditions, the ER luminal domains of these sensor proteins are associated or linked to the intraluminal calcium-dependent protein-78 (GRP78 or BIP) and upon ER stress, GRP78 binds to unfolded proteins, being dissociated from Ire1α, PERK and ATF6α, and leading to its activation (Malhi and Kaufman 2011). PERK and Ire1α are activated by dimerization and subsequent autophosphorylation. On the other hand,

ATF6α which is synthetized as a 90kDa protein (90kDa-ATF6α) is activated by a specific proteolytic cleavage. It is transported to the Golgi apparatus, and activated by site-1/2 proteases producing the active form (50kDa-ATF6α) (Gotoh, Endo et al. 2011).

The responses that make up the UPR include (Fig. 10):

- The reduction of global protein synthesis through phosphorylation of α-subunit of eukaryotic initiation factor (eIF2α) by activated PERK.
- The synthesis of chaperones and other proteins to improve the folding capacity of the ER.
- The degradation of unfolded or misfolded proteins through the ubiquitin-proteasome system, also called ER-associated degradation (ERAD).
- When ER stress is prolonged and severe and it is not be able to recover its function, as a last resort, apoptosis is triggered for removing misfolded/unfolded proteins and damaged cells (Hoyer-Hansen and Jaattela 2007; Zhang, Cao et al. 2015). It is known that at least three pathways are involved in ER stress-mediated apoptosis:
  - Transcriptional activation of the gene for CHOP (CCAAT/enhancer binding protein (C/EBP) homologous protein).
  - The activation of Ire1-TRAF2 (TNF-α receptor-associated factor 2)-AKS1 (apoptosis signal-regulating kinase 1) –MAP (mitogen-activated protein) kinase pathway.
  - The activation of the ER-associated caspase-12 (Gotoh, Endo et al. 2011).

Under physiological conditions, CHOP is expressed at low levels but under conditions of ER stress, CHOP transcription is strongly induced by the three ER stress signaling pathways. Despite this, PERK pathway always plays a dominant role in CHOP induction (Gotoh, Endo et al. 2011).

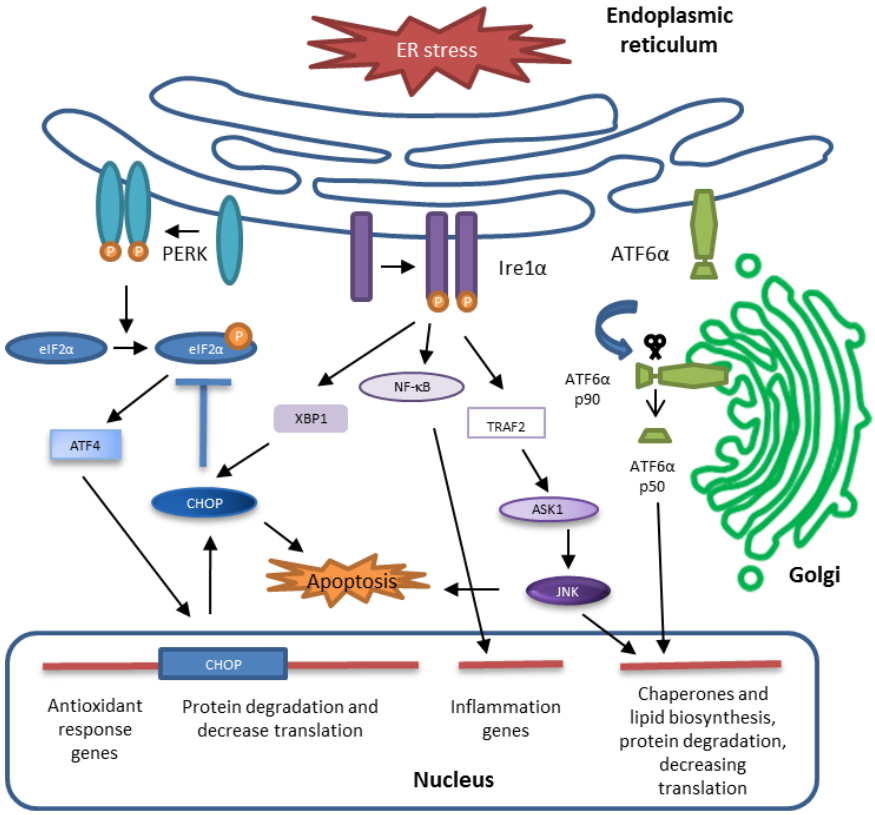

Figure 10. The major signal transduction pathways in the unfolded protein response .ER- endoplasmic reticulum; PERK- double-stranded RNA-activated protein kinase–like endoplasmic reticulum kinase; eIF2α-α- subunit of eukaryotic initiation factor; ATF4- activation transcription factor 4; CHOP- CCAAT/enhancer binding protein homologous protein; Ire1α- Inositolrequiring enzyme-1; XBP1- X-box binding protein 1; NF-κB - nuclear factor κ-light-chain enhancer of activated B cells; TRAF2- TNF-α receptor-associated factor 2; ASK1- apoptosis signal-regulating kinase 1; JNK- c-Jun N-terminal kinase; ATF6α- activating transcription factor-6-α.

Furthermore, Marciniak and colleagues reported that CHOP induces *de novo* protein synthesis, via eIF2α dephosphorylation, leading

to the accumulation of high molecular weight proteins complex in the ER, and promoting ER function decline (Marciniak, Yun et al. 2004).

Alterations in the function of ER have been associated with the triggering of inflammatory responses and autophagy, and the development of insulin resistance and obesity (Lavallard, Meijer et al. 2012; Park, Kim et al. 2014; Kim, Kang et al. 2015).

Autophagy

Although autophagy can ultimately trigger a type of cell death known as PCD type II, it is a primarily survival mechanism [Rautou, 2010 #37]. Autophagy is a dynamic process by which cell membranes sequester long-lived proteins, protein aggregates, portions of cytoplasm and even subcellular organelles for degradation by lysosomal proteases in order to recover their components [Coto-Montes, 2012 #17]. Three types of autophagy have been identified: microautophagy, chaperone-mediated autophagy (CMA) and macroautophagy (Fig. 11). Macro- and microautophagy are well preserved in all eukaryotic cells, while CMA is restricted to mammalian cells. The three types of autophagy differ in the way of cargo delivery to lysosomes.

During **microautophagy**, small portions of the cytosol are directly taken up by the lysosomes by invagination of their membranes (Wang and Klionsky 2003). **Chaperone-mediated autophagy** (CMA) involves the degradation of proteins and peptides containing the specific amino acid sequence KFERQ through binding a constitutive chaperone, the heat shock-cognate protein (hsc70). Then, this specific targeted proteins are recognized by LAMP2A (lysosome-associated membrane protein type 2A), which facilitates the translocation of these proteins across the lysosomal

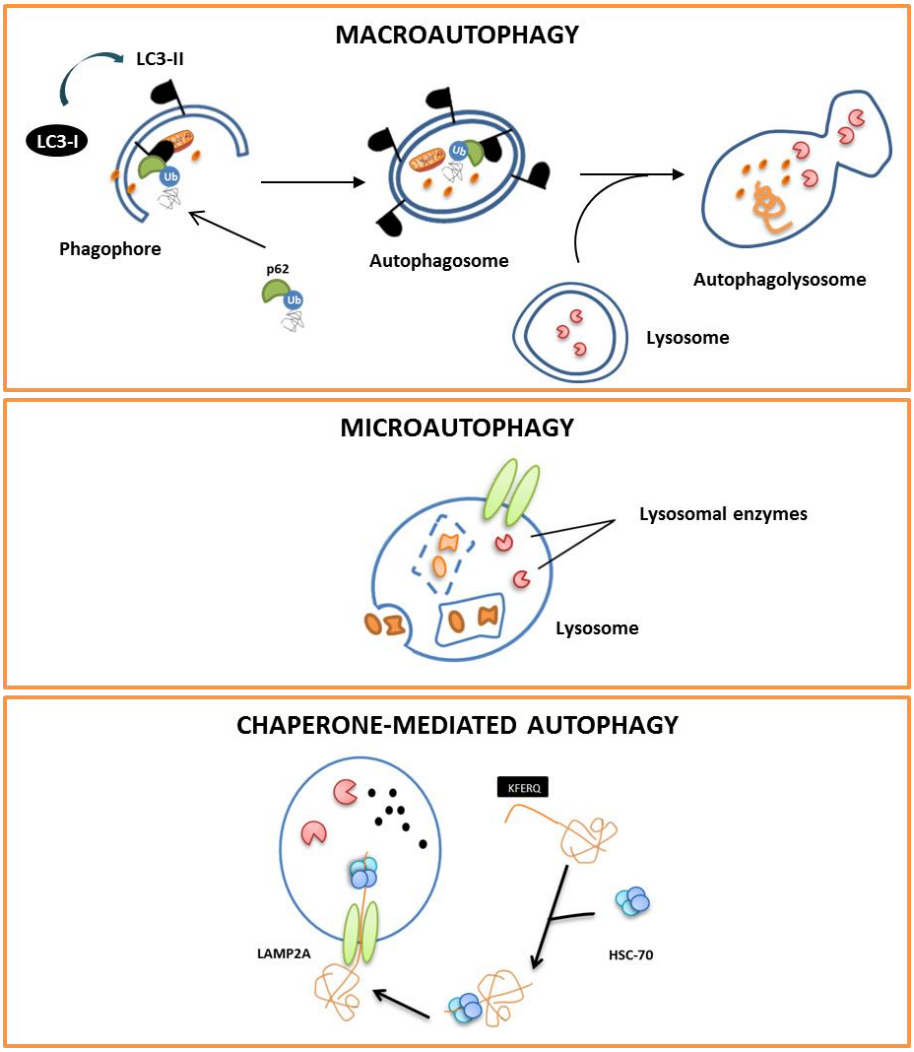

Figure 11. Types of autophagy. The diagram shows the three main forms of autophagy: macroautophagy, microautophagy and chaperone-mediated autophagy. In microautophagy, portions of cytosol are internalized by invagination of the lysosomal membrane. In macroautophagy, large portions of cytoplasm are sequestered in double-membrane structures fuse with lysosomes. In chaperone-mediated autophagy, specific cytosolic proteins are transported inside the lysosome through a chaperone / receptor complex. ER- endoplasmic reticulum, PI3K- phosphatidylinositol 3 kinase , LAMP2- lysosome-associated membrane protein type 2, LC3- microtubule-associated protein light chain 3, HSC-70- heat shock cognate protein 70. Adapted from the thesis of Vega-Naredo, 2010 (Vega-Naredo 2010).

membrane, resulting in their unfolding and degradation (Cuervo and Wong 2014).

The morphological hallmark of **macroautophagy** (hereafter referred to as autophagy) is the formation of a double-membrane structure, called an autophagosome [Xie, 2007 #55]. Upon autophagy induction, a membrane structure referred to as the phagophore (the precursor to the autophagosome) gradually expands and engulfs a portion of the cytosol or specific molecular loads for delivery into the lysosomes for degradation [Yorimitsu, 2005 #57]. Initially, the origin of autophagosome membranes was attributed to ER (Axe, Walker et al. 2008; Hayashi-Nishino, Fujita et al. 2009; Yla-Anttila, Vihinen et al. 2009), but currently, there are studies that suggest that other membrane sources such as mitochondria and the Golgi apparatus can also take part in the formation of the autophagosomal membrane (Mari, Tooze et al. 2011). This process, which entails the sequential expansion of the phagophore, provides autophagy with the capacity to sequester essentially any cellular component for the delivery and subsequent degradation in the lysosomal compartment [Wang, 2011 #77]. As consequence of a failed attempt at preserving cell survival, several autophagosomes are formed throughout cell, swallowing much of the cytoplasmic components and resulting in a type of cell death with autophagic characteristics denoted as PCD type II [Coto-Montes, 2012 #17].

Several proteins are implicated in the formation of the phagophore and autophagosome. These so-called autophagy-related (ATG) genes and proteins were originally identified in yeast, and subsequently they orthologs in mammals have been identified. Autophagy consists of three sequential steps: initiation, nucleation and elongation/enclosure (Fig. 12).

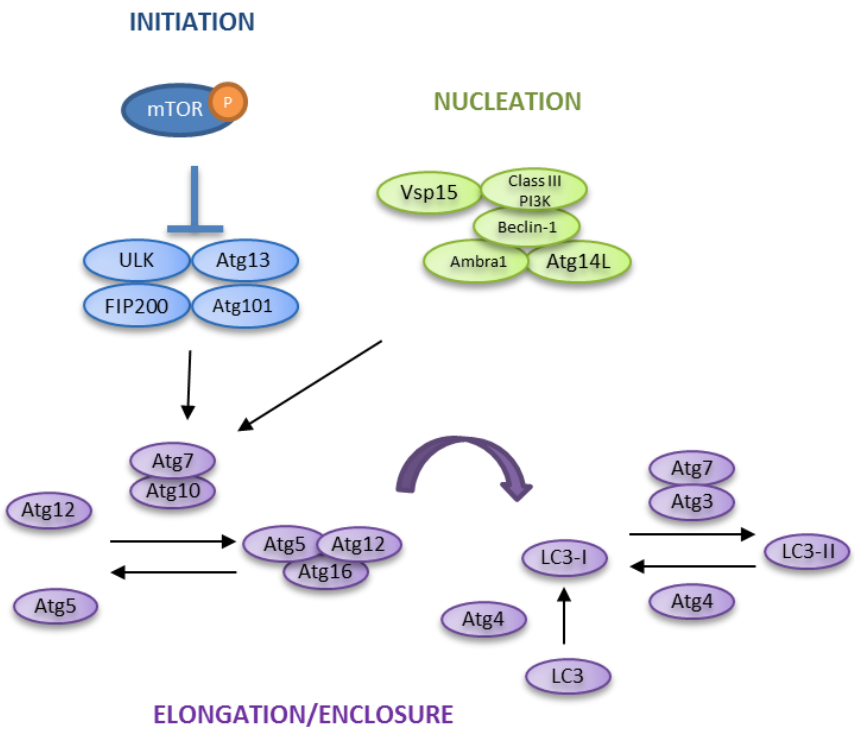

Figure 12. Three major of macroautophagy: Initiation, nucleation and elongation/enclosure. mTOR- mammalian target of rapamycin; Atg- autophagy related protein, Class III PI3K- class III phosphatidylinositol 3-kinase; LC3- microtubule-associated protein 1 light chain 3. Figure adapted from (Lavallard and Gual 2014).

The initiation of autophagy is controlled by the ULK kinase complex (ULK-Atg3-FIP200), which also contains Atg101. The serine/threonine kinase mammalian target of rapamycin (mTOR) is the main inhibitor of autophagy. When it is phosphorylated, interacts with ULK inactivated them, preventing the autophagosome formation.

- Nucleation: this is the step in which the autophagosome is formed. This step involves the interaction of Beclin-1 with the factors (Ambra-1 and Atg14L) that modulate the Beclin-1 binding with the vacuolar protein sorting 34 (Vsp34). This, is a class III

phosphadidylinositol 3-kinase which has a lipid kinase activity essential for the autophagosome formation.

- Elongation/Enclosure: two conjugation systems take part in the formation and elongation of the phagophore: Atg12-Atg5 and LC3 (microtubule-associated protein 1 light chain 3)
    - Atg12-Atg5: they are conjugated by two ligases, Atg7 and Atg10, and when they are joined, Atg12-Atg5 complex is associated with Atg16, leading to Atg12-Atg5-Atg16 complex.
    - LC3 (the orthologue of yeast Atg8) is required for autophagosome transport and maturation. LC3 is synthesized in an unprocessed form, proLC3, which is cleavage in the C-terminus amino acids by Atg4, leading to the soluble form LC3-I (Skop, Cahova et al. 2012). Then, LC3-I is conjugated to phosphatidylethanolamine, mediated by Atg7 and Atg3 participation. This new phosphatidylethanolamine-conjugated form is called LC3-II and it is part of autophagosomes and autolysosomes (Skop, Cahova et al. 2012).
- Finally, the autophagosomes are fused with lysosomes forming the autophagolysosome, and leading to the degradation of the cellular constituents sequestered.

Sequestosome 1, also called p62, is a protein that specifically marks organelles and protein aggregates for autophagic degradation. When it is attached for material degradation, it interacts with LC3-II to be degraded in the autophagolysosome with other waste components (Komatsu 2011). A blockage in autophagy prevents the degradation of these marked structures, and p62 is accumulated with them. Many studies have shown

that, when autophagy is impaired, p62 is accumulated along with ubiquitinated aggregates (Mizushima and Yoshimori 2007; Komatsu 2011; Aghajan, Li et al. 2012), leading to increased oxidative stress (Mathew, Karp et al. 2009). Interestingly, p62 can activate mTOR resulting in a negative feedback (Manley, Williams et al. 2013).

p62 is a scaffold protein with multiple domains that has multiple functions as transduction, cell proliferation, cell survival, cell death, inflammation, tumorigenesis, inflammation (Manley, Williams et al. 2013) and oxidative stress response through nuclear factor (erythroid-derived 2)-like 2 (Nrf2) activation (Komatsu 2011). In addition, p62 has also been implicated in various signal transduction pathways associated with obesity and insulin resistance (Geetha, Zheng et al. 2012). For example, p62 have been described as a negative regulator of PPARγ (peroxisome proliferator-activated receptor gamma) (Rodriguez, Duran et al. 2006; Lee, Pfluger et al. 2010), the ligand-activated transcription factor and master regulator of the genes involved in lipogenic pathways and adipocyte differentiation (Videla and Pettinelli 2012).

Regulation of autophagy:

There are several mechanisms involved in the regulation of autophagy that include multiple signal-transduction pathways.

The main signaling pathways involved in the regulation of autophagy are: the insulin–PI3K–Akt–mTOR pathway, the ERK (extracellular signal-regulated kinases) pathway and the p38 MAPK (mitogen-activated protein kinases) pathway (Lavallard, Meijer et al. 2012).

- Insulin-PI3K-Akt-mTOR pathway: as we saw above, the insulin binding to its receptor leads to the phosphorylation of Akt. This Akt activation, prevents the formation ofTSC1/2 complex (tuberous sclerosis complex1/2) and ultimately leads to mTOR activation. Thus, in presence of insulin, autophagy is inhibited through the activation of mTOR.
- ERK pathway activates autophagy in response to amino acid depletion, but ERK can also inhibit autophagy depending on the cell type and the stimuli.
- The p38 MAPK pathway is also a negative or positive regulator of autophagy depending on the cell type and stimuli specific.

In addition, there are short and long term regulatory mechanisms in which the three pathways that were explained above are involved.

- The short term regulation involves amino acids, energy balance, ROS, ER stress and acetylation/deacetylation of proteins.
- The long-term regulation that involves FoxO proteins (class O of forkhead box transcription factors), that take part in the regulation of glucose metabolism and the cell cycle and death, and the transcription factor EB, which is involved in the control of lysosomal biogenesis. (Lavallard, Meijer et al. 2012).

Autophagy and obesity-related alterations

Many works suggest the involvement of autophagy in several obesity-related processes. Autophagy regulates food intake, insulin resistance, and plays a key role against lipotoxicity (Lavallard, Meijer et al. 2012). Furthermore, it is closely linked to white adipose tissue differentiation and maturation, including the conversion of white adipose tissue towards brown adipose tissue (Singh, Xiang et al. 2009; Zhang, Goldman et al. 2009; Goldman, Zhang et al. 2010), and it is also crucial in the development of hepatic disorders associated with obesity (Lavallard and Gual 2014). During a sustained availability of lipids, as occurs in obesity, the autophagic turnover of the liver is inhibited, so it cannot degrade lipid droplets, leading to hepatic steatosis (Lavallard and Gual 2014). Besides, altered autophagic activity is implicated in the progression of type 2 diabetes through impaired β-cell function and development of insulin resistance (Barlow and Thomas 2015).

Apoptosis

In multicellular organisms, when some cells threaten tissue/organism integrity or are no longer necessary, they enter into a tightly regulated program for cell suicide known as PCD type I or apoptosis. The cell death caused by apoptosis, unlike what happens with necrosis, occurs in a controlled way, so that neighbouring cells are not affected by the waste materials. This process is characterized by, cell shrinkage and condensation, cytoskeleton collapse, nuclear envelope disassembles, and nuclear DNA breakage into fragments. Finally, the remains of the cell are engulfed and recycled by a neighbouring cell or a macrophage without causing a major host inflammatory and/or immune response.

This process is and energy dependent process mediated by proteolytic enzymes called caspases, which trigger cell death by cleaving specific proteins in the cytoplasm and nucleus. Initially, caspases are synthesized in the cell as inactive precursors, or pro-caspases. In presence of the appropriated stimulus, pro-caspases are cleaved and activated by other caspases resulting in a proteolytic cascade. The activation of this process can be initiated by either extracellular (extrinsic pathway) or intracellular (intrinsic pathway) death signal. On the other hand, in addition to the apoptosis mediated by caspases, there is a caspase-independent cell death, that is also triggered by intrinsic factors.

Activation of the intracellular cell death pathway takes place when the cell entry into a new stage of the cell cycle or is damaged or stressed. In the best understood pathway, mitochondria induce the activation of the transcription of genes encoding B-cell lymphoma 2 (Bcl-2) family proteins that promote the release of electron carrier protein cytochrome c from mitochondria into the cytosol. Some members of this family, like Bcl-2 itself and Bcl-X_L, inhibit apoptosis, blocking the release of cytochrome c. On the contrary, other Bcl-2 members, such as Bax (Bcl-2 associated X protein) are pro-apoptotic. These pro-apoptotic proteins tend to oligomerize constituting mitochondrial channels that lead to MOMP, and the consequent release of cytochrome c from the mitochondrial intermembrane space to the cytosol (Loureiro, Mesquita et al. 2013). Since anti-apoptotic proteins such as Bcl-2 interact with their pro-apoptotic counterparts to prevent their olymerization, the balance between pro- and anti-apoptotic proteins is crucial for MOMP. As explained in previous sections, the uncontrolled production of ROS can also affect this balance

enhancing MOMP and initiating apoptosis through cytochrome c release into the cytoplasm.

On the other hand, Bax and other pro-apoptotic proteins responsible for MOMP can also regulate the mitochondrial permeability transition pore (mPTP) (Loureiro, Mesquita et al. 2013). The mPTP is a multiprotein complex formed in the contact sites between MIM and MOM, and allows the no selective passage of molecules less than 1500 Da between the cytoplasm to the mitochondrial matrix (Taddeo, Laker et al. 2014). The mPTP includes VDAC, also called porin, in the MOM; the adenine nucleotide translocase (ANT), in the MIM; and cyclophilin-D which has a peptidyl-proplyl isomerase activity, crucial for protein folding (Andreeva, Heads et al. 1999)., and it is located in the mitochondrial matrix (Crompton 2000).

Under physiological conditions, the mPTP components are dispersed, and under the appropriated stimulus, they are assembled forming a pore of 1.0 to 1.3 nm radius. mPTP opening is usually triggered by ROS, mitochondrial Ca^{2+} overload and Bcl2 family proteins (Crompton 2000). The effects of mPTP opening include the dissipation of protein concentration gradient between the mitochondrial matrix and the cytoplasm, the decrease of the electrochemical gradient and thereby lowering ATP production; and the mitochondrial swelling which produce the physical rupture of the MOM, and the release of molecules, including the apoptosis inductor cytochrome c, from the mitochondrion to the cytosol.

Apotosis and obesity

The typical accumulation of fatty acids in the liver of obese individuals, makes this organ more vulnerable to infections, mitochondrial dysfunction and oxidative damage, releasing pro-fibrogenic and pro-inflammatory mediators. All these factors can collectively stimulate inflammation, apoptosis and fibrosis, contributing to the progression of hepatic diseases to cirrhosis (Jung and Choi 2014).

In addition, apoptosis and obesity are also related through the absence of Fas (transmembrane receptors involved in extrinsic pathway) apoptosis inhibitory molecule, that has been implicated in the development of spontaneous obesity and hepatosteatosis (Huo, Ma et al. 2016).

MELATONIN

Melatonin (N-acetyl-5-methoxy tryptamine) is an ancient molecule, ubiquitously presented in nature, that has been identified in most living organism, including bacteria, algae, fungi, animals and plants (Tan, Manchester et al. 2011; Cipolla-Neto, Amaral et al. 2014) (Fig. 13). Melatonin in mammals is synthesized and secreted primarily by the pineal gland under a circadian rhythm in response to darkness. Melatonin plays a key role in the regulation of sleep and circadian rhythms. In addition, it plays a well-known role as a direct free radical scavenger and an indirect antioxidant, stimulating a set of antioxidant enzymes (Reiter, Tan et al. 2003). In

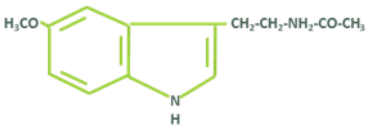

Figure 13. Chemical structure of melatonin (N-acetyl-5-Hydroxytryptamine).

addition to pineal melatonin, there is a non-pineal synthesis in several cells, tissues and organs with autocrine and paracrine actions that are probably related with its properties to protect against oxidative stress (Zephy and Ahmad 2014). This extrapineal melatonin makes little contribution to the circadian rhythm of melatonin in the blood (Tan, Manchester et al. 2011).

Besides, melatonin is also implicated in many other physiological functions with effects almost on all tissues and organs (Rivara, Pala et al. 2015), such as tumour growth inhibition, immune defense, thermoregulation and reproductive activity in seasonally reproductive animals (Carrillo-Vico, Guerrero et al. 2005; Witt-Enderby, Radio et al. 2006; Reiter, Tan et al. 2010).

Melatonin effectiveness lies in its highly lipophilicity and weakly hydrophobicity, which allows it to cross cell membranes easily. Then, it can be distributed throughout the body at cellular and subcellular levels (Coto-Montes, Boga et al. 2012). Melatonin can exercise their functions by binding to specific receptors or in a receptor-independent manner probably through its free radical scavenging actions (Reiter, Tan et al. 2003). In mammals, there are several two kind of melatonin receptors: the membrane receptors MT1 and MT2, and nuclear orphan receptors, from the retinoic acid receptor (RZR) superfamily, such ROR (Hardeland 2009).

Melatonin synthesis occurs from the essential amino acid L-tryptophan (Ramis, Esteban et al. 2015). Melatonin synthesis involved four enzymes: tryptophan-5-hydroxylase, 5-hydroxytryptophan decarboxylase, serotonin N-acetyltransferase and hydroxyindole-O-methyltransferase (also known as acetylserotonin methyltransferase) (Fig. 14) (Ramis, Esteban et al. 2015).

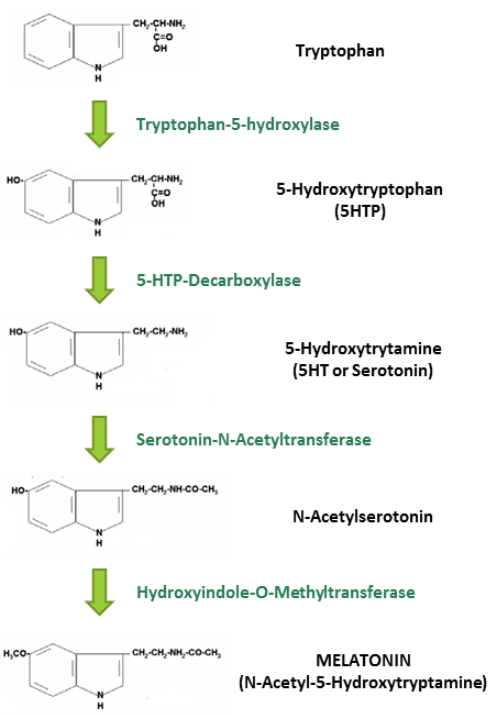

Figure 14. Melatonin synthesis.

Naturally, the secretion of melatonin in vertebrates exhibits a circadian pattern (Fig. 15), showing its maximum serum levels at night and lowest levels during the day, regardless of whether the animal is nocturnal or diurnal (Tan, Manchester et al. 2011). Environmental light regulates the synthesis of pineal melatonin. The light stimulus is taken through photoreceptor retinal ganglion cells, and it is transported through the optic nerve to the suprachiasmatic nucleus (SCN) of the hypothalamus, which has adrenergic neuronal endings that reach the pineal gland, where melatonin biosynthesis

Figure 15. Circadian secretion of melatonin. Figure adapted from (Gerstner and Yin 2010).

and release is regulated (Fig. 16). Melatonin synthesis occurs exclusively during darkness, because light exposure shut down its production (Tan, Manchester et al. 2011; Cipolla-Neto, Amaral et al. 2014). Furthermore, the duration of the nocturnal secretion peak is proportional to night-time duration (Cipolla-Neto, Amaral et al. 2014). Thus, there is a longer secretion peak in short photoperiodic season than in long photoperiods so, in winter there are greater melatonin levels than in summer (Tan, Manchester et al. 2011). It has been reported that short-day photoperiod exposure is an important signal to weight gain and adipose storage. In wild

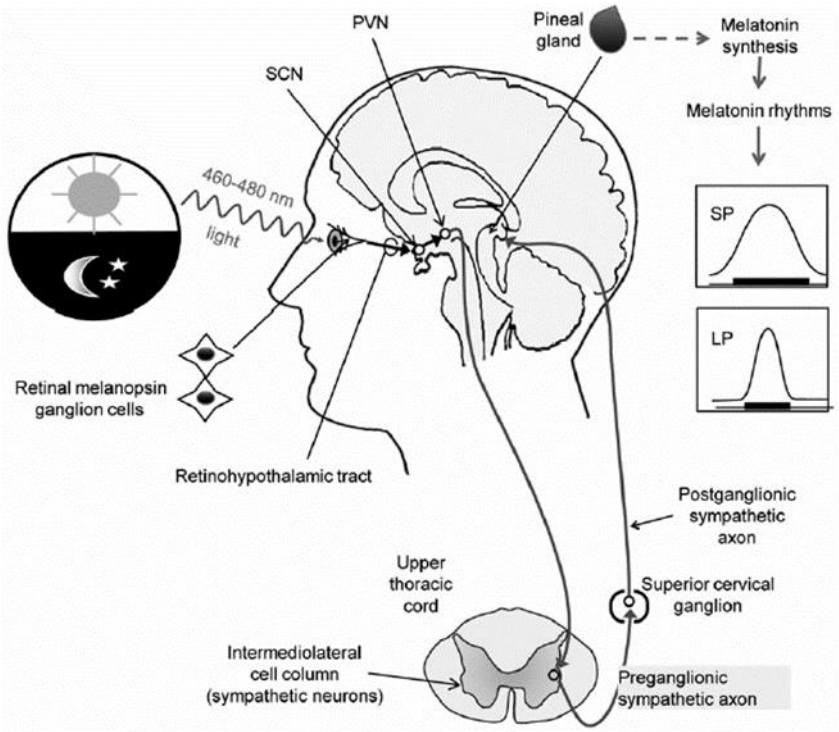

Figure 16. Diagram of the relation between light capture by the retina and regulation of the production of melatonin by the pineal gland. LP- long photoperiod, PVN- paraventricular nucleus, SCN- suprachiasmatic nucleus, SP- short photoperiod. This figure was taken from (Tan, Manchester et al. 2011).

animals, weight gain during the winter is a survival mechanism against possible food shortage during this season (Tan, Manchester et al. 2011). Therefore, it is assumed that melatonin is the molecule that transduces the environmental photoperiod into appropriate endocrine signals (Banerjee, Udin et al. 2011; Tan, Manchester et al. 2011), playing an important role in synchronizing physiology and behavior with the environmental conditions.In addition to the sedentary lifestyle of modern society, other typical characteristics of modern countries such as sleep deprivation and the use of artificial light, TV, and monitors, alter melatonin secretion pattern and circadian rhythms (Szewczyk-Golec, Wozniak et al. 2015). Numerous experimental observations indicate that melatonin has an association with an improved body-weight maintenance and adiposity and other characteristics of obesity through the stimulation of non-shivering thermogenesis or stimulating the recruitment of brown adipose tissue in small mammals (Tan, Manchester et al. 2011), whereas melatonin deficiency has been linked to the development of obesity (Reiter, Tan et al. 2012; Cipolla-Neto, Amaral et al. 2014; Kim, Jeong et al. 2015).

The fact that both melatonin and leptin follow a circadian rhythm of secretion with maximum values at night, and play a key role in the regulation of body weight and adiposity, suggests that one can influence the expression and action of the other. The literature includes examples in which melatonin can both increase (Alonso-Vale, Andreotti et al. 2005) and decrease leptin secretion (Kus, Sarsilmaz et al. 2004). Besides, other works also reported the ability of melatonin in enhancing leptin signaling synergistically with insulin in different animal models (Alonso-Vale, Andreotti et al. 2005; Banerjee, Udin et al. 2011).

The aim of this thesis was the study of the most important alterations usually described during obesity such as insulin resistance, mitochondrial dysfunction, systemic inflammation, increased oxidative stress and dysregulation of cellular quality control systems on the liver of leptin-deficient mice (ob/ob). In addition, we sought to evaluate the effects of the treatment with melatonin on these ob/ob mice.

OBJETIVES

OBJETIVES

Alterations in daily patterns of leptin, food intake and cell metabolism are key players during the pathogenesis of obesity. Therefore, the main aims of this thesis were the identification of the most important metabolic alterations produced as a result of a leptin deficiency in the liver of obese mice and the evaluation of the effects of melatonin administration in these key alterations. To pursue these aims, we used leptin-deficient ob/ob mice and wildtype counterparts. Thus, we hypothesised that leptin deficiency-induced obesity is accompanied by cellular alterations in mitochondria, inflammation and cellular quality control systems that may be partially reverted by reinforcing the nocturnal melatonin peak.

For this purpose, the following experimental objectives were pursued along this work:

1. Study glucose and lipid metabolism and in the liver of leptin-deficient (ob/ob) mice.
2. Study the mitochondrial function/dysfunction associated with leptin deficiency in the liver of ob/ob mice.
3. Study of the redox metabolism and the inflammatory response in the liver of leptin-deficient (ob/ob) mice.
4. Evaluate the cellular quality control systems in the liver of ob/ob mice.
5. Determine the effect of melatonin administration on the studied alterations.

MATERIAL AND METHODS

ANIMALS AND TREATMENTS

Study 1

Eight six-week-old male leptin-deficient obese B6.V-Lepob/J (ob/ob) mice were purchased from Charles River Laboratory (Charles River Laboratories Spain, SA, Barcelona, Spain). The mice were housed two per cage under 12:12 h dark-light cycle at 22 ± 2 ºC. The animals received tap water and a standard chow diet *ad libitum*. All the animals were weighed at the beginning (baseline) and the end of the experiment.

After a two-week acclimatization period, a randomized group of four ob/ob mice were treated with melatonin for two weeks, and the remaining four ob/ob mice were maintained as a control group for same period. At 2 h after lights off, intraperitoneal injections of melatonin were administered daily at a dose of 500 µg/kg body weight (M5250, Sigma Aldrich, St Louis, MO, USA). Melatonin was dissolved in 0.5 % ethanol/ saline. The animals in the control group received vehicle at an equal dosage, route and treatment duration. Fresh melatonin and vehicle solutions were prepared twice a week, and the melatonin dose was adjusted to the body weight throughout the study.

Study 2

Thirty-two six-week-old male leptin-deficient obese B6.V-Lepob/J (ob/ob) mice and thirty-two six-week-old male wild-type C57BL/6J were purchased from Charles River Laboratory (Charles River Laboratories Spain, SA, Barcelona, Spain).

The mice were housed two per cage under 12:12 h dark-light cycle at 22 ± 2 ºC, and received tap water and a standard chow diet *ad libitum*.

All the animals were weighed at the beginning (baseline) and the end of the experiment of the experiment.

After a two-week acclimatisation period, the animals were randomly divided into four groups: untreated wild-type mice (WC), untreated ob/ob mice (ObC), melatonin-treated wild-type mice (WM) and melatonin-treated ob/ob mice (ObM). At 2h after lights off, intraperitoneal injections of melatonin (M5250, Sigma Aldrich) were administered daily at a dose of 500 µg/ kg body weight for 4 weeks. Melatonin was dissolved in 0.5 % ethanol/saline. The animals in the control groups received vehicle at a comparable dosage, route and treatment duration. Fresh melatonin and vehicle solutions were prepared twice a week, and the melatonin dose was adjusted to the body weight throughout the study.

The experiment protocol in both cases was approved by the Oviedo University Animal Care and Use Committee. All experiments were performed according to the Spanish Government Guide and the European Community Guide for Animal Care (Council Directive 86/609/EEC).

In both studies, animals were sacrificed by decapitation, and the liver of each mouse was immediately removed and frozen at -80°C until further use. If not indicated otherwise, the liver (50 mg) were homogenised using a Polytron homogeniser at 4°C in 1 mL of lysis buffer (50 mM sodium phosphate buffer, pH 7.5, 1 mM NaF, 1 mM Na_3VO_4, 1mM PMSF and 0.1 % Triton-X 100). The tissue homogenates were then subsequently centrifuged at 3000 rpm for 6 min at 4°C, and the supernatants were collected and stored at -80°C until use.

The Bradford method was used to quantify the protein amount in liver supernatants, using bovine serum albumin (BSA) as standard protein. (Bradford 1976).

LIGHT MICROSCOPY

For morphological analysis, liver pieces were fixed, sectioned, stained and observed by using a Nikon Eclipse E200 microscopy.(Nikon Instruments, Tokyo, Japan).

Fixation, embedding, and sectioning A piece of liver from two mice from each experimental condition was divided into pieces of 4 mm thick, and immersed in a fixing solution of 4% formaldehyde (20910.294, MERCK, Darmstadt, Germany) for until inclusion. After removing the formaldehyde, the samples were dehydrated through a battery of alcohols (30, 50, 70, 96 and 100%) during 15 min in each alcohol. Then, the pieces were immersed in 100% xylene (28975.291, MERCK) for 5-15 min. After that, the samples were immersed in a mixture of paraffin (107158, MERCK) and xylene (1:1) for 30 min and transferred to paraffin for 1 h at 60 °C. The paraffin was removed, freshly paraffin was added for 1 h at 60ºC.Finally, the blocks were made following the usual procedure and stored until sectioning. The paraffin blocks were then cut into 5-7 µm sections with a microtome (Leica RM2155, Leica Instruments GmbH, Nussloch, Germany) and these sections were adhered to slides (Superfrost Plus, Menzel GmbH and Co KG, Braunschweig, Germany).

Staining

The slides were deparaffinised and rehydrated through xylene and battery of ethyl alcohol (100, 96, 70, 50 and 30%) and the brought into tap water. They were stained with the alum hematoxylin (H9627, Sigma Aldrich) during 5-10 min to stain nuclei and rinsed in running tap water. After that, the sections were stained with eosin 0.2-0.5% during 5-10 min, dehydrated, cleared and mounted.

OXIDATIVE DAMAGE DETECTION

Lipid peroxidation assay

The concentration of the end-products of lipid peroxidation was measured by determining MDA and 4-HNE content. For this purpose, we used a chromogenic reagent (N-methyl-2phenylindole) which reacts with MDA and 4-HNE forming a stable chromophore at 45°C with an absorbance maximum of 586 nm.

First, a 1,1,3,3,-tetramethoxypropane (108383, Sigma Aldrich) standard curve was prepared in the concentration range of 0-20 µM by diluting it with homogenization buffer. Both standard and problem tubes (Glass tubes, TU05-130-250, labbox) got 1-methyl-2-phenylindole n acetonitrile (1:3) 10.3 mM (404888, Sigma Aldrich) and methanesulfonic acid (806022, MERCK) was added in all tubes (both the standard curve as the problem ones). Then, all tubes were covered with parafilm, shaken and after an incubation of 40 min at 45°C, the tubes were kept on ice 15 min and centrifuged at 10000 g 5 min at 4°C. Supernatant were added to the 96 wells plate (BioTek Power Wave XS, Vermont, USA) and read at 586 nm. The results were expressed as nmol MDA+4-HNE/ g protein.

Protein carbonylation assay

The protein carbonyl concentrations, as a measure of protein oxidative damage (PD), were determined according to the method described by Levine (Levine, Garland et al. 1990), with modifications from Coto-Montes and Hardeland (Coto-Montes and Hardeland 1999).

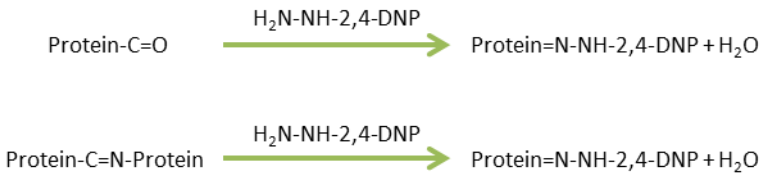

Figure 17. Protein carbonylation scheme.

Samples were incubated with 2,4-dinitrophenylhydrazine (2,4-DNP) 10 mM (D2630, Sigma Aldrich) diluted in HCl 2M (20252290, MERCK) to mark carbonyl protein, and samples incubated in HCl were used as blank. After 1h of incubation, trichloroacetic acid (TCA) 20% (T4885, Sigma Aldrich) was added into each tube to precipitate proteins. Tubes were centrifuged at 11000 g for 3 min and the precipitate was washed three times with ethanol (VWR, 20821.310) in ethyl acetate (31990-2, Sigma Aldrich) (1:1) under stirring. The supernatant of the last wash was discarded and guanidine 6M (G7028, Sigma Aldrich) diluted in phosphate buffer 10mM (pH 2.3) were added to denature and resuspend precipitated proteins during a 15 min incubation at 37°C. Samples were read at 366 nm in a 96 wells plate and read. The data were presented as nmol carbonyl protein/ mg protein.

ANTIOXIDANT ACTIVITY

Superoxide dismutase activity

SOD (EC 1.15.1.1), which catalyses the dismutation of $O_2^{\bullet-}$ to H_2O_2, was measured according to the previously described method of Martin and colleagues (Martin, Dailey et al. 1987). SOD inhibits haematoxylin auto-oxidation to the coloured compound called hematein (Fig. 18).

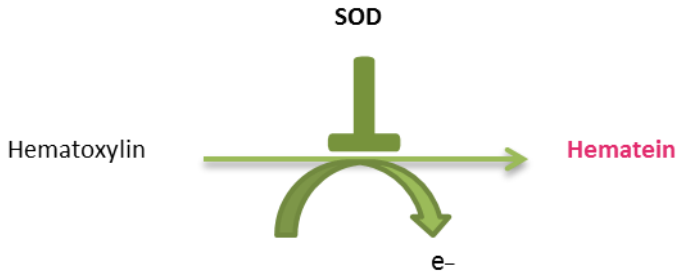

Figure 18. Inhibition of autoxidation of hematoxylin to the color compound hematein by superoxide dismutase (SOD).

After oxygenate a potassium phosphate buffer 50 mM pH 7.5 + EDTA 0.1 mM (ED2P, Sigma Aldrich) for 30 min at 4°C and 30 min at room temperature, was added to the sample in a 96 wells plate. Then hematoxylin 5mM diluted in 50 mM de KH_2PO_4 were added to all wells, and the plate was read at 560 nm for 10 min at 25°C. The results were expressed as SOD units/ mg protein.

Catalase activity

CAT (EC 1.11.1.6) activity was assayed according to the previously described methods of Lubinsky and Bewley, (Lubinsky and Bewley 1979), based on the conversion of hydrogen peroxide (H_2O_2) into O_2 and H_2O, using H_2O_2 as a substrate.

H_2O_2 30% (95294, Sigma Aldrich) diluted in sodium phosphate buffer 50 mM, pH 7 was added to the samples and the conversion of H_2O_2 into O_2 and H_2O was read in all wells of a 96 wells ultraviolet plate at 240 nm for 4 min at 25°C. The data were expressed as CAT units/ mg protein.

Total antioxidant activity

Liver total antioxidant activity (TAA) was determined using the 2,2'-azino-bis(3-ethylbenzothiazoline-6-sulphonic acid (ABTS) /H_2O_2/ Horseradish peroxidase (HRP) method modified (Arnao MB 2001; de Gonzalo-Calvo, Neitzert et al. 2010).

A radical mixture of sodium phosphate buffer 50 mM, ABTS 2mM, HRP 0.25 µM and H_2O_2 40 µM, was kept cold and dark 3-4 h until the absorbance was constant and did not vary. Then was added to the sample and after incubate the plate for 15 min, the absorbance was measured at 730 nm. The difference between the initial and final absorbance was used as an indicator of antioxidant activity. TAA was expressed as Trolox (Tx) equivalents that produce the same antioxidant effect that the study sample (1mol Tx reacts with 2 mol of ABTS radical). Results were expressed in equivalents of mg Tx/ mg protein.

PROTEASOME ACTIVITY

Proteasome activity was assessed in homogenised tissue using a 20S proteasome activity assay kit (APT280, Chemicon, CHEMICON International, Inc, Temecula, CA, USA). The assay is based on detection of the fluorophore 7-amino-4-methylcoumarin (AMC) after its cleavage from the labelled substrate LLVY-AMC by the chymotrypsin-like activity of the proteasome. Free AMC was detected by fluorimetric quantification (380/460 nm) using multiplate reader (Synergy HT, BioTek, Vermont, USA). Results were presented as arbitrary fluorescence units/ mg protein.

WESTERN BLOT ANALYSIS

Tissue homogenates (25-200 µg of protein per sample) were mixed with Laemmli sample buffer (1610737, BioRad Laboratories, Inc., USA) to increase sample density and promote the reduction of the intra and inter-molecular disulfide bonds and the denaturation of the proteins with the consequent gain of an overall negative charge, favoring a separation based on protein molecular weight. The samples were then boiled at 100°C for 5 min to complete protein denaturation and loaded in 7%-16% sodium dodecyl sulfate (SDS)-polyacrilamide gels. A molecular weight size marker (Precision Plus Protein All Blue Standards, BioRad) was also run in the outer lanes of all gels. The SDS-polyacrilamide gels fitted in a Mini-PROTEAN 3 System (Bio-Rad) filled with running buffer (25mM Tris, 192mM glycine, 0.1% SDS) and connected to a PowerPac Basic Power Supply (Bio-Rad) at 120V. Protein electrophoretic separation was performed at room temperature. After that, the SDS-polyacrilamide gel was transferred to a Polyvinylidene difluoride membrane (PVDF Immobilon TM-P; Millipore Corp., Bedford, MA, USA) which was previously activated in methanol and equilibrated in transfer buffer (25mM Tris,

190mM glycine and 20% methanol), using a cooled Mini Trans-Blot Cell System (BioRad) filled with transfer buffer and run at 100 mA during 180 minutes.

Once protein transfer was completed, the membrane was identified and incubated with Ponceau S solution (0.1% Ponceau S (w/v) in 5% acetic acid) for 5 minutes. Afterwards, membranes were washed 3 times with Tris-buffered saline Tween-20 (TBS-T; 154 mM NaCl, 50 mM Tris-HCl pH 8.0 and 0.1% Tween-20) for 5 minutes and incubated with blocking solution, 5-10% non-fat dry milk (Bio-Rad) in TBS-T overnight at 4°C under continuous stirring (Stuart SRT6 tube roller, VWR, Leuven, Belgium), to block non-specific binding.

In the next day, the membrane was washed three times with TBS-T, 10 min each, and then incubated with the primary antibody (Table 1) previously diluted in TBS buffer containing 1% (w/v) skim milk, overnight at 4ºC under continuous stirring. After three 5 min washes in TBS-T, the membranes where incubated with the corresponding HRP-conjugated secondary antibody diluted in TBS buffer for 2 h at room temperature, followed by three 10 min washes in TBS-T.

The membrane was developed using a chemiluminescent HRP substrate (WBKLS0500, Millipore Corporation, Billerica, USA) according to the manufacturer's protocol. Chemiluminiscence data was collected using a G:BOX Syngene (All data presented are representative from at least three separate experiments. The levels of proteins were semiquantitatively analyzed by using Image Studio Lite 3.1 software. The densitometry results were normalized to β-actin as a loading control and showed as percentage of wild-type control animals.

Table 1. Antibodies used

Antibody	Reference	Manufacture
Adiponectin (C45B10)	2789	Cell Signaling
Akt	9272	Cell Signaling
AMPK (F6)	2793	Cell Signaling
Anti-Goat IgG	A5420	Sigma-Aldrich
Anti-Mouse IgG	7076	Cell Signaling
Anti-Rabbit IgG	7074	Cell Signaling
ATF6α (H-280)	sc-22799	Santa Cruz Biotechnology
Bax	2772	Cell Signaling
Bcl-2 (C-2)	sc-7382	Santa Cruz Biotechnology
Beclin-1	3738	Cell Signaling
CHOP (L63F7)	2895	Cell Signaling
CI-20 (NDUFB8)	ab110242	Abcam
CII-30 (SDHB)	ab14714	Abcam
CIII-Core 2 (UQCRC2)	ab14745	Abcam
CIV-I (MTCO1)	ab14705	Abcam
CV-a (ATP5A)	ab14748	Abcam

Cyclophilin D	ab110324 (MSA04)	Abcam
Drp1 (D6C7)	9482S	Cell Signaling
eIF2α (D7D3)	5324	Cell Signaling
Ire1α (14C10)	3294	Cell Signaling
LAL	ab36597	Abcam
LAMP2A	Ab18528)	Abcam
LC3	PD014	Medical & Biological Laboratories
Mfn2 (D2D10)	8570S	Cell Signaling
NF-κB p65	4764	Cell Signaling
Nrf2 (C-20)	sc-722	Santa Cruz Biotechnology
p62	H00008878-M01	Abnova
Perilipin (H-300)	sc-67164	Santa Cruz Biotechnology
phospho-Akt (Ser473)	9271	Cell Signaling
phospho-AMPKα (Thr172)	2535S	Cell Signaling
phospho-NF-κB p65 (Ser536)	3033	Cell Signaling
phospho-eIF2α (Ser51)	3398	Cell Signaling
phospho-mTOR (Ser2448)	5536	Cell Signaling

PI3K	4255	Cell Signaling
Porin	ab14734 (MSA03)	Abcam
PPARγ	sc-7273	Santa Cruz Biotechnology
Sirt1 (H-300)	sc-15404	Santa Cruz Biotechnology
β-actin	AC-15	Sigma-Aldrich

PROTEIN IDENTIFICATION BY PEPTIDE MASS FINGERPRINT

Hepatic protein homogenates (25 µg) were mixed with Laemmli sample buffer (1610737, BioRad Laboratories, Inc., USA) and boiled at 100°C for 5 min to complete protein denaturation. Both samples and pre-stained molecular weight standards (Precision Plus Protein All Blue Standards, BioRad) were loaded to 1 mm SDS- polyacrilamide gel (resolving gel contained 11% and the stacking gel 4% of 30% (w/v) acrylamide:bisacrylamide). Gels were run at 120V and stained in a mixture of 30% (v/v) methanol, 10% (v/v) acetic acid and 0.01% (w/v) Coomassie Brilliant Blue R-250 and destained using a mixture of 40% (v/v) methanol and 10% (v/v) acetic acid. Stained gel images were captured using a GS-800 Imaging Densitometer (Bio-Rad) and semiquantitatively analyzed using Image Studio Lite 3.1 software.

The processing of the bands of interest was conducted following the protocol described by Oliván and colleagues (Oliván, Fernández-Suárez et al. 2016). Bands of interest was sent for identification to the proteomics laboratory of Inbiotec S.L. (León, Spain), where the proteins were digested following the method of Havlis and colleagues (Havlis, Thomas et al.

2003)[18] and processed for further analysis as indicated by Jami and colleagues (Jami, Barreiro et al. 2010). The samples were analyzed with a 4800 Proteomics Analyzer matrix-assisted laser desorption/ionization-time of flight (MALDI-TOF/TOF) mass spectrometer (ABSciex, MA, USA). A 4700 proteomics analyzer calibration mixture (Cal Mix 5, ABSciex) was used as external calibration. All mass spectrometry (MS) spectra were internally calibrated using peptides from the trypsin digestion. The analysis by MALDI-TOF/TOF mass spectrometry produced peptide mass fingerprints, and the peptides observed (up to 65 peptides per spot) were collected and represented as a list of monoisotopic molecular weights with a signal to noise (S/N) ratio greater than 20 using the 4000 Series Explorer v3.5.3 software (ABSciex). All known contaminant ions (trypsin- and keratin- derived peptides) were excluded for later MS/MS analysis. Hence, from each MS spectra, the 10 most intensive precursors with S/N greater than 20 were selected for MS/MS analyses with CID in 2-kV ion reflector mode and precursor mass windows of ±7 Da. The default calibration was optimized for the MS/MS spectra.

For protein identification, mascot generic files combining MS and MS/MS spectra were automatically created and used to interrogate a non-redundant protein database using a local license of Mascot v 2.2 from Matrix Science through the Global Protein Server v 3.6 (ABSciex). The search parameters for peptide mass fingerprints and tandem MS spectra obtained were set as follows: i) NCBInr (2012.06.26) sequence databases were used; ii) taxonomy: All entries (18713758 sequences, 6412106995 residues); iii) fixed and variable modifications were considered (Cys as S carbamidomethyl derivative and Met as oxidized methionine); iv) one missed cleavage site was allowed; v) precursor tolerance was 100 parts

per million and MS/MS fragment tolerance was 0.3 Da; vi) peptide charge: 1+; and vii) the algorithm was set to use trypsin as the enzyme.

Protein candidates produced by this combined peptide mass fingerprinting/tandem MS search were considered valid when the global Mascot score was greater than 85 with a significance level of $p< 0.050$.

REAL-TIME RT-PCR

Total RNA was extracted using the TRI reagent (Sigma Aldrich, St Louis, MO, USA), and cDNA was synthesized using a High Capacity cDNA Reverse Transcription Kit (Invitrogen, Life Technologies) according to the manufacturer's protocols. Gene expression was analyzed by a real-time PCR assay using the StepOne Real Time PCR System (Life Technologies, Calsbad, CA, USA) following Applied Biosystem's SYBR Green Master Mix protocol (Invitrogen, Life Thechnologies, Carlsbad, CA, USA). The relative messenger RNA (mRNA) expression was calculated using the $2^{-\Delta\Delta CT}$ method, and the data for each gene in the liver were expressed as the fold change normalized to GAPDH mRNA levels and relatively to the samples from untreated wild-type mice (WC). Single PCR products of the correct size were observed in all cases. Primer sequences are described in Table 2.

Table 2. Gene Mouse Primers

Beclin-1	Forward	GATGGAAGGGTCTAAGACGTCCAA
	Reverse	TTTCGCCTGGGCTGTGGTAAG
p62	Forward	AACTCATGGCCGAGAAGGACTC
	Reverse	TTTGATTGTATTTCCTTGTGGTCCA
LC3B	Forward	GACCTTCAAGCAGCGCCG
	Reverse	TAGCATTGAGCTGCAAGCGC
LAMP2a	Forward	GAAGTTCTTATATGTGCAACAAAGAGCAG
	Reverse	CTAAAATTGCTCATATCCAGCATGATG
PPARα	Forward	TGAAGAACTTCAACATGAACAAG
	Reverse	TTGGCCACCAGCGTCTTC
PPARγ	Forward	ACTATGGAGTTCATGCTTGTGAAGGA
	Reverse	TTCAGCTGGTCGATATCACTGGAG
AdipoR1	Forward	CCCACCATGCCATGGAGA
	Reverse	GCCATGTAGCAGGTAGTCGTTGT
AdipoR2	Forward	CAGGAAGATGAGGGCTTTATGG
	Reverse	GAGGAAGTCATTATCCTTGAGCCA
Insulin receptor	Forward	TGAACGCCAAGAAGTTTGTG
	Reverse	CAGCCAGGCTAGTGATTTCC

TFAM	Forward	ACCTCGTTCAGCATATAACGTTTATGTA
	Reverse	GCTCTTCCCAAGACTTCATTTCAT
GAPDH	Forward	CAATGACCCCTTCATTGACC
	Reverse	TGGAAGATGGTGATGGGATT

ENZYME-LINKED IMMUNOSORBENT ASSAY (ELISA)

Liver levels of TNF-α and IL-6 were determined using commercially available enzyme-linked immunosorbent assay kits (Invitrogen, Life Thechnologies). All assays were performed as outlined in the protocols enclosed in each kit.

Standards and sample were added to TNF-α or IL-6 coated onto a 96 wells plate. In a first incubation, the corresponding antibody antigen binds simultaneously to the immobilized antibody on one site, and to the solution phase biotinylated antibody on a second site. After removal of excess second antibody, Streptavidin-Peroxidase is added and incubated, to bind to the biotinylated antibody to complete the four-member sandwich. After this second incubation, the pate is washed to remove the unbound enzyme. Then, a substrate solution is added, and acted upon by the bound enzyme to produce color, whose intensity is directly proportional to the concentration of interleukin present in the original sample. Results were expressed as pg/mg protein.

MITOCHONDRIAL FUNCTION

Isolation of mitochondria

Mitochondria isolation was performed following the protocol of Oliveira and Silva (Silva and Oliveira 2012) with modifications made in our research group (Fig. 19).

Mouse abdominal cavity was opened with a scissor and the liver was removed, placed in a liver isolation buffer (LIB, 250mM sucrose, 10 mM HEPES 0.5 mM EGTA and 1mg/ mL BSA (fatty acid free), pH 7.4. and cut slowly in little pieces with a scissor. After wash the liver pieces with LIB to remove all blood, they were tightly manually homogenized in a glass Teflon Potter-Elvehjem homogenizer with 7mL LIB/g liver, being careful to maintain temperature under 4°C. The tubes with the homogenate were centrifuged and the floating fat was carefully aspirated and removed. Supernatant was poured to new refrigerated centrifuge tubes, filled up with LIB and centrifuged at 12000 × g during 10 min. Supernatant was discharged, the tubes were filled up with LRB and the pellet was gently homogenized with a smooth paintbrush. Finally, supernatant was discharged and isolated mitochondria were resuspended in 300 µL of LRB.

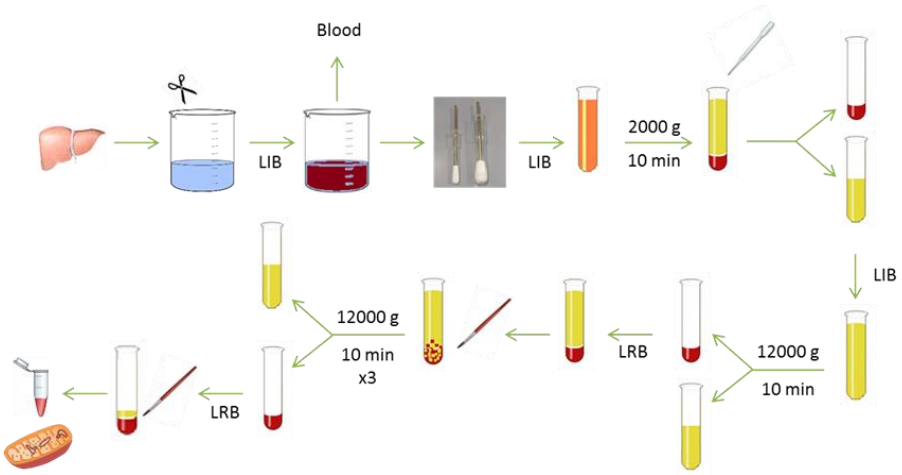

Figure 19. Flowchart for mitochondrial isolation. All the material was kept on ice during the isolation procedure. Liver was cut in little pieces with scissor and washed to remove all the blood. Liver pieces were manually homogenized in a glass Teflon potter, centrifuged, and the supernatant was poured to new tubes. After a second centrifugation, the supernatant was discarded and pellet washed three times with LRB. Finally, the last pellet is resuspended in 300ul of LBR.

Mitochondria were stored on ice until start oxygen respiration assays, and their protein content was determined by Bradford method (Bradford 1976).

Oxygen consumption

Oxygen consumption assays were performed following the protocol of Oliveira and Silva (Silva and Oliveira 2012). Oxygen consumption was measured in a suspension of isolated mitochondria at 37°C and monitored polarographically with a Clark-type oxygen electrode (Oxygraph, Hansatech Instruments Ltd, Pentney, UK) (Fig. 20).

Figure 20. Oxygraph picture.

This electrode consists of a platinum cathode which is maintained at a potential of -0.7 mV relative to an Ag-AgCl reference employee. The electrode is coated with a thin oxygen-permeable membrane of polyethylene.

Protocol:

1. Temperature was properly defined at 30°C.
2. O_2 scale was properly calibrated using distilled water.
3. The desired volume of respiration buffer (135 mM sucrose, 65 mM KCl, 5 mM KH_2PO_4, 5 mM HEPES, and 2.5 mM MgCl2 (pH 7.4)) was introduced (up to 1 mL of buffer).
4. Mitochondrial suspension was added with the desired protein concentration (1mg/mL).
5. Energization was achieved with 10 mM glutamate + 5 mM malate followed by 175 nmol ADP, or with 5mM succinate in presence of 1 µM rotenone followed by 125 nmol ADP.
6. Having consumed all ADP nmol, 1 µl oligomycin was added to determine oxygen consumption with inhibited ATP synthase.
7. Finally the maximum capacity of mitochondrial respiration was determined after adding the decoupling of the electron transport chain Carbonyl cyanide-4-(trifluoromethoxy) phenylhydrazone (FCCP) 1µM.

   The oxidation rates were expressed in nanoatoms of oxygen consumed per minute per milligram of protein (natom oxygen/min*mg protein).

By the measuring mitochondrial oxygen consumption assays, we get the following respiratory parameters:

- Sate 3 that reflects the maximal ATP synthesis or maximum O_2 consumption rate (respiration) in the presence of ADP.
- State 4, or respiration in the absence of ADP or without ATP synthesis due to leakage or entry passive proton from the cytosol into the mitochondrial matrix.
- RCR, which represents the ration between sate 3 and 4 and determine the coupling between substrate oxidation and phosphorylation (Silva and Oliveira 2012).
- ADP/O that determines the oxidative phosphorylation efficiency, and is expressed as the ratio between the amount of ADP added (in nmol) and the oxygen (in natom) consumed during state 3 (Silva and Oliveira 2012).

ATP levels

The determination of the ATP levels was performed by a bioluminescence assay. A commercial available ATP bioluminescent kit (FLAA, Sigma Aldrich) was used to quantify ATP content in isolated mitochondria, cytosolic and ATP produced after oxygen consumption assays energized with glutamate/malate or succinate. This assay is based on the reaction of ATP with recombinant firefly luciferase and its substrate luciferin. The ATP production was determined by following the light emission from two reactions:

1) ATP reacts with luciferin to form adenyl-luciferin and inorganic pyrophosphate.

2) Adenyl-luciferin combines with oxygen to form oxyluciferin, which emits light that can be quantified using a chemiluminometer. The light emitted is directly proportional tothe concentration of ATP.

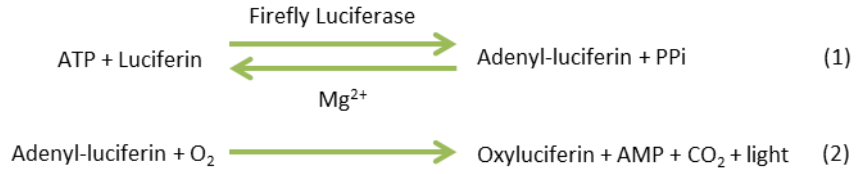

Figure 21. Action mechanism of the luciferase kit. In the first reaction firefly luciferase causes ATP reaction with luciferin to give adenyl-luciferin and inorganic phosphate, and in the second reaction, this new compound in contact with oxygen, the light emitted is proportional to the ATP present in the sample.

Measurements were conducted according to the manufacturer's instructions with modifications adapted to the conditions of our samples. A standard curve was made in the range of 0.074 nM to 6 nM, and standard or sample previously diluted 1:100 were added in a white 96 well plate (353296, Falcon). After dissolve the ATP assay mix it was swirled and incubated at room temperature for 3 min. Then it was added to each well and the luminescence was measured against the standard curve using multiplate reader (Synergy HT, BioTek, Vermont, USA). The concentrations of ATP were expressed as nmol ATP/ mg protein.

STATISTICAL ANALYSIS

The statistical software package GraphPad Prism 6 for Windows (GraphPad Software, Inc. La Jolla, CA, USA) was used for all statistical analyses. The data are presented as means ± standard deviation of the mean (SD). The normality of the data was analysed using the Kolmogorov-Smirnov test. The effect of melatonin and the

phenotype was analysed by using a two-way ANOVA, and differences between groups were analysed with the Bonferroni post hoc test. The differences were considered statistically significant when $p<0.050$.

RESULTS

EFFECT OF 2-WEEKS MELATONIN TREATMENT ON OB/OB MICE

Oxidative stress status

To compare the effect of 2-week melatonin treatment in the oxidative state of liver from ob/ob mice, we studied the concentrations of protein carbonyl and lipid peroxidation products as an index of oxidative

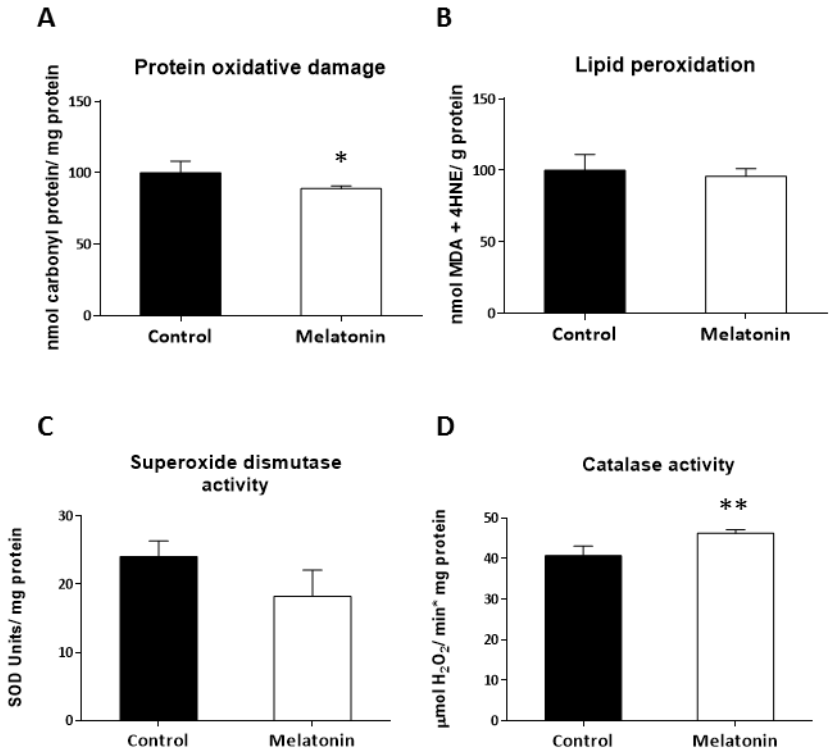

Figure 22. Effect of treatment with melatonin in oxidative situation. (A) Protein damage expressed as nmol carbonyl protein/ mg protein, (B) lipid peroxidation presented as nmol MDA+4-HNE/ g protein, (C and D) superoxide dismutase (SOD) activity was expressed as SOD Units / mg protein and catalase activity µmol H_2O_2/ min* mg protein. The data are expressed as the means ± SD, calculated from at least three separate measurements performed in triplicate. *p<0.050; **p<0.010.

damage, and the activities of the antioxidant enzymes SOD and CAT. Thus, we observed that, although LPO values were similar in both groups (Fig. 22B), melatonin caused a significant decrease in damaged proteins compared with the control group ($p<0.050$) (Fig. 22A). Besides, CAT activity levels were significantly higher in the liver of melatonin-treated mice than in the control group ($p<0.010$) (Fig. 22D). However, although SOD activity was reduced in the liver of melatonin-supplemented animals, this effect was not statistically significant (Fig. 22C). So, just 2 weeks of daily melatonin (500 μg/ kg body weight) administration reduced oxidative stress and damage in the liver of leptin-deficient mice.

Autophagy

The analysis of LAMP2A immunoblotting as a marker of CMA showed non-significant differences between both experimental groups (Fig. 23A).

To characterize macroautophagy in the liver of ob/ob mice, we performed western blot analysis using antibodies against Beclin-1, LC3 and p62. The immunoblot analysis of Beclin-1, which plays an essential role promoting autophagy, showed a significant decrease in the melatonin-treated group compared with the control ($p<0.010$) (Fig. 23B), suggesting that melatonin downregulates autophagy in the liver of ob/ob mice.

The immunoblot analysis of LC3 showed two bands corresponding to LC3-I and its lipidated form, LC3-II (18 and 16 kDa, respectively) in the liver of ob/ob mice (Fig. 23C and D). The expression of LC3-II, a marker of autophagosomes, showed no significant differences were observed in LC3-I or LC3-II expression between both experimental groups. However, the LC3-II/LC3-I ratio was increased in melatonin-treated mice ($p<0.010$) (Fig. 23E).

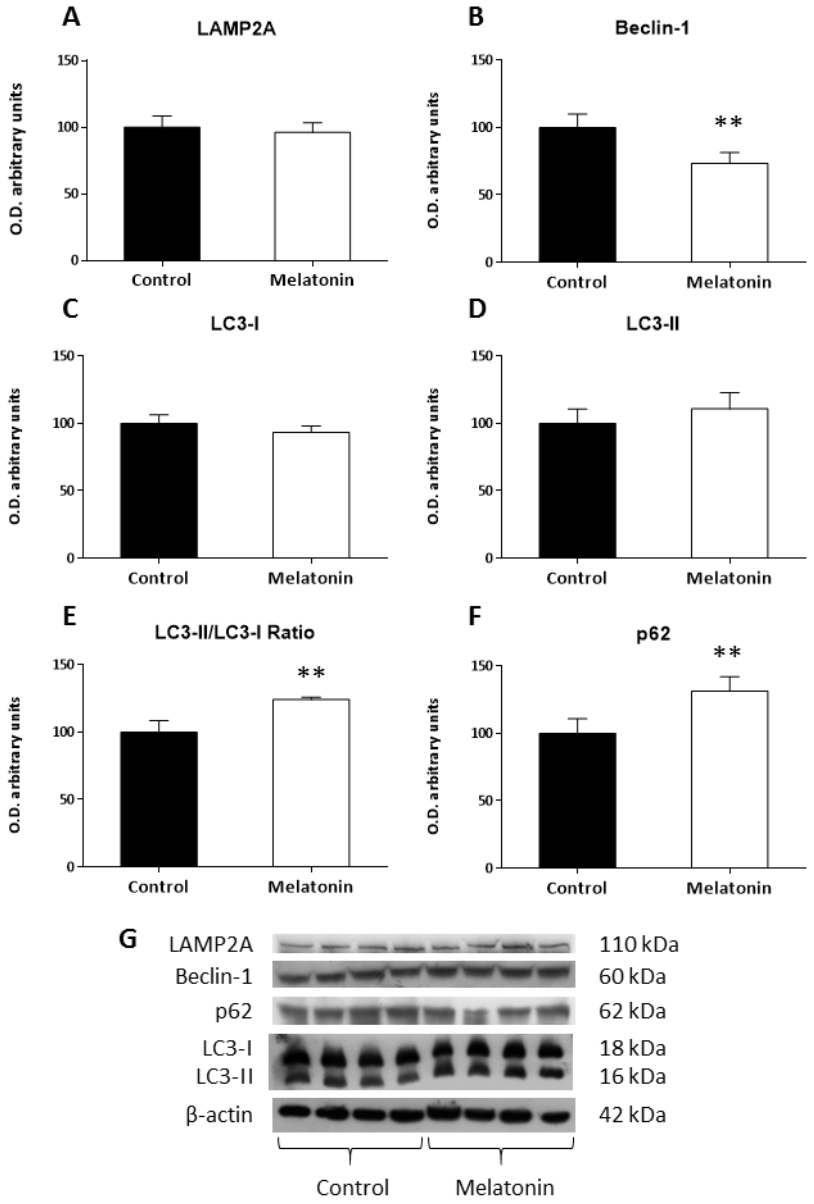

Figure. 23. Autophagy markers in liver from melatonin-treated and untreated ob/ob mice. Bar charts shows the semi-quantitative optical density (arbitrary units of blot bands) of (A) lysosome-associated membrane protein type 2A (LAMP2A); (B) Beclin-1; (C-E) microtubule-associated protein 1 light chain 3 forms (LC3-I and II) and (F) sequestosome-1 or p62 from western blot experiments normalised to β-actin and showed as percentage of controls. The data are expressed as the means ± SD, calculated from at least three separate experiments performed in triplicate. **p<0.010.

Sequestosome 1, or p62, is a selective substrate for autophagy, which interacts with LC3 during autophagosome formation and subsequently is degraded in the lysosome with other selected substrates (Komatsu 2011). Due to this, it is may be used as a marker to study autophagic flux. The immunoblot results showed a significant increase in p62 protein expression in the group treated with melatonin during two weeks indicating a blockade in the autophagic pathway ($p<0.010$) (Fig. 23F).

Taken together, these results indicate that melatonin administration reduced autophagy levels in the liver of ob/ob mice, leading to the accumulation of p62.

Adipogenesis

PPARγ is a member of a nuclear hormone receptor superfamily, predominantly found in adipose tissue but also expressed in liver and muscle tissue (Ros Perez and Medina-Gomez 2011). This protein plays an essential role in adipogenesis and fat storage (Nunn, Bell et al. 2007). Our

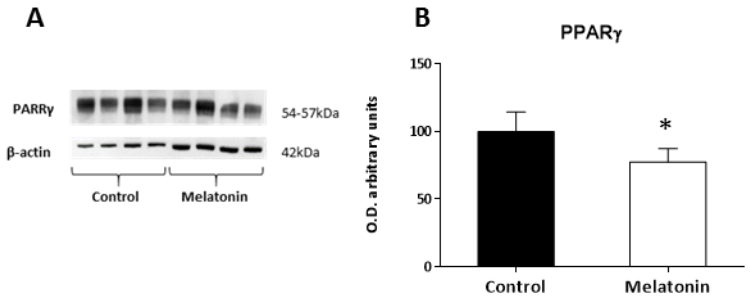

Figure 24. (A) Western blot analysis of peroxisome proliferator-activated receptor gamma (PPARγ) and β-actin as a load control from the liver of ob/ob mice. (B) Bar chart showing the semi-quantitative optical density (arbitrary units of blot bands) normalised with β-actin and relative to the WC sample. The data are expressed as the means ± SD, calculated from at least three separate experiments performed in triplicate. *$p<0.050$.

immunoblot analysis of PPARγ showed a significant decrease in the expression of this protein after melatonin treatment compared with non-treated animals. (*p<0.050) (Fig. 24). Moreover, after only two weeks of exogenous melatonin treatment, the obese mice showed a significant reduction in body weight (p<0.050) (Table 3).

This result along with the decrease in the levels of PPARγ associated with melatonin treatment suggest that the administration of this indolamine improves body weight and adipogenesis in the liver of leptin-deficient mice.

Table 3. Body weight changes of ob/ob mice

	Baseline	Sacrifice	Δweight
Control (n=4)	37.08 ± 2.61	37.95 ± 2.04	0.86 ± 1.17
Melatonin (n=4)	38.40 ± 1.36	35.99 ± 2.57	-2.41 ± 1.54*

Table 3. Effect of melatonin and vehicle treatment on body weight changes from baseline to the end of the study. The data are expressed as the means ± SD. Control Δweight vs. Melatonin Δweight. *p<0.050.

In summary, the data obtained here suggested that two weeks of melatonin treatment reduces oxidative stress and blocks autophagy while reducing adipogenesis and body weight of leptin-deficient obese mice.

EFFECT OF 4-WEEKS MELATONIN TREATMENT ON WILD-TYPE AND OB/OB MICE

Taking into an account the results from the study 1 about the effects of melatonin in reducing adipogenesis and body weight of obese mice, we decided to perform a more ambitious study about the obesity-related alterations (insulin resistance, mitochondrial dysfunction, systemic inflammation, increased oxidative stress and dysregulation of cellular quality control systems like the unfolded protein response and autophagy) using wild-type and leptin-deficient ob/ob mice and treating both types of strains with melatonin but during four weeks to better understand the cellular pathways involved in these actions.

Body and tissue parameters

First we measured daily food intake and physical parameters such as body, liver and white adipose tissue weight, as well as mass gain and body mass index (BMI) in the four experimental groups: untreated and melatonin-treated wild-type mice, and untreated and melatonin-treated ob/ob mice. Thus, we found that obesity induced by a leptin deficiency affected all parameters studied, increasing them significantly compared with wild-type mice ($p<0.050$). Furthermore, melatonin treatment produced no changes in the physical measurements of wild-type mice. However, although 4 weeks-treatment with melatonin did not reduce body weight of ob/ob mice as it was observed during the 2 weeks-treatment, body weight did not change and white adipose tissue weight was reduced despite that food intake was increased ($p<0.010$) (Table 4).

Table 4. Food intake, body, white adipose tissue and liver weights

	WC	WM	ObC		ObM	
Food intake (g/day)	2.72±0.11	2.88±0.28	4.18±0.33	##	5.23±0.75	** ###
Body weight (g) at Baseline	22.40±1.59	23.85±1.87	45.13±4.66	###	43.95±5.49	###
Body weight (g) at Sacrifice	24.19±1.55	24.86±2.08	49.93±5.01	###	46.42±9.67	###
Body weight (g) changes	1.47±0.65	1.01±0.40	4.80±0.95	###	4.85±0.63	###
Liver weight (g) at Sacrifice	1.04±0.16	0.93±0.21	2.67±0.62	###	3.08±0.26	###
Liver/Body weight ratio at Sacrifice (mg/g)	43.94±5.83	41.63 ±3.40	56.87±6.18	#	61.81±5.22	###
White adipose tissue weight (g) at Sacrifice	0.53±0.23	0.55±0.23	3.31±0.52	###	2.33±0.55	** ###
White adipose tissue /Body weight ratio at Sacrifice (mg/g)	22.11±10.12	22.15±9.24	65.40±7.86	###	51.29±5.72	* ###
BMI	3.14±0.18	3.05±0.22	6.54±0.45	###	6.01±1.09	###

Table 4. Effect of the 4 weeks treatment with melatonin on body and tissue parameters (food intake, body, white adipose tissue and liver weights) of wild type mice and leptin-deficient mice (ob/ob). The data are expressed as the means ± SD that were calculated from at least three separate measurements performed in triplicate. WC- untreated wild-type; WM- wild-type plus melatonin; ObC- untreated ob/ob; ObM- ob/ob plus melatonin; BMI- body mass index. Statistical comparisons: # wild-type vs. ob/ob and * treated with melatonin vs. untreated counterpart. The number of symbols marks the level of statistical significance: one for $p<0.050$; two for $p<0.010$ and three for $p<0.001$.

The morphological analysis of the liver revealed a higher lipid droplets deposition and therefore hepatic steatosis in ob/ob mice with respect to wild-type mice. Apparently, there were no histological differences after the treatments with melatonin (Fig. 25).

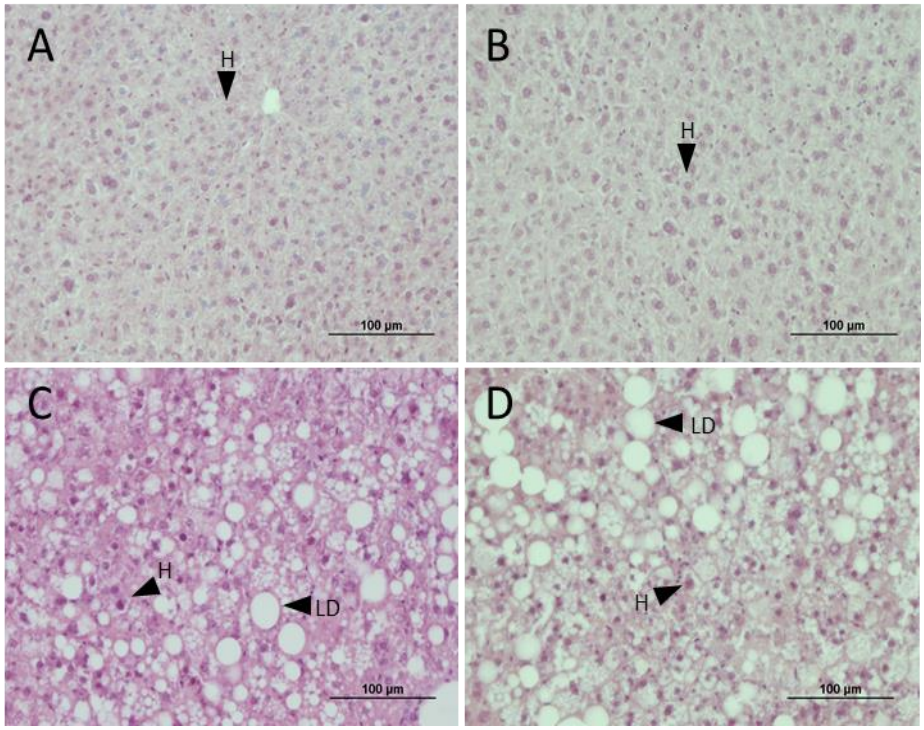

Figure 25. Light microscopy images of hematoxylin-eosin stained sections of livers from (A) wild-type mice, (B) wild-type mice treated with melatonin, (C) ob/ob mice, and (D) ob/ob mice treated with melatonin. Scale bars: 100 µm. LD- lipid droplet; H- hepatocyte.

Electrophoretic pattern

SDS-PAGE gels of liver extracts allowed separation and quantification of a total of 14 bands of protein (280 to 16 kDa) (Fig. 26), he results of identification of these protein bands by MS/MS MALDI TOFF are shown in Table 5.

Table 5. **Protein identification by peptide mass fingerprint of individual bands of liver extracts separated by SDS-PAGE**

Band	Protein Name	Accession No.	Protein Score	Protein Score C. I. %	Protein MW (kDa)
B1	fatty acid synthase, isoform CRA_a [Mus musculus]	gi|148702861	232	100	276.7
B2	carbamoyl-phosphate synthase [ammonia], mitochondrial precursor [Mus musculus]	gi|124248512	449	100	165.8
B3	Liver glycogen phosphorylase [Mus musculus]	gi|15489037	220	100	97.8
B4	alpha-fetoprotein, partial [Mus musculus]	gi|191765	181	100	48.8
B5	glutamate dehydrogenase 1 [Mus musculus]	gi|148692928	319	100	54.5
B6	betaine--homocysteine S-methyltransferase 1 [Mus musculus]	gi|7709990	288	100	45.4
B7	3-ketoacyl-CoA thiolase B, peroxisomal precursor [Mus musculus]	gi|22122797	304	100	44.5
B8	aldolase 2, B isoform, isoform CRA_b [Mus musculus]	gi|148670365	274	100	30.3
B9	uricase [Mus musculus]	gi|6678509	341	100	35.2
B10	Glycine N-methyltransferase [Mus musculus]	gi|15679953	166	100	33.2
B11	carbonic anhydrase 3 [Mus musculus]	gi|31982861	304	100	29.6
B12	glutathione S-transferase Mu 1 [Mus musculus]	gi|6754084	367	100	26.1
B13	PREDICTED: major urinary protein 2-like isoform 1 [Mus musculus]	gi|377835020	518	100	21.0
B14	Chain A, Mouse Sod1	gi|306440452	151	100	16.0

Table 5. Protein identification by MALDI-TOF mass spectrometry of liver extracts of wild-type and leptin-deficient (ob/ob) mice. WC- untreated wild-type; WM- wild-type plus melatonin; ObC- untreated ob/ob; ObM- ob/ob plus melatonin; MW- molecular weight.

It is worthwhile to mention that some of the bands analysed have metabolic functions, so its decline (B2, B3, B5, B7, B11, B13) or increase (B1 and B8) have important metabolic consequences in the liver of leptin-deficient mice.

Because of these proteins are involved in different ways, the results of interest bands MALDI-TOF will be described in different sections of results.

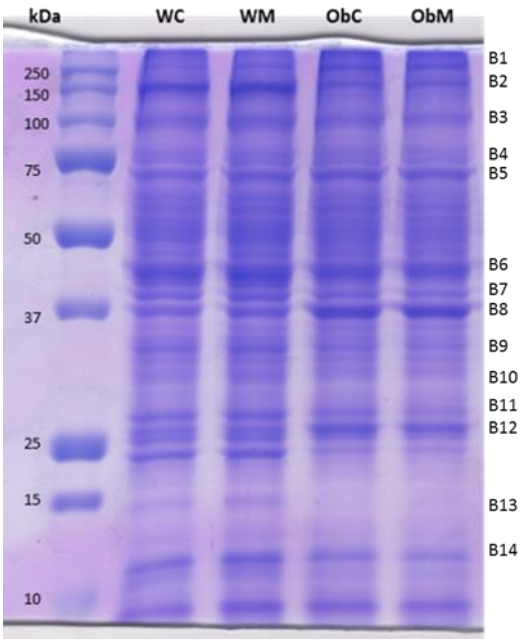

Figure 26. SDS-PAGE gel image of protein extracts of the liver from wild-type mice and leptin-deficient (ob/ob) mice. WC- untreated wild-type; WM- wild-type plus melatonin; ObC- untreated ob/ob; ObM- ob/ob plus melatonin. Band names are denoted by B (band) followed by a number.

Lipid metabolism

Insulin resistance is linked to impaired adipogenesis during obesity (Gustafson, Hedjazifar et al. 2015). In fact, insulin is a potent adipogenic hormone that triggers the differentiation of pre-adipocytes into mature adipocytes (Klemm, Leitner et al. 2001). Here we analyzed PPARγ mRNA expression as a key regulator of adipocyte differentiation and lipid storage which controls energy and glucose homeostasis (Yu, Matsusue et al. 2003; Zhang, Yu et al. 2014). Furthermore, we also studied PPARα because is a key transcription factor in the regulation of lipid metabolism in the liver. Our results showed that leptin-deficient mice expressed significantly higher levels of both PPARγ and PPARα ($p<0.001$) (Fig. 27A and B)

suggesting that ob/ob mice presented higher liver adipogenesis as indicated by the light microscopy study (Fig. 27).

Melatonin treatment also decreased both PPARγ and PPARα mRNA levels in ob/ob animals ($p<0.001$) (Fig. 27A and B).

Adiponectin have been associated with obesity, insulin resistance and type 2 diabetes promoting differentiation of pre-adipocytes, augmenting programmed gene expression responsible for adipogenesis, and increasing lipid content and insulin responsiveness of the glucose transport system in adipocytes (Fu, Luo et al. 2005). Adiponectin levels were statistically higher in ob/ob mice compared with those found in wild-type groups ($p<0.001$). However, in this case, melatonin treatment exerted no effects on any phenotype (Fig. 27E).

When we studied the mRNA expression of adiponectin receptor 1 and 2 (AdipoR1 and AdipoR2), we saw that both receptors showed equal expression patterns. Leptin-deficient animals exhibited higher expression levels of both receptors compared with their wild-type counterparts ($p<0.001$) and melatonin caused a significant decrease in their mRNA expression in both phenotypes ($p<0.050$) (Fig. 27C and D).

Within the experimental block MALDI-TOF two proteins are involved in lipid metabolism section. Thus, fatty acid synthase obtained from band 1 analysis was significantly increased in the liver of leptin-deficient mice ($p<0.001$) (Fig. 27G). Melatonin treatment had a dual effect depending on the mouse strain, so fatty acid synthase expression was significantly decreased in ob/ob mice ($p<0.001$), but increased in wild-type treated mice ($p<0.001$).

The analysis of the SDS-PAGE band 7 revealed that there were differences in the expression of peroxisomal precursor of 3-ketoacyl CoA thiolase B, which catalyzes the final step in the peroxisomal β-oxidation of straight-chain acyl-CoA (Fidaleo, Arnauld et al. 2011).

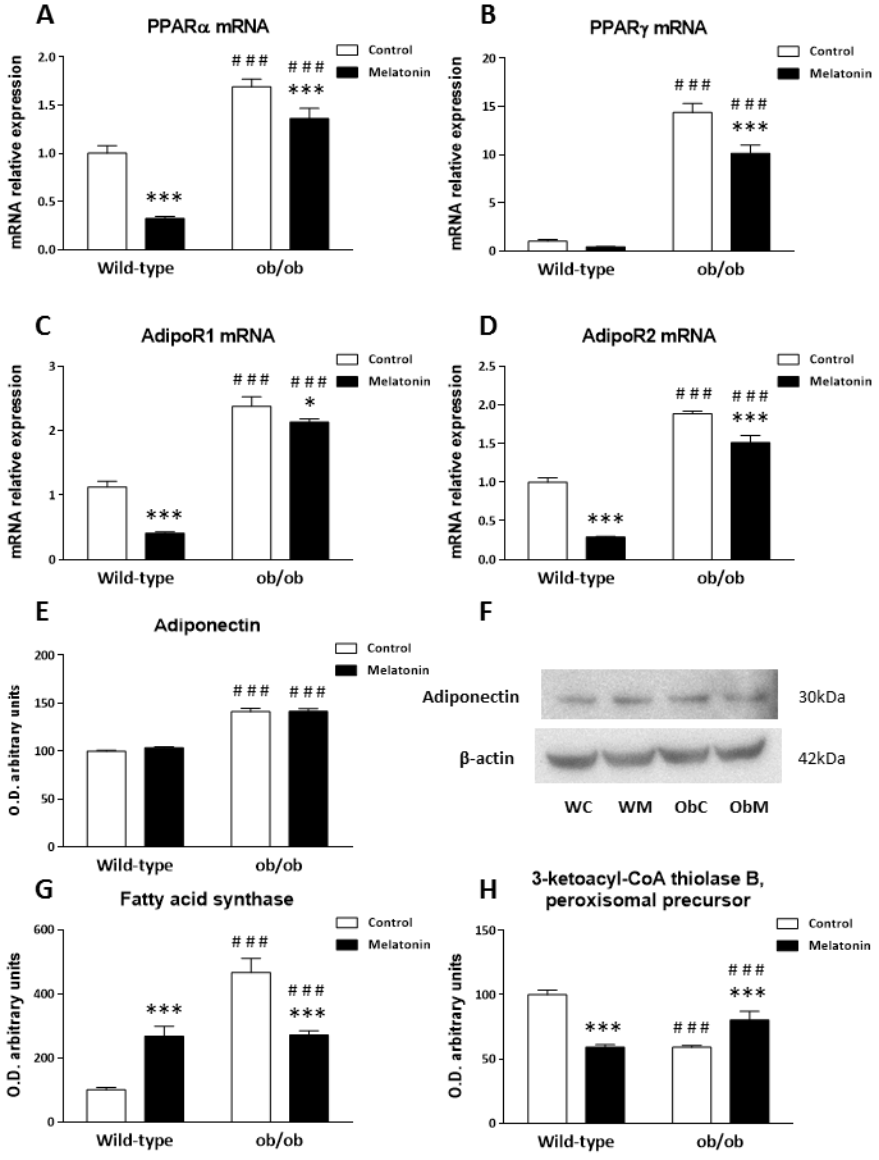

Figure 27. Adipogenic, lipogenic and adiponectin related markers in the liver of wild-type and ob/ob mice. (A and B) mRNA expression of the peroxisome proliferator-activated receptor alpha (PPARγ) and gamma (PPARγ). (C and D) mRNA expression of the adiponectin receptors (AdipoR1 and AdipoR2). (E-G) Bar chart showing the semi-quantitative optical density (arbitrary units of blot bands) of (E) adiponectin from western blot normalised to β-actin, and (F) fatty acid synthase expression and (G) 3-ketoacyl-CoA thiolase B, peroxisomal precursor obtained from protein band 1 and 7 analysis by matrix-assisted laser desorption/ionization-time of flight (MALDI-TOF/TOF) mass spectrometry. (G) Western blot of adiponectin and β-actin as load control. The data are expressed as the means ± SD that were calculated from at least three separate measurements performed in triplicate. WC- untreated wild-type; WM- wild-type plus melatonin; ObC- untreated ob/ob; ObM- ob/ob plus melatonin. Statistical comparisons: # wild-type vs. ob/ob and * treated with melatonin vs. untreated counterpart. The number of symbols marks the level of statistical significance: one for $p<0.050$ and three for $p<0.001$.

Thus, there was a decrease in the expression of peroxisomal precursor of 3-ketoacyl CoA thiolase B ($p<0.001$) in the liver of leptin-deficient mice (Fig. 27H). Again, melatonin treatment had different effects on the two mouse strains, but this time ob/ob treated mice increased this protein levels ($p<0.001$), and wild-type treated mice reduced its expression ($p<0.001$).

Lysosomal acid lipase (LAL) and perilipin are proteins that take part in the intracellular lipid metabolism. LAL is an enzyme involved in the turnover of endogenous lipid stores (lipid droplets) and lipophagy (Pearson, Mellett et al. 2014) that are constitutive negative regulators of glucose-stimulated insulin secretion (Pearson, Mellett et al. 2014). In addition, it was described a reduced LAL in patients with non-alcoholic fatty liver disease (Baratta, Pastori et al. 2015). On the other hand, perilipins are associated with the stability of lipid droplets by acting as a protective layer preventing the action of lipases.

Accordingly with their obese phenotype, we found that ob/ob animals exhibited a significant decrease in LAL levels and an increase in

perilipin content than wild-type mice ($p<0.001$). Melatonin treatment led to an enhancement on LAL expression on both strains ($p<0.010$) (Fig. 28A). This suggests a general action of melatonin in inducing the hydrolysis of triglycerides and cholesteryl esters into lysosomes. However, in ob/ob mice, we also observed a higher expression of perilipin ($p<0.001$) (Fig. 28B) that probably counteracts the actions of melatonin-induced LAL.

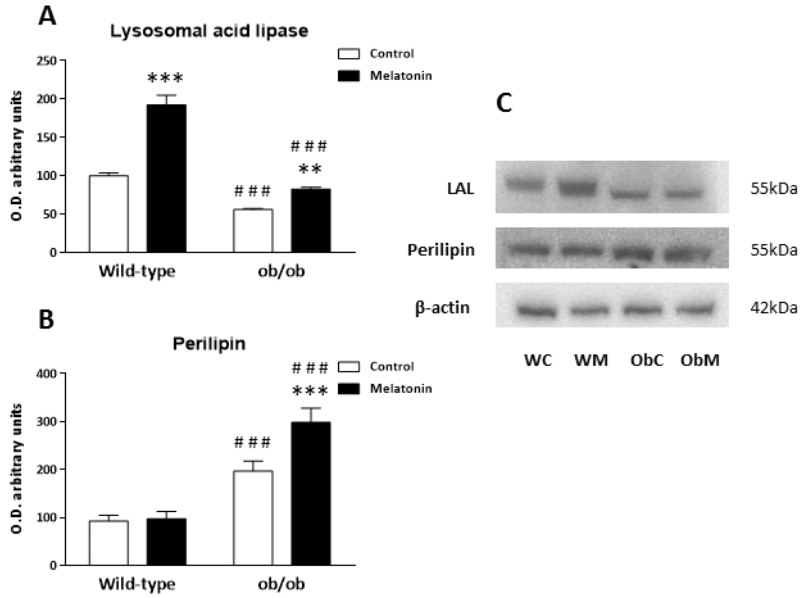

Figure 28. Lipid droplets markers from the liver of wild-type and ob/ob mice. (A and B) Bar chart showing the semi-quantitative optical density (arbitrary units of blot bands) of lysosomal acid lipase (LAL) and perilipin from western blot normalised to β-actin. (C) Western blot of LAL and perilipin and β-actin as load control. The data are expressed as the means ± SD that were calculated from at least three separate measurements performed in triplicate. WC- untreated wild-type; WM- wild-type plus melatonin; ObC- untreated ob/ob; ObM- ob/ob plus melatonin. Statistical comparisons: # wild-type vs. ob/ob and * treated with melatonin vs. untreated counterpart. The number of symbols marks the level of statistical significance: two for $p<0.010$ and three for $p<0.001$.

Glucose metabolism and insulin signalling

As mentioned before, insulin resistance is closely associated with obesity. To elucidate the effect of the absence of leptin in the mechanism of insulin action, we studied some key molecules from the insulin signaling pathway. We measured the expression of the insulin receptor at transcriptional level, the amount of PI3K and phosphorylated Akt (Ser473) as representative molecules of the signaling cascade. We also studied Sirt1 expression, due to its role in glucose homeostasis and insulin signaling activation (Wang, Kim et al. 2011).

Our results on insulin receptor mRNA levels showed that ob/ob mice had an upregulated expression of this receptor by approximately 2-fold of the wild-type group ($p<0.001$) and melatonin supplementation was able to decrease transcript expression in both types of mice ($p<0.001$) (Fig. 29A).

The immunoblot analysis of PI3K showed that ob/ob mice expressed significantly higher protein levels compared with wild-type animals ($p<0.001$), that were further increased by the treatment with melatonin in both phenotypes ($p<0.010$) (Fig. 29B). Akt activation behaved parallel to PI3K results. Although, there was no differences in total Akt expression between both strains, its phosphorylated form (p-Akt) were significantly higher in ob/ob animals ($p<0.001$). Melatonin treatment increased Akt phosphorylation also in both phenotypes ($p<0.001$) (Fig. 29C and D).

Sirt1 plays a pivotal role in several cellular processes, such as metabolism and insulin resistance (Lim, Kim et al. 2012). We found that in our experimental model, ob/ob mice presented a deficit in Sirt1 levels compared with those found in wild-type mice ($p<0.001$). In this case,

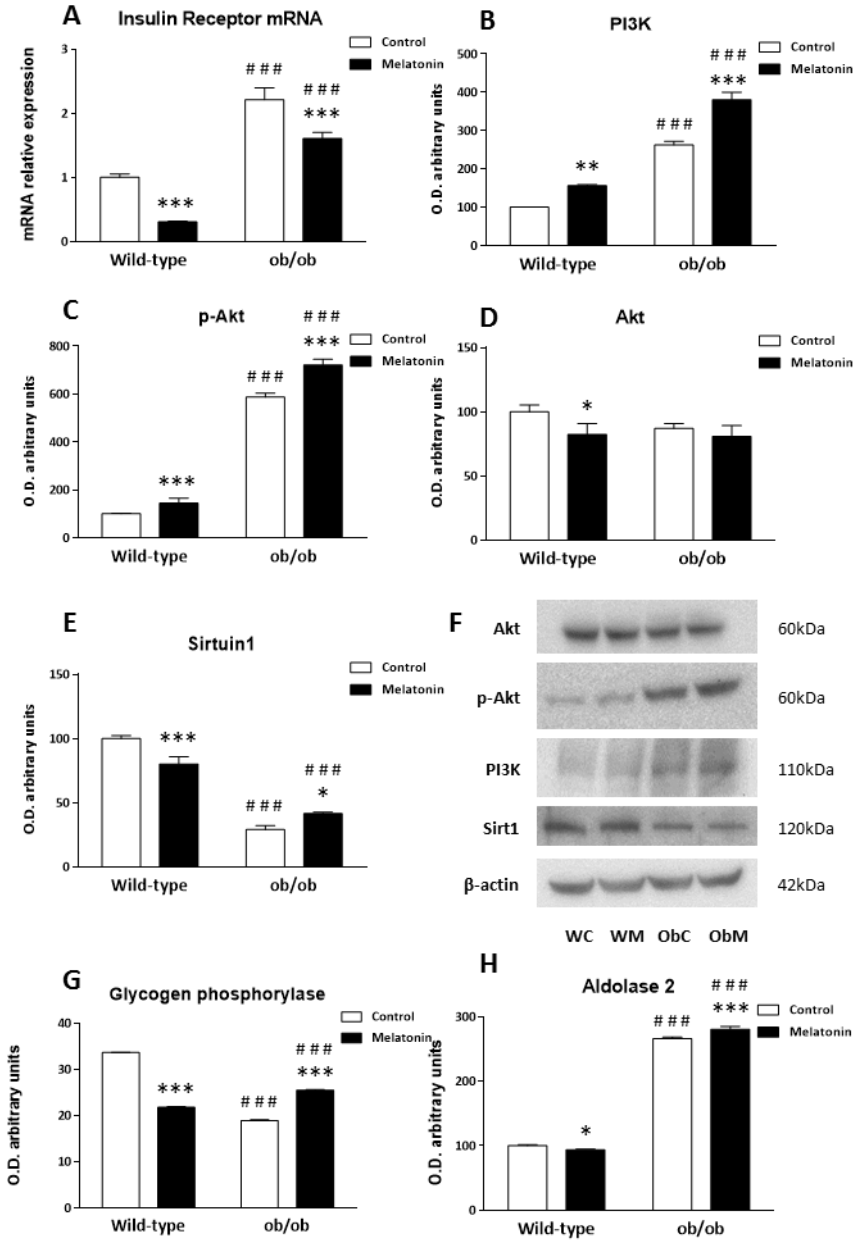

Figure 29. Insulin signalling situation markers from the liver of wild-type and ob/ob mice. (A) mRNA expression of the insulin receptor. (B-H) Bar chart showing the semi-quantitative optical density (arbitrary units of blot bands) of (B) phosphatidylinositol 3-kinase (PI3K), (C and D) Akt and its phosphorylated form (p-Akt), (D) Sirtuin1 (Sirt1) from western blot normalised to β-actin, and (G) glycogen phosphorylase and (H) aldolase 2 expression obtained from protein band 3 and 8 analysis by matrix-assisted laser desorption/ionization-time of flight (MALDI-TOF/TOF) mass spectrometry. (F) Western blot of PI3K, Akt forms, Sirt1, and β-actin as load control. The data are expressed as the means ± SD that were calculated from at least three separate measurements performed in triplicate. WC- untreated wild-type; WM- wild-type plus melatonin; ObC- untreated ob/ob; ObM- ob/ob plus melatonin. Statistical comparisons: # wild-type vs. ob/ob and * treated with melatonin vs. untreated counterpart. The number of symbols marks the level of statistical significance: one for $p<0.050$; two for $p<0.010$ and three for $p<0.001$.

melatonin behaves differently depending on the mouse phenotype. Thus, Sirt1 levels were diminished in melatonin-treated wild-type mice ($p<0.050$) and increased in melatonin-treated ob/ob mice ($p<0.001$) (Fig. 29E).

The analysis of SDS-PAGE band 3 revealed changes in the glycogen phosphorylase expression in the liver of studied animals. This protein, involved in the degradation of glycogen was significantly decreased in the liver of leptin-deficient mice ($p<0.001$) (Fig. X29). As it happened with the effect of melatonin on the expression of Sirt1, glycogen phosphorylase was also increased in ob/ob treated mice ($p<0.001$) and decreased in wild-type animals ($p<0.001$).

The band 8 of the SDS-PAGE gel analysed by MALDI-TOF showed that leptin-deficient mice expressed much higher levels of aldolase 2 compared to wild-type ($p<0.001$) (Fig. 29H). Furthermore, melatonin increased further this glycolytic enzyme content in both treated groups ($p<0.050$).

Our data suggest that leptin deficiency, despite activate the signaling pathway of insulin PI3K / Akt and increase insulin receptor mRNA levels, courses with a defective insulin signaling in liver from obese mice, reflected by low levels of SIRT1, that melatonin treatment seems to improve.

AMPK as energy sensor

Adenosine 5'monophosphate kinase activated protein (AMPK) is a cellular energy sensor that play central role in maintaining energy homeostasis. It is activated under conditions in which cellular energy demands are increased, due to high levels of intracellular AMP or low levels of ATP (Bijland, Mancini et al. 2013), to stimulate ATP production (Zhang, Zhou et al. 2009).

Both total AMPK and its active phosphorylated form (p-AMPK (Thr 172)) were significantly increased in leptin-deficient mice compared with wild-type animals ($p<0.001$), suggesting that ob/ob mice switch on catabolic pathways that generate ATP. The supplementation with melatonin exerted no effects on wild-type mice but increased AMPK activation in ob/ob mice ($p<0.001$) (Fig. 30).

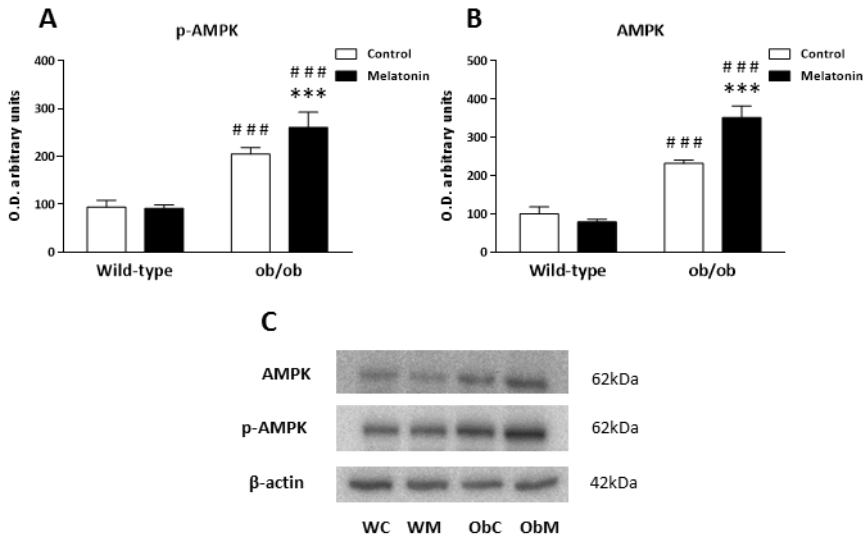

Figure 30. (A and B) Bar chart showing the semi-quantitative optical density (arbitrary units of blot bands) of adenosine monophosphate-activated protein kinase (AMPK) and its phosphorylated form (p-AMPK) (C) Western blot of AMPK forms and β-actin as load control. The data are expressed as the means ± SD that were calculated from at least three separate measurements performed in triplicate. WC- untreated wild-type; WM- wild-type plus melatonin; ObC- untreated ob/ob; ObM- ob/ob plus melatonin. Statistical comparisons: # wild-type vs. ob/ob and * treated with melatonin vs. untreated counterpart. The number of symbols marks the level of statistical significance: three for $p<0.001$.

Mitochondrial biogenesis

To measure mitochondrial mass, we determined relative abundance of mitochondrial housekeeping protein (Yazdi, Moradi et al. 2013), porin, against cellular housekeeping protein β actin in the whole tissue protein extract to determine possible effect of obesity on the liver mitochondrial mass. Thus, the deficiency in leptin induced the upregulation of the porin expression ($p<0.001$), which was significantly reduced in after the treatment with melatonin ($p<0.010$) (Fig. 31).

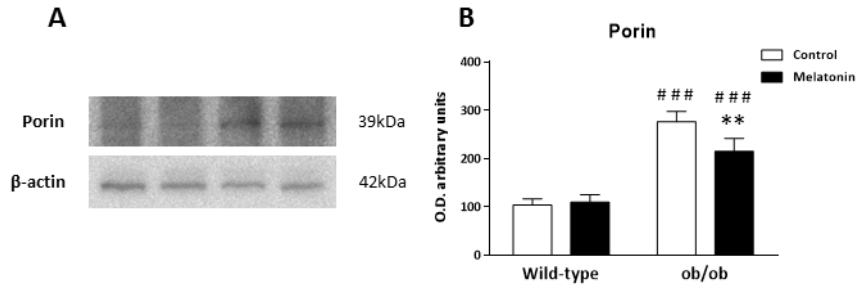

Figure 31. (A) Western blot analysis Porin and β-actin as a load control from the liver of wild-type and leptin-deficient mice (ob/ob). (B) Bar chart showing the semi-quantitative optical density (arbitrary units of blot bands) normalised to β-actin. The data are expressed as the means ± SD that were calculated from at least three separate measurements performed in triplicate. WC- untreated wild-type; WM- wild-type plus melatonin; ObC- untreated ob/ob; ObM- ob/ob plus melatonin. Statistical comparisons: # wild-type vs. ob/ob and * treated with melatonin vs. untreated counterpart. The number of symbols marks the level of statistical significance: two for $p<0.010$ and three for $p<0.001$.

Mitochondrial transcription factor A (TFAM) is a key activator of mitochondrial DNA transcription as well as a participant in mitochondrial genome replication. It is transcribed from the nuclear DNA in response to increased demand for mitochondrial structures. Therefore, it is used as a good marker for mitochondrial biogenesis. When we analyzed TFAM mRNA levels in the liver from ob/ob mice, we found that they expressed this transcription factor by approximately 3-fold than the wild-type group ($p<0.001$). Thus, mitochondrial biogenesis seems to be triggered in leptin-deficient mice. Both experimental groups treated with melatonin significantly reduced the TFAM mRNA expression levels. ($p<0.050$) (Fig. 32).

These results suggest that the deficiency in leptin lead to an increased mitochondrial biogenesis in the liver of obese mice compared with wild-type, which is decreased after treatment with melatonin

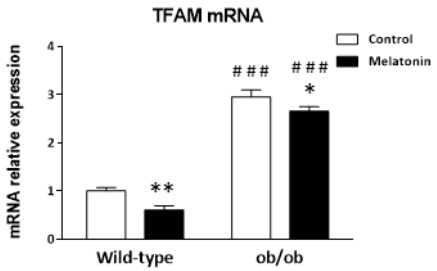

Figure 32. Biogenesis marker in the liver of wild-type and ob/ob mice. mRNA expression of the mitochondrial transcription factor A (TFAM). The data are expressed as the means ± SD that were calculated from at least three separate measurements performed in triplicate. WC- untreated wild-type; WM- wild-type plus melatonin; ObC- untreated ob/ob; ObM- ob/ob plus melatonin. Statistical comparisons: # wild-type vs. ob/ob and * treated with melatonin vs. untreated counterpart. The number of symbols marks the level of statistical significance: one for $p<0.050$; two for $p<0.010$ and three for $p<0.001$.

Mitochondrial dynamics.

As we said before, mitochondrion is a very dynamic organelle, whose fusion and fission is fundamental to the regulation of mitochondrial bioenergetics.

To evaluate mitochondrial dynamics in our model of obesity, we measured the protein expression of Mfn2, a protein involved in mitochondrial fusion, and Drp1, involved in mitochondrial fission. The analysis of the data obtained from Mfn2 immunoblotting showed that its expression was significantly increased in the liver from ob/ob mice ($p<0.050$) (Fig. 33A). Otherwise, Drp1 expression in ob/ob mice was lower than in wild-type animals ($p<0.050$), confirming the stimulation of mitochondrial fusion processes in leptin-deficient mice (Fig. 33B).

The treatment with melatonin in wild-type animals had no effects on any of the proteins studied but, in ob/ob mice, it induced an upregulation of both proteins ($p<0.050$) (Fig. 33A and B). To dissect the

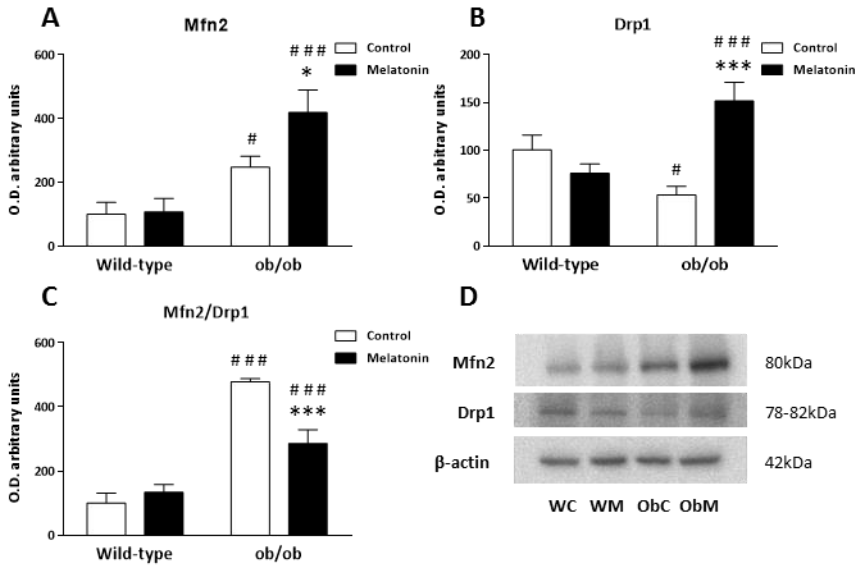

Figure 33. (A and B) Bar chart showing the semi-quantitative optical density (arbitrary units of blot bands) of mitofusin 2 (Mfn2) and dynamin related protein 1 (Drp1). (C) Bart chart showing the Mfn2/Drp1 ratio. (D) Western blot of Mfn2 and Drp1 and β-actin as load control. The data are expressed as the means ± SD that were calculated from at least three separate measurements performed in triplicate. WC- untreated wild-type; WM- wild-type plus melatonin; ObC- untreated ob/ob; ObM- ob/ob plus melatonin. Statistical comparisons: # wild-type vs. ob/ob and * treated with melatonin vs. untreated counterpart. The number of symbols marks the level of statistical significance: one for $p<0.050$ and three for $p<0.001$.

relative contribution of melatonin to the overall processes of mitochondrial dynamics, we calculated the Mfn2/Drp1 ratio, finding that melatonin in ob/ob mice probably counteracts the stimulation of mitochondrial fusion detected in these obese mice ($p<0.001$) (Fig. 33C).

Respiratory complexes expression

Western blot analysis of subunits from electron transport chain complexes were obtained in total liver extracts. Firstly, were normalised to cellular housekeeping protein β actin and then normalized with porin, as a mitochondrial housekeeping protein, to take into account the differences observed before in the mitochondrial mass between both mice strains (Yazdi, Moradi et al. 2013).

Based on the above data, we hypothesized that OXPHOS machinery was remodeled in leptin-deficient mice. We compared the expression of subunits of the mitochondrial electron transport chain complexes, namely NADH dehydrogenase (ubiquinone) 1 b subcomplex 8 (NDUFB8) from complex I; succinate dehydrogenase (ubiquinone) iron-sulfur subunit (SDHB) from complex II; ubiquinol-cytochrome c reductase core protein II (UQCRC2) from complex III; cytochrome c oxidase subunit I (MTCO1) from complex IV and ATP synthase subunit α (ATP5A) from complex V by immunodetection.

No significant differences in the content of complex I subunit between the four experimental groups were found (Fig. 34A), and both complex III and IV subunits did not change in ob/ob animals compared with wild-type mice (Fig. 34C and D). However, complex II, and ATP synthase subunits were significantly reduced in the ob/ob mice compared with wild-type strain ($p<0.050$) (Fig. 34B and E), pointing to an alteration in hepatic electron transport chain content levels associated with obesity.

On the other hand, melatonin treatment, besides increasing the expression of the complex II subunit in ob/ob mice also increased complexes III and IV subunits in both strains, and ATP synthase subunit α in control mice ($p<0.001$), suggesting that melatonin reshapes electron transport chain in the liver of both wild-type and ob/ob mice.

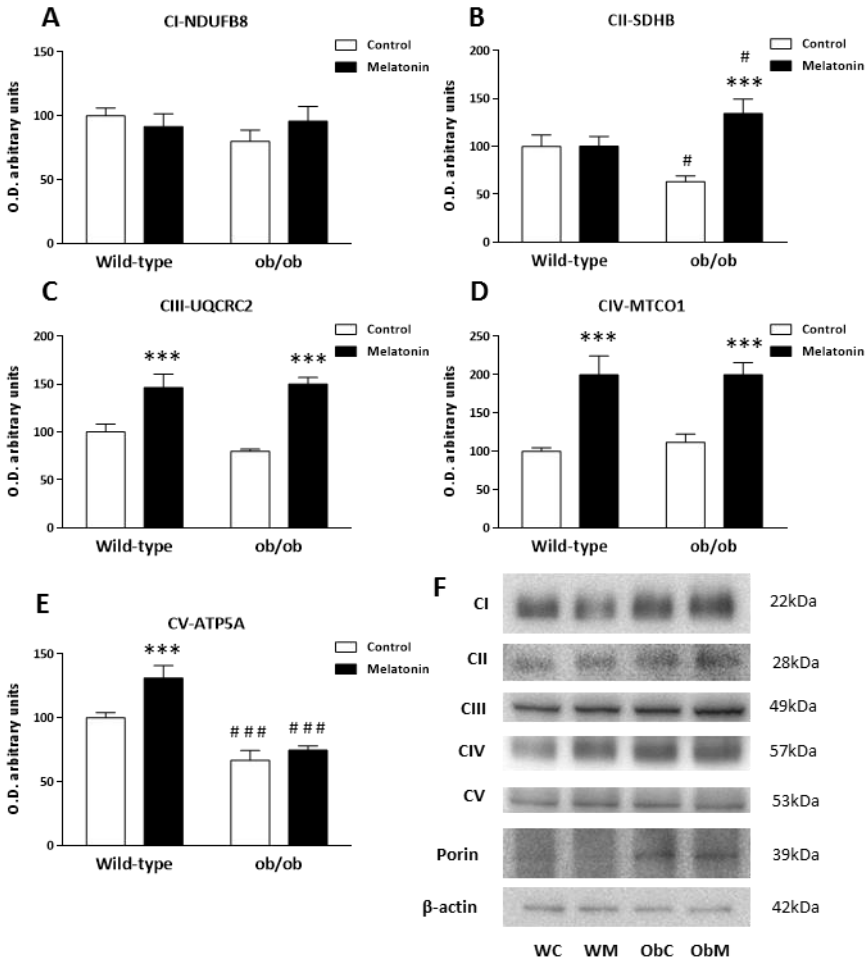

Figure. 34. Oxidative phosphorylation profile from the liver of wild-type and ob/ob mice. (A-E) Bar chart showing the semi-quantitative optical density (arbitrary units of blot bands) of NADH dehydrogenase (ubiquinone) 1 b subcomplex 8 (NDUFB8) from complex I (CI), iron-sulfur subunit (SDHB) from complex II (CII), ubiquinol-cytochrome c reductase core protein II (UQCRC2) subunit from complex III (CIII), cytochrome c oxidase subunit I (MTCO1) from complex IV (CIV), and ATP synthase subunit α (ATP5A) from complex V (CV). The immunoblots were normalised with β-actin as a total extract load control, and after that, the complexes were normalised again with porin as a mitochondrial mass marker. (F) Western blot of CI, CII, CIII, CIV, CV, and β-actin and porin as load controls. The data are expressed as the means ± SD that were calculated from at least three separate measurements performed in triplicate. WC- untreated wild-type; WM- wild-type plus melatonin; ObC- untreated ob/ob; ObM- ob/ob plus melatonin. Statistical comparisons: # wild-type vs. ob/ob and * treated with melatonin vs. untreated counterpart. The number of symbols marks the level of statistical significance: one for $p<0.050$ and three for $p<0.001$.

Mitochondrial function

To evaluate mitochondrial function, we measured oxygen consumption in isolated mitochondria from livers of both strains. According to data obtained from state 3 respiration, which is defined as ADP-stimulated respiration, obtained using **glutamate/malate** as respiration substrates, there were no differences in the maximum production of ATP in presence of ADP between the four experimental

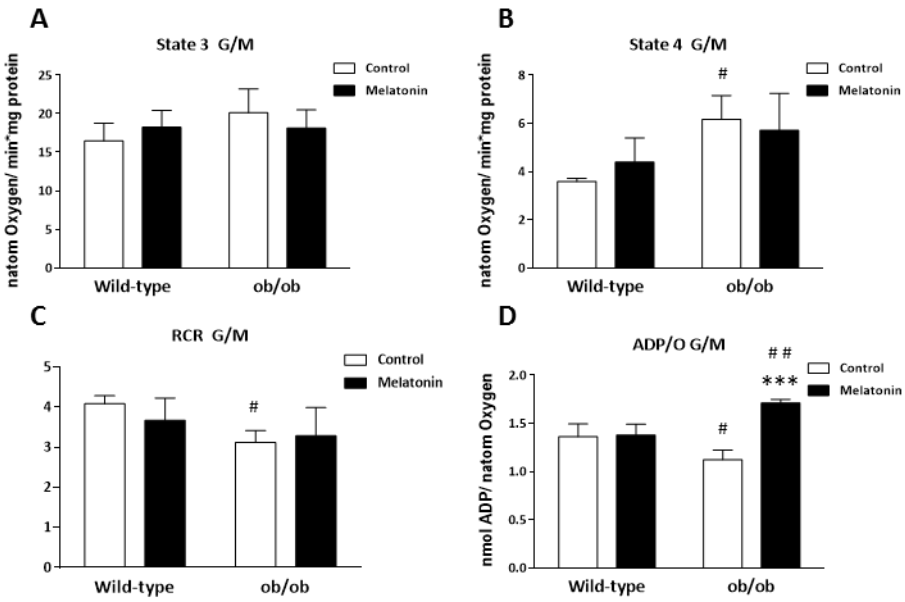

Figure 35. Data represent mitochondrial oxygen consumption rates collected with a Clark electrode. The energization was obtanied from glutamate /malate (G/M) with 175 nmol ADP (A) State 3 represents the maximum consumption of oxygen in the presence of ADP and (B) state 4 described oxygen consumption in without ADP consumption (both expressed as natom oxygen/min*mg protein). (C) Respiratory control ratio (RCR) determines the coupling between substrate oxidation and oxidative phosphorylation. (D) ADP/O is the efficiency of oxidative phosphorylation, expressed as nmol ADP/ natom oxygen. The data are expressed as the means ± SD that were calculated from at least three separate measurements performed in triplicate. WC- untreated wild-type; WM- wild-type plus melatonin; ObC- untreated ob/ob; ObM- ob/ob plus melatonin. Statistical comparisons: # wild-type vs. ob/ob and * treated with melatonin vs. untreated counterpart. The number of symbols marks the level of statistical significance: one for $p<0.050$ and three for $p<0.001$.

groups (Fig. 35A). Despite this, when analysing state 4 respiration (respiration in the absence ATP synthesis), we found that ob/ob mice showed increased state 4 values than wild-type mice ($p<0.050$) suggesting that the activity of the electron transport chain was higher in ob/ob mice. The treatment with melatonin did not induce any change in state 4 respiration in both types of animals (Fig. 35B).

When we calculated the RCR, the ratio between state 3 and 4 that determines the coupling between substrate oxidation and oxidative phosphorylation, in the presence of glutamate/malate, we observed a significant decrease in the degree of oxidative phosphorylation coupling in ob/ob ($p<0.010$) (Fig. 35C). These results suggest that probably part of the isolated mitochondria from ob/ob mice are damaged and cannot maintain a chemiosmotic gradient and then, in the presence of substrates, electron transport runs freely and cannot be coupled to ATP synthesis. The treatment with melatonin did not altered RCR values.

The analysis of the effectiveness of oxidative phosphorylation (ADP/O) in the presence of glutamate/malate showed a worse degree of effectiveness in ob/obthan in wild-type mice ($p<0.050$). In this case, melatonin produced a significant increase in the efficiency of oxidative phosphorylation in ob/ob animals ($p<0.001$) (Fig. 35D).

When we used **succinate** as a substrate for the electron transport chain and therefore without taking into account respiration since complex I, the state 3 was significantly higher in leptin-deficient mice than in wild-type mice ($p<0.050$), and again, melatonin did not caused any change (Fig. 36A).

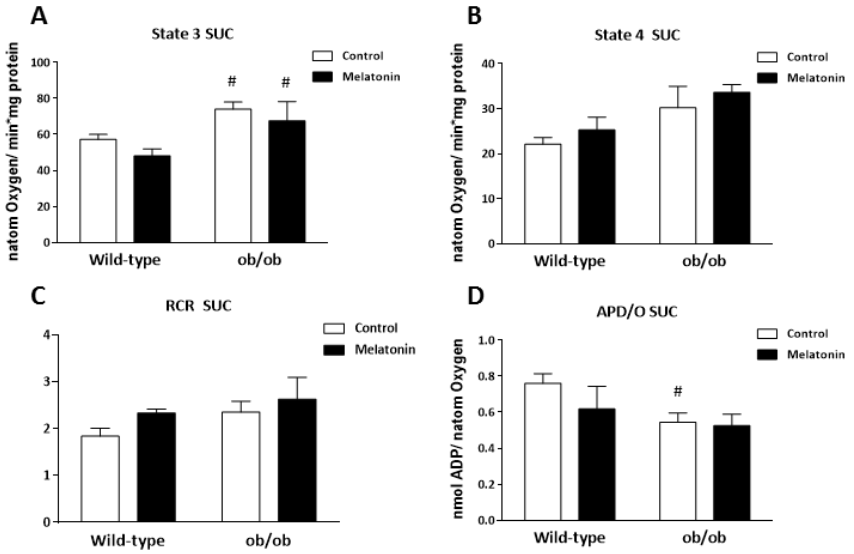

Figure 36. Data represent mitochondrial oxygen consumption rates collected with a Clark electrode. The energization was obtanied from succinate (SUC + rotenone with 125 nmol ADP (A) State 3 represents the maximum consumption of oxygen in the presence of ADP and (B) state 4 described oxygen consumption in without ADP consumption (both expressed as natom oxygen/min*mg protein). (C) Respiratory control ratio (RCR) determines the coupling between substrate oxidation and oxidative phosphorylation. (D) ADP/O is the efficiency of oxidative phosphorylation, expressed as nmol ADP/ natom oxygen. The data are expressed as the means ± SD that were calculated from at least three separate measurements performed in triplicate. WC- untreated wild-type; WM- wild-type plus melatonin; ObC- untreated ob/ob; ObM- ob/ob plus melatonin. Statistical comparisons: # wild-type vs. ob/ob and * treated with melatonin vs. untreated counterpart. The number of symbols marks the level of statistical significance: one for $p<0.050$.

No significant differences were appreciated in the state 4 respiration or RCR in the presence of succinate between the four experimental conditions. Despite this, a trend to higher levels of state 4 respiration was detected in ob/ob mice (Fig. 36B and C).

As observed when we used glutamate/malate energization, the ADP/O ratio in the presence of succinate was significantly lower in ob/ob mice compared with their respective controls ($p<0.050$) but, in this case,

melatonin failed in recovering oxidative phosphorylation efficiency (Fig. 36D).

ATP content

In view of the results on the respiration assays, and to see if obesity affect ATP production, we measured the basal levels of mitochondrial and cytosolic ATP, as well as the amount of ATP produced after energization with glutamate / malate and succinate.

Thus, we found that mitochondrial ATP content were lower ($p<0.001$) and cytosolic ATP were higher ($p<0.001$) in ob/ob mice than wild-type (Fig. 37A and B). On the other hand, melatonin treatment increased cytosolic ATP levels in wild-type mice ($p<0.050$) and both mitochondrial and cytosolic ATP content in ob/ob mice ($p<0.050$).

Taking these results about the basal ATP levels into an account, we decided to measure mitochondrial ATP content after mitochondrial energization and subsequent oxygen consumption measurements to determine the levels of ATP produced during respiration. The amount of ATP produced during oxygen consumption assays was calculated as the difference between the ATP content in mitochondria after respiration and basal mitochondrial ATP.

As basal mitochondrial ATP levels, ATP produced during respiration energized with glutamate/malate was significantly lower in leptin-deficient mice compared with wild-type animals ($p<0.010$). However, although melatonin slightly increased ATP content, it was not significantly (Fig. 37C).

By contrast, the ATP produced during energization with succinate, although was slightly lower in ObC mice, did not result in statistically

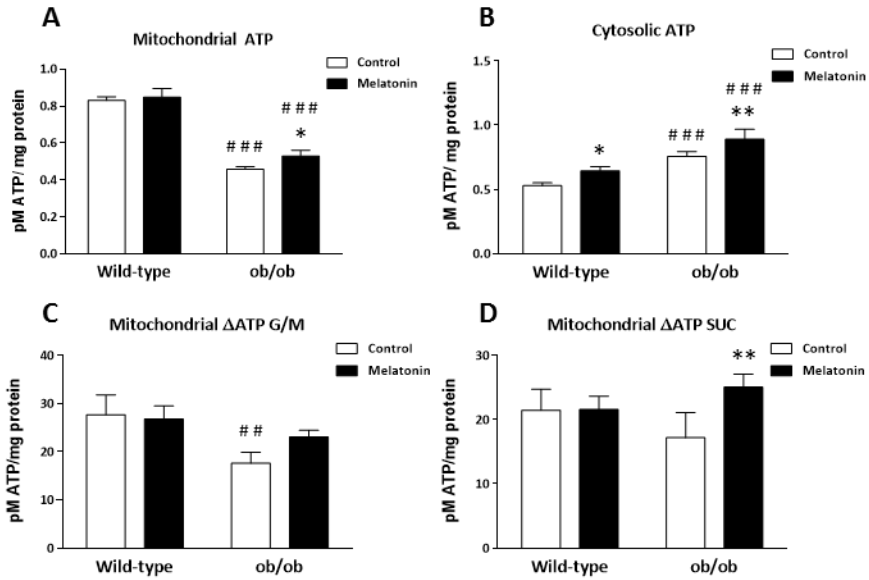

Figure 37. Basal (A) mitochondrial and (B) cytosolic ATP content, and ATP produced after (C) glutamate / malate and (D) succinate energization, calculated as the difference between the ATP content in mitochondria after respiration and basal mitochondrial ATP. ATP content is presented as pM ATP/ mg protein. The data are expressed as the means ± SD that were calculated from at least three separate measurements performed in triplicate. WC- untreated wild-type; WM- wild-type plus melatonin; ObC- untreated ob/ob; ObM- ob/ob plus melatonin. Statistical comparisons: # wild-type vs. ob/ob and * treated with melatonin vs. untreated counterpart. The number of symbols marks the level of statistical significance: one for $p<0.050$; two for $p<0.010$ and three for $p<0.001$.

significant differences, while melatonin treatment caused a significant increase in ATP production after succinate in ob/ob treated mice ($p<0.010$) (Fig. 37D).

In summary, our results indicate a worse oxidative phosphorylation and increased non mitochondrial ATP production in the liver of leptin-deficient mice, that melatonin is able to increase significantly.

MOMP and mPTP

The maintenance of the integrity of mitochondrial membranes is essential to guarantee a correct mitochondrial function. Bcl-2 and Bax are proteins that play a key role in the MOMP, whereas cyclophilin D it is the regulatory component the mPTP. Thus, these three proteins are fundamental in controlling mitochondrial membrane permeability and the subsequent process of mitochondrial apoptosis.

The study of Bcl-2 protein levels showed that its expression was significantly diminished in ob/ob mice compared with the expression detected in wild-type mice ($p<0.001$) (Fig. 38A). In addition, the expression of the pro-apoptotic protein Bax was higher in ob/ob mice ($p<0.001$) (Fig. 38B) suggesting that leptin-deficient mice presented a higher mitochondrial permeability than their wild-type counterparts. Although melatonin treatment reduced Bax levels in both types of mice ($p<0.010$) and increased Bcl-2 in ob/ob mice ($p<0.001$) suggesting a protective effect, we found a downregulation on Bcl-2 expression in melatonin-treated wild-type mice ($p<0.001$).

Among the mitochondrial permeability transition pore components, cyclophilin D is the most studied and has been found overexpressed under pathological conditions increasing the vulnerability of the permeability transition pore to stress-induced opening (Matas, Young et al. 2009; Lopez-Erauskin, Galino et al. 2012). Here, our results showed higher levels of cyclophilin D in leptin-deficient mice ($p<0.001$) supporting the idea about an impairment in mitochondrial membrane integrity in leptin-deficient obese mice. On the other hand melatonin treatment increased cyclophilin D expression ($p<0.050$) (Fig. 38D).

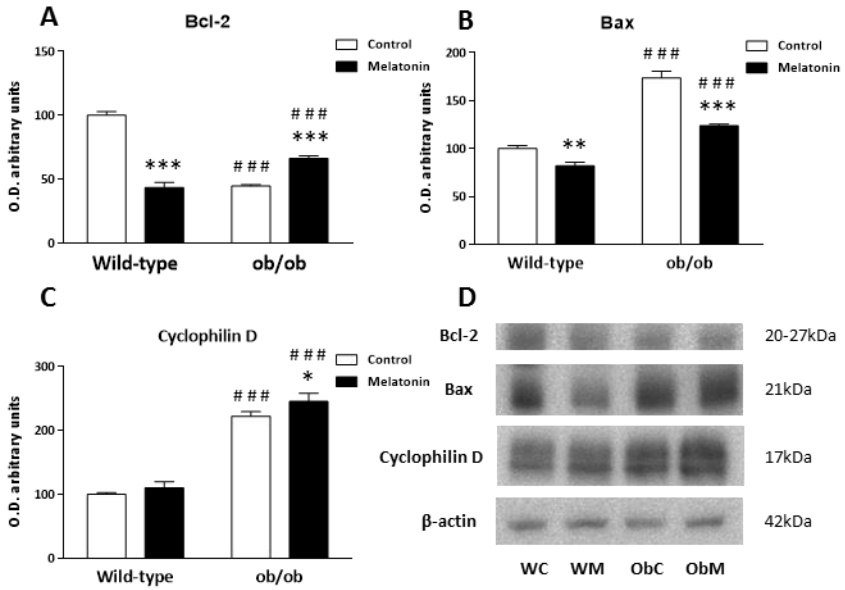

Figure 38. Mitochondrial membrane permeability markers from the liver of wild-type and ob/ob mice. (A, B) Bar chart showing the semi-quantitative optical density (arbitrary units of blot bands) of B-cell lymphoma 2 (Bcl-2), Bcl-2 associated X protein (Bax) and cyclophilin D from western blot normalised to β-actin. (C) Bax/Bcl-2 ratio as an indicator of mitochondrial outer membrane pore (MOMP) formation. (E) Western blot of Bcl2, Bax and Cyclophilin and β-actin as a load control. The data are expressed as the means ± SD that were calculated from at least three separate measurements performed in triplicate. WC- untreated wild-type; WM- wild-type plus melatonin; ObC- untreated ob/ob; ObM- ob/ob plus melatonin. Statistical comparisons: # wild-type vs. ob/ob and * treated with melatonin vs. untreated counterpart. The number of symbols marks the level of statistical significance: one for $p<0.050$ and three for $p<0.001$.

Oxidative stress status

To evaluate oxidative stress status in the four experimental groups, we measured markers of oxidative damage and antioxidant defence in livers from both strains.

The levels of protein carbonyls were measured as an index of oxidative damage to proteins. We found a higher levels of oxidatively damaged proteins in ob/ob mice than in the wild- type mice ($p<0.050$). In addition, melatonin was able to reduce protein carbonilation in both phenotypes ($p<0.001$) (Fig. 39A). The levels of MDA and 4-HNE were measured as an index of lipid peroxidation and again the ob/ob mice

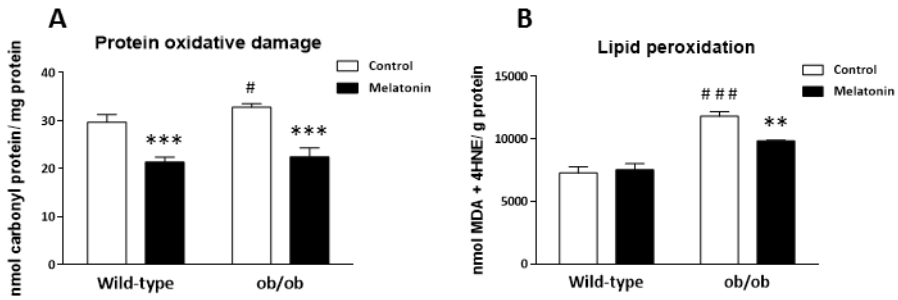

Figure 39. Protein and lipid oxidative damage in the liver of wild-type and ob/ob mice. (A) Protein damage is expressed as nmol carbonyl protein/mg protein. (B) Liver´s lipid peroxidation is presented as nmol MDA+4-HNE/ g protein. The data are expressed as the means ± SD that were calculated from at least three separate measurements performed in triplicate. WC- untreated wild-type; WM- wild-type plus melatonin; ObC- untreated ob/ob; ObM- ob/ob plus melatonin. Statistical comparisons: # wild-type vs. ob/ob and * treated with melatonin vs. untreated counterpart. The number of symbols marks the level of statistical significance: one for $p<0.050$; two for $p<0.050$ and three for $p<0.001$.

presented a higher accumulation of these end-products of lipid peroxidation peroxidation only in ob/ob mice ($p<0.010$) (Fig. 39B).

Antioxidant capacity was study by measuring the activity of the antioxidant enzymes SOD and CAT and the total antioxidant activity (TAA)

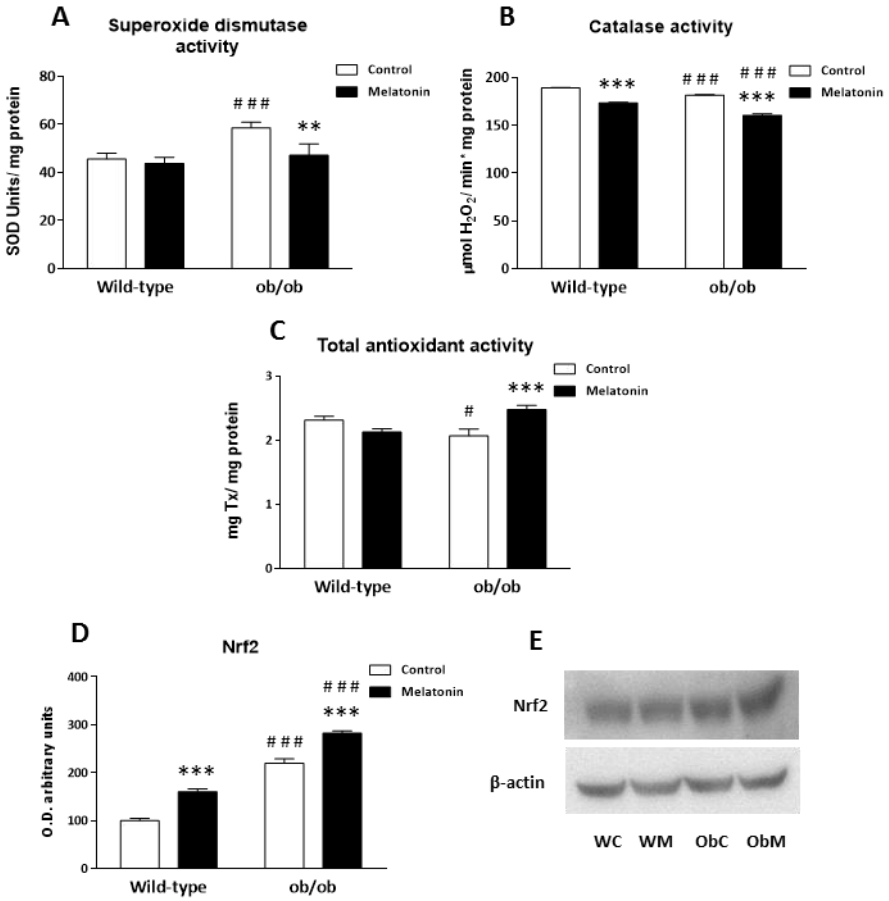

Figure 40. Antioxidant enzymatic and non-enzymatic capacity of the liver of wild-type and ob/ob mice. (A and B) Superoxide dismutase (SOD) activity was expressed as SOD units (U)/ mg protein and catalase activity as µmol H_2O_2 /min*mg protein. (C) Total antioxidant activity expressed in equivalents of mg Trolox (Tx)/mg protein. (D and E) Bar chart showing the semi-quantitative optical density (arbitrary units of blot bands) of nuclear factor erythroid-derived 2-like 2 (Nrf2) normalised to β-actin and western blot analysis of Nrf2 and β-actin from the liver of wild-type and ob/ob mice. The data are expressed as the means ± SD that were calculated from at least three separate measurements performed in triplicate. WC- untreated wild-type; WM- wild-type plus melatonin; ObC- untreated ob/ob; ObM- ob/ob plus melatonin. Statistical comparisons: # wild-type vs. ob/ob and * treated with melatonin vs. untreated counterpart. The number of symbols marks the level of statistical significance: one for p<0.050; two for p<0.010 and three for p<0.001.

using the ABTS cation radical method. SOD activity was significantly higher in the ob/ob group compared with the wild-type strain ($p<0.001$) and melatonin caused a significant decrease in its activity but only in ob/ob mice ($p<0.010$) (Fig. 39A). On the opposite, CAT activity was lower in ob/ob animals ($p<0.001$) and melatonin treatment resulted in a significant decrease in the activity of this enzyme in both phenotypes ($p<0.001$) (Fig. 39B). The assay to measure the TAA demonstrated significantly lower antioxidant activity in ob/ob animals ($p<0.050$). Nonetheless, melatonin treatment displayed opposite effects in both phenotypes. The antioxidant activity was higher in melatonin-treated ob/ob mice ($p<0.001$) and lower in treated wild-type mice (Fig. 39C).

To confirm if these different redox status are consequence of variations in redox signalling pathways, we evaluated the expression of Nrf2, an essential transcription factor which regulates the expression of several detoxify and antioxidant molecules. Nrf2 immunoblot showed that the expression of this transcription factor was significantly higher in ob/ob animals ($p<0.001$), and the melatonin treatment led to an upregulation of this transcription factor in both strains ($p<0.001$) (Fig. 39D and E).

Thus, as well as we saw in after two weeks treatment, melatonin improves the oxidative stress found in the liver of leptin-deficient mice through direct and indirect actions.

Inflammation

As described before, hepatocytes of obese individuals accumulate lipids causing hepatic steatosis and triggering an inflammatory response that is closely linked to oxidative stress and other obesity-related alterations such as ER stress or insulin resistance. We studied the inflammatory response in our cellular model by detecting the activation level of the transcription factor NF-κB and by measuring the pro-inflammatory cytokines IL-6 and TNF-α.

Immunoblot analysis of the activated form of NF-κB, p65 phosphorylated at Ser536, showed that ob/ob mice had an enhanced inflammatory response than wild-type mice ($p<0.001$) which was reduced after the melatonin treatment ($p<0.010$) (Fig. 41A). Besides, ob/ob mice exhibited higher levels of total p65 ($p<0.010$) and the treatment with melatonin did not affect its protein expression (Fig. 41B).

In the same way, IL-6 and TNF-α levels were higher in ob/ob animals compared with wild-type mice ($p<0.001$) and, when they were treated with melatonin, the levels of these pro-inflammatory cytokines were reduced ($p<0.001$) (Fig. 41E and F). On the other hand, the treatment with melatonin did not alter any of the inflammation markers in wild-type mice.

In summary, leptin deficiency results in an exacerbated inflammatory response in the liver of obese mice, that melatonin significantly reduces.

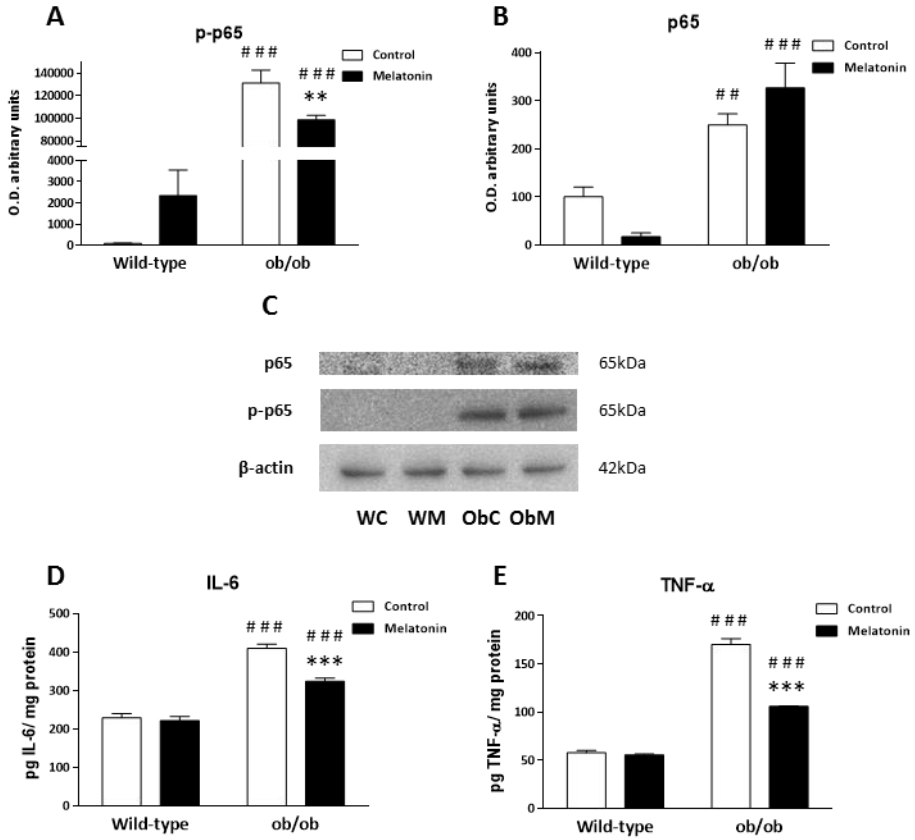

Figure. 41. Inflammatory markers from the liver of wild-type and ob/ob mice. (A and B) Bar chart showing the semi-quantitative optical density (arbitrary units of blot bands) of NF-κB p65 and its phosphorylated form phosphop65 (p-p65) western blot, normalised to β-actin. (C) Western blot of NF-kappa-B p65 subunit and its phosphorylated form. (D) Interleukin 6 (IL-6) levels. (E) Tumor necrosis factor α (TNF-α). Both IL-6 and TNF-α results are expressed as pg/mg protein. The data are expressed as the means ± SD that were calculated from at least three separate measurements performed in triplicate. WC- untreated wild-type; WM- wild-type plus melatonin; ObC- untreated ob/ob; ObM- ob/ob plus melatonin. Statistical comparisons: # wild-type vs. ob/ob and * treated with melatonin vs. untreated counterpart. The number of symbols marks the level of statistical significance: two for $p<0.010$ and three for $p<0.001$.

Proteasome activity

To initiate the study of the protein quality control processes, we measured the activity of the proteasome, the system responsible for the degradation of short half-life proteins. Thus, the deficiency in leptin induced the upregulation of the proteasome activity ($p<0.001$), which was significantly reduced in both phenotypes after the treatment with melatonin ($p<0.050$) (Fig. 42).

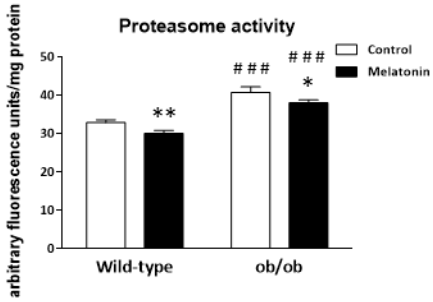

Figure 42. Proteasome activity from the liver of wild-type and ob/ob mice. Proteasome activity are expressed as arbitrary fluorescence units. The data are expressed as the means ± SD that were calculated from at least three separate measurements performed in triplicate. WC- untreated wild-type; WM- wild-type plus melatonin; ObC- untreated ob/ob; ObM- ob/ob plus melatonin. Statistical comparisons: # wild-type vs. ob/ob and * treated with melatonin vs. untreated counterpart. The number of symbols marks the level of statistical significance: one for $p<0.050$; two for $p<0.010$ and three for $p<0.001$.

Unfolded protein response

Metabolic machinery overload produced in the liver of obese individuals is usually accompanied by the accumulation of misfolded proteins in the lumen of the ER that detonates UPR (Ozcan, Cao et al. 2004). To study the effect of melatonin in the ER stress in the liver of leptin-deficient mice we measured key proteins of the three main branches that make up the response to unfolded or misfolded proteins.

Immunoblot analysis of eIF2α and its phosphorylated form (p-eIF2α) was performed as representative markers of PERK pathway and showed that, although ob/ob animals exhibited lower levels of total eIF2α ($p<0.05$) (Fig. 43A), they also displayed the highest p-eIF2α levels ($p<0.001$) (Fig. 43B) demonstrating the activation of PERK pathway in leptin-deficient mice.

In addition, we found that melatonin treatment decreased the protein expression of this phosphorylated form in both phenotypes ($p<0.001$) (Fig. 43D).

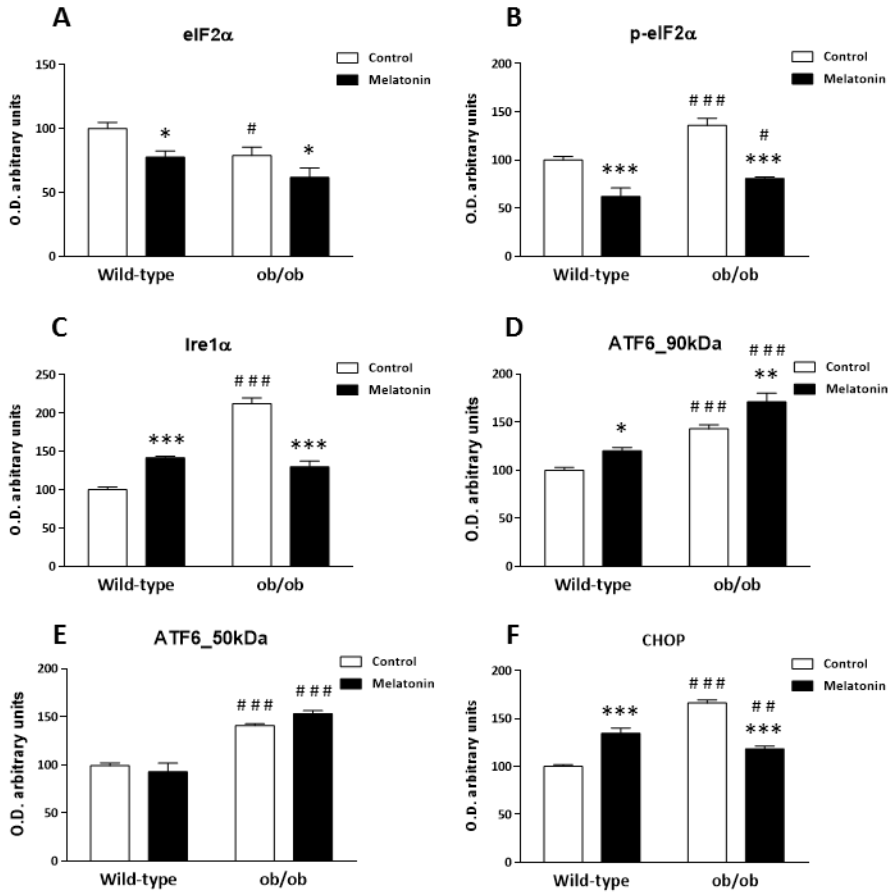

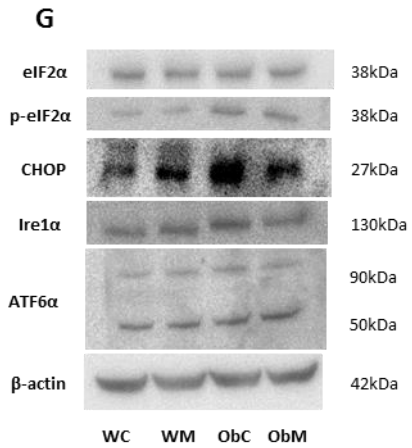

Figure 43. Unfolded protein response markers from the liver of wild-type and ob/ob mice. (A-B) Bar chart showing the semi-quantitative optical density (arbitrary units of blot bands) of activating transcription factor-6-α (ATF6α) forms, (A and B) of α-subunit of eukaryotic initiation factor (eIF2α) and its phosphorylated form (peIF2α), (E) of inositolrequiring enzyme-1 (Ire1) and (F) C/EBP homologous protein (CHOP) form western blot normalised to β-actin. (G) Western blot of ATF6α, eIF2α, Ire1α, CHOP and β-actin as load control. The data are expressed as the means ± SD that were calculated from at least three separate measurements performed in triplicate. WC- untreated wild-type; WM- wild-type plus melatonin; ObC- untreated ob/ob; ObM- ob/ob plus melatonin. Statistical comparisons: # wild-type vs. ob/ob and * treated with melatonin vs. untreated counterpart. The number of symbols marks the level of statistical significance: one for $p<0.050$; two for $p<0.010$ and three for $p<0.001$.

According to the preceding results, Ire1α expression, was highest in ob/ob animals ($p<0.001$), but in this case, the effect of melatonin varied depending on the phenotype. Melatonin increased Ire1α expression in wild-type mice ($p<0.001$) but decreased Ire1α expression in ob/ob ($p<0.001$) (Fig. 43C).

As occurred with the other ER stress markers, the quantification of ATF6α levels showed that ob/ob animals presented higher amounts of both 90kDa inactive ATF6α ($p<0.001$) and 50kDa active fragment of ATF6α than wild type mice ($p<0.001$). In this case, although melatonin treatment

increased the 90kDa form of ATF6α levels in both types of mice ($p<0.050$), it did not change the levels of the active ATF6α. (Fig. 43D and E).

The three ER stress pathways converge on the protein CHOP that is able to induce cell death by promoting protein synthesis in the stressed ER (Marciniak, Yun et al. 2004). Here, we found that leptin-deficient animals exhibited higher levels of this protein than wild-type mice ($p<0.001$) but, as observed with Ire1α results, CHOP expression was differently influenced by melatonin depending on the phenotype. Thus, CHOP levels were increased by melatonin in wild-type mice ($p<0.001$), and decreased in ob/ob animals ($p<0.001$) (Fig. 43F).

Taken together, our results indicate that the liver of mice-deficient in leptin has triggered the response to misfolded proteins, and therefore reticulum stress. Melatonin treatment improves ER stress associated with leptin deficiency through PERK and Ire1α pathways.

Autophagy

The generation of inflammatory responses and oxidative damage in livers from leptin-deficient mice probably requires the activation of degradation systems to eliminate the damaged materials and thus prevent its accumulation and spread. Since leptin seems to play an important role in the neuroendocrine control of autophagy (Malik, Marino et al. 2011), we conduct a comprehensive characterization of the autophagic machinery by measuring CMA and the phosphorylated active form of mTOR, as the main inhibitor of autophagic response, and the expression of the main markers of macroautophagy. To evaluate the occurrence of CMA, we analysed LAMP2A mRNA levels showing that ob/ob mice significantly upregulated its hepatic mRNA expression by approximately 2-fold the wild-type levels ($p<0.001$). In both phenotypes, melatonin

supplementation caused a decrease in LAMP2A mRNA levels ($p<0.001$) (Fig. 44A).

The immunoblot analysis revealed higher p-mTOR levels in the ob/ob group than in wild-type mice ($p<0.001$), while melatonin treatment caused a significant decrease in p-mTOR levels in both phenotypes

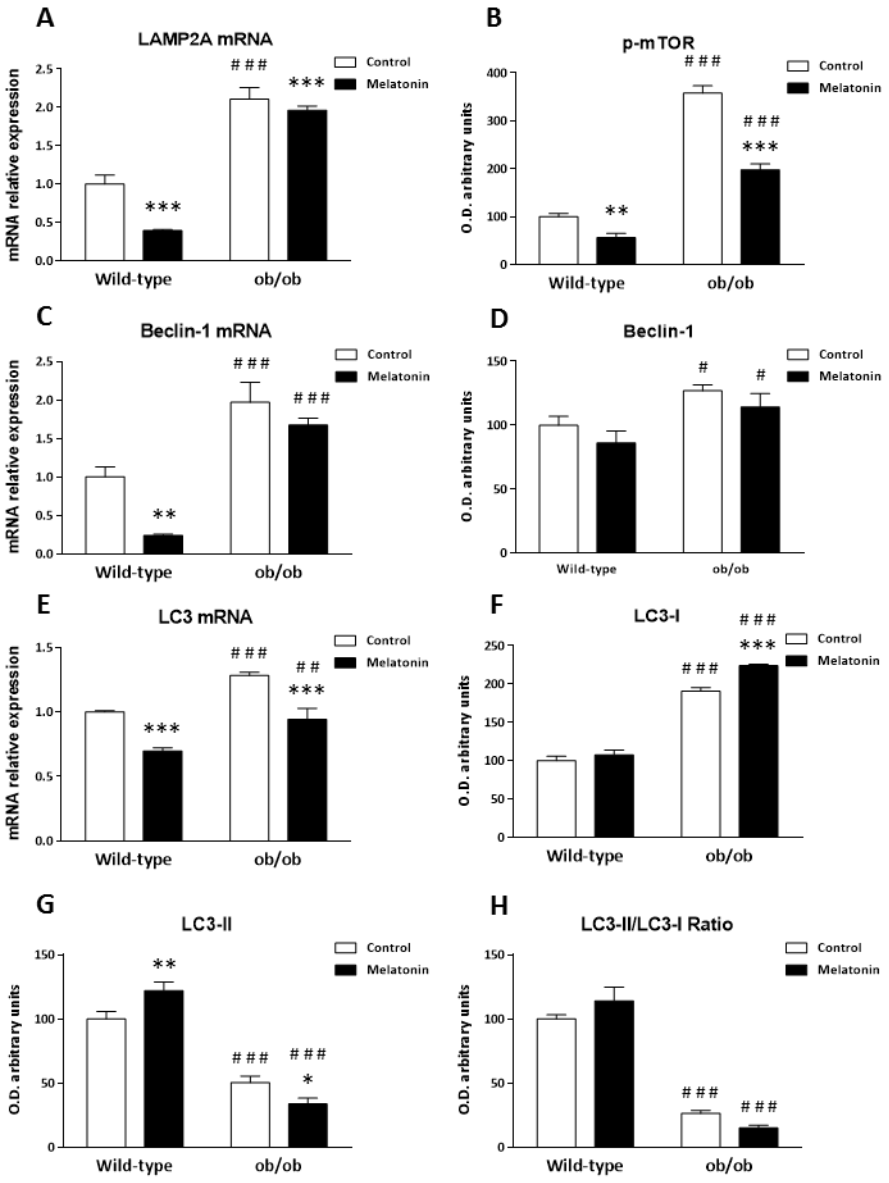

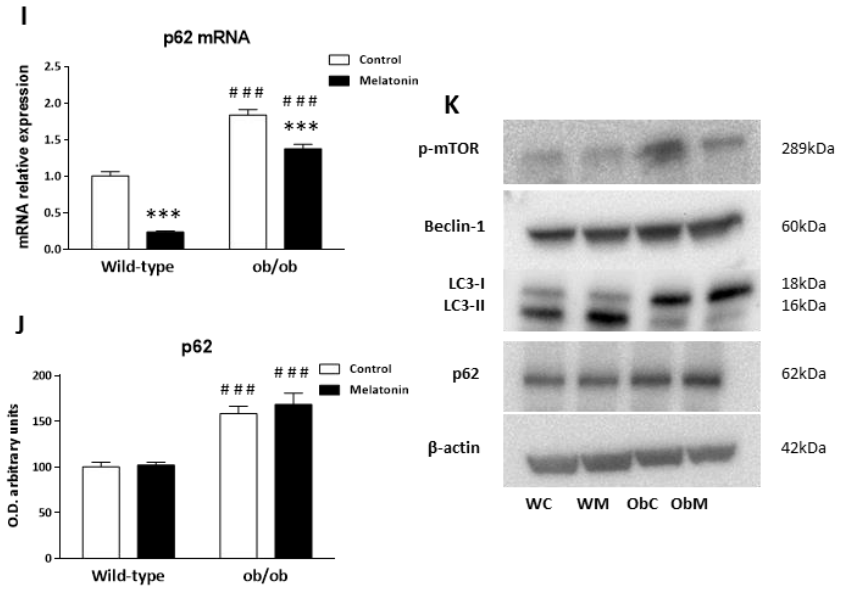

Figure 44. Autophagy markers from the liver of wild-type and ob/ob mice. (A) mRNA expression of lysosome-associated membrane protein type 2A (LAMP2A) as chaperon mediated autophagy marker. (C, E and I) mRNA expression of Beclin-1, microtubule-associated protein 1 light chain 3 isoform B (LC3B) and sequestosome-1 or p62. (B, D, F-H and J) Bar chart showing the semi-quantitative optical density (arbitrary units of blot bands) of phosphorylated mammalian target of rapamycin phospho-mTOR (p-mTOR), Beclin-1, LC3-I and II and p62 from western blot normalised to β-actin. (K) Western blot of p-mTOR, Beclin-1, LC3-I, LC3-II, p62 and β-actin as load control. The data are expressed as the means ± SD that were calculated from at least three separate measurements performed in triplicate. WC- untreated wild-type; WM- wild-type plus melatonin; ObC- untreated ob/ob; ObM- ob/ob plus melatonin. Statistical comparisons: # wild-type vs. ob/ob and * treated with melatonin vs. untreated counterpart. The number of symbols marks the level of statistical significance: one for $p<0.050$; two for $p<0.010$ and three for $p<0.001$.

($p<0.010$) (Fig. 44B). These results suggest that leptin deficiency inhibits autophagy and melatonin activates the pathway. However, Beclin-1 results suggest the opposite. In comparison with wild-type mice, ob/ob mice upregulated the hepatic mRNA expression of Beclin-1 by approximately 2-fold of wild-type animals ($p<0.001$). Furthermore, melatonin treatment caused a decline in Beclin-1 mRNA levels in both

phenotypes ($p<0.010$) (Fig. 44C). Accordingly, the immunoblot analysis of Beclin-1 showed higher levels of this protein in ob/ob mice ($p<0.050$), suggesting the upregulation of autophagy by the deficiency of leptin. Despite this and although Beclin-1 mRNA expression was inhibited by melatonin in both types of mice, melatonin treatment did not seem to affect Beclin-1 protein expression in any of the strains (Fig. 44D).

To further investigate these discrepancies, we analysed LC3 mRNA and protein expression. Liver from leptin-deficient ob/ob mice presented a statistically significant upregulation LC3 transcripts by approximately 30% compared with wild-type mice ($p<0.001$). In both phenotypes, melatonin treatment caused a significant decrease in LC3 mRNA expression of approximately 30% ($p<0.001$) (Fig. 44E). These results support the information obtained from Beclin-1 about a possible switch in endocrine and metabolic signalling pathways that favours autophagy ob/ob animals than in the wild-type group ($p<0.001$) but melatonin treatment caused a significant increase in LC3-I levels ($p<0.001$) (Fig. 44F).in ob/ob mice and a role of melatonin in exerting the opposite effect. Immunoblot analysis confirmed a higher LC3-I protein expression in

On the contrary, the autophagosomal marker LC3-II displayed lower levels in leptin-deficient mice than in the wild-type animals ($p<0.001$). Melatonin treatment had a dual effect depending on the mouse phenotype, since mice of the wild-type strain treated with melatonin increased LC3-II levels, whereas leptin-deficient mice reduced the presence of this protein ($p<0.050$) (Fig. 44G). Based on this, our results suggest that melatonin increases the number of autophagosomes in wild-type mice, but reduces its number in ob/ob animals.

To measure autophagic flux, we quantified p62 mRNA and protein expression. Thus, we found that leptin-deficient mice had significantly higher p62 protein levels and upregulated p62 mRNA expression by approximately 80% compared with wild-type mice ($p<0.001$) indicating that ob/ob mice have a lower autophagic flux than their respective controls. Nonetheless, melatonin treatment did not alter p62 protein levels in any strain but significantly reduced its mRNA expression in both types of mice ($p<0.001$) (Fig. 44I and J).

Based on our results, we can say there is a blockage in the development of autophagy in the liver of leptin-deficient mice, and as happened after two weeks of melatonin treatment, there was a greater blockage of autophagy in the liver of ob/ob mice after four weeks of treatment.

DISCUSSION

DISCUSSION

In recent decades, big resources has been spent in making people aware of the dangers of obesity and its comorbidities. However, the awareness campaigns against physical inactivity, promoting healthy diets, and the tremendous effort, resources and time spent on elucidating the molecular mechanisms of obesity and its comorbidities have not been enough to stop the pandemic which represents obesity today.

Obesity is a complex multi-factorial chronic disease that is characterized by numerous dysfunctions that affecting the whole body, making difficult to understand the mechanisms underlying the development of these diseases.

Melatonin, due to its antioxidant properties, and its involvement in many physiological functions such as the regulation of seasonal body weight variation, glucose intake, or adiposity, as well as to the lack of reported toxicity and association with serious adverse effects (Tan, Manchester et al. 2011), has attracted special attention as a potential therapeutic target in numerous anti-obesity studies. However, melatonin roles in obesity are not fully understood, so in this study we delve into the study of the beneficial role of melatonin in the liver of genetically obese mice.

A feature of leptin deficient mice is that the lack of this hormone makes them develop an excessive appetite and leading to weight gain uncontrollably. This metabolic overload due to the continuous supply of energy involves an increase in free radical production, responsible for the obesity characteristic oxidative stress. To characterize the oxidative status, we compared antioxidant capacity to cope oxidative damage. Thus, we

saw that our obese mice, that had ingested a large amount of food, also showed higher oxidative damage. Is noteworthy that, although obese mice showed increased SOD activity levels, CAT activity was significantly reduced in these mice, suggesting that SOD acts as a pro-oxidant in obese mice.

Melatonin, is one of the most known antioxidants, making it a good molecule study to try to mitigate the effects of obesity and its associated disorders. So as we expected, both short and long melatonin treatment reduced oxidative damage in the liver of obese mice. Although both treatment durations led to a decrease in SOD activity, it was only significant in the long treatment. On the other hand, melatonin affected CAT activity differently in obese treated mice according to treatment duration. After the short treatment CAT activity was increased, while obese mice treated for four weeks viewed decreased this enzyme activity. This leads us to think that short melatonin treatment is acting as indirect antioxidant by increasing the CAT activity, and as a direct antioxidant, through $O_2^{\cdot -}$ scavenging, which would reduce the need for an increase in SOD activity parallel to CAT. The difference in antioxidant activities found between both duration treatments could be due to that in the long treatment, melatonin has more time to act as a direct antioxidant, reducing oxidative damage and therefore decreasing the need to enhance the antioxidant activities. This is supported by higher total antioxidant activity and Nrf2 levels observed in obese mice treated with melatonin.

The close connection between oxidative stress and autophagy is well established (Scherz-Shouval and Elazar 2011; Lavallard, Meijer et al. 2012; Vega-Naredo, Caballero et al. 2012). An increase in ROS levels activate autophagy as a mechanism of protection against oxidative stress and damage (Coto-Montes, Boga et al. 2012) so, our next step was

investigate the ability of trigger autophagy response to counteract the oxidative stress associated with obesity. Thus, showed an increase in p-mTOR expression, together with a reduction in autophagy flux markers, pointing to an impairment of autophagosome formation and the interruption of autophagy activity in the liver of obese mice compared with wild-type ones. The autophagy impairment associated with obesity is confirmed by higher p62 mRNA and protein expression. As we said in the introduction, p62 is a selective substrate for autophagy, which binds to ubiquitinated protein aggregates, marking them for autophagic degradation (Komatsu 2011), so it is also a maker for autophagic flux (Mizushima and Yoshimori 2007). Thus, when p62 binds to LC3, this protein becomes internalised into the autophagosome (Komatsu 2011). Many studies have shown that, when autophagy is impaired, p62 is accumulated along with ubiquitinated aggregates (Mizushima and Yoshimori 2007; Komatsu 2011; Aghajan, Li et al. 2012), leading to increased oxidative stress (Mathew, Karp et al. 2009).

This blockage in autophagy represents the loss of a crucial proteolytic mechanism which is usually observed in other diseases, such as cancer (Ding, Ma et al. 2015), viral infection (Ding, Zhang et al. 2014) and neurodegenerative disorders such as Alzheimmer (Ling and Salvaterra 2009). The amino acids loading from the excessive food intake, is may be the cause of both high oxidative stress and autophagy blocking shown in liver of obese mice.

Treatment of obese animals with melatonin does not appear to be capable of reversing autophagy blockage, but it decreases further regardless of the duration of treatment. However, autophagy inhibition occurs at different stages depending on the duration of treatment.

The short treatment reduced Beclin-1 levels in the liver of obese mice, pointing to an inhibition of autophagy at nucleation level. Although, a higher LC3-II/LC3-I ratio was observed in the melatonin short-treated group, the results of the autophagic flux study must be interpreted with caution. Although the conversion of soluble LC3-I to lipid-bound LC3-II is typically associated with autophagosome formation, this process does not necessarily result in complete autophagy (Gimenez-Xavier, Francisco et al. 2008). Increased LC3-II levels might reflect the increased conversion of LC3-I into LC3-II but also indicate the reduced degradation of this protein through the inhibition of autophagic activity (Skop, Cahova et al. 2012). p62 expression was enhanced in obese after short melatonin treatment, supporting Beclin-1 results, and therefore the autophagy inhibition after melatonin treatment.

Regarding to obese mice subjected to prolonged treatment, they showed a lower conversion of LC3-I into LC3-II, and therefore an autophagy blocking at autophagosome transport and maturation level. Both p62 mRNA and protein support this fact, since despite ObM translated least p62, there were equivalent levels of protein than ObC, suggesting that p62 was not degraded and it was accumulated.

However, despite the reduction in autophagy activity, melatonin also reduced oxidative damage. We must consider that autophagy is primarily a cellular cleaning system, whereby organelles are destroyed for the sake of the common good. If the factor which induces damage is removed by melatonin, autophagy becomes unnecessary.

It is well stablished that autophagy plays a key role in lipid metabolism and storage (Czaja 2010; Lavallard, Meijer et al. 2012; Singh and Cuervo 2012). Autophagy limits hepatic lipid content by conducting the breakdown of the triglycerides and cholesterol stored in lipid droplets

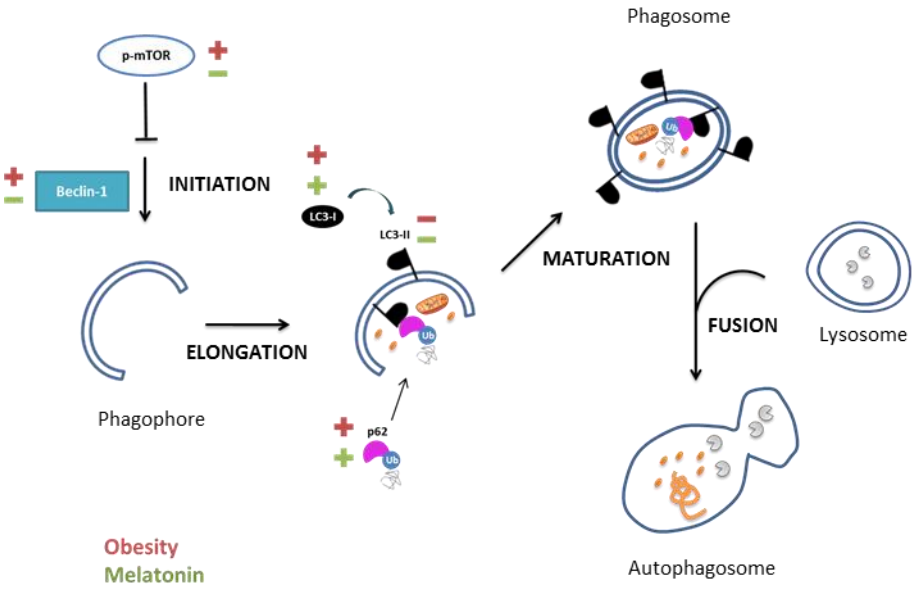

Figure 45. Effect of obesity and melatonin treatment in the hepatic autophagic flux. Despite the increased (plus) levels of p-mTOR, Beclin-1 and LC3-I, obesity (in red) causes a blockage of autophagy, as reflected in the lower (minor) levels of LC3-II, and the accumulation of p62. Melatonin treatment (in green) in turn, further reduces the levels of autophagic activity. p-mTOR, phosphorylated mammalian target of rapamycin; LC3, microtubule-associated protein 1 light chain 3 forms (LC3-I and its phosphatidylethanolamine-conjugated form LC3-II); p62 or sequestrosome-1.

(Singh, Kaushik et al. 2009). This process that regulate the lipid droplet turnover is known as lipophagy. However, not only autophagy regulates lipid metabolism but the inverse relationship also exists, since lipid stores affect autophagic function (Czaja 2010), establishing a negative feedback.

The blockage of autophagy and the reduced levels of LAL observed in obese mice, lead to defective lipid turnover and therefore, an increased number of lipid droplets.

Phospholipid monolayer surrounding lipid droplets is coated by several proteins, including perilipins (Singh and Cuervo 2012; Carr and Ahima 2015), which protect the lipid storage until it is digested. Thus,

higher perilipins levels showed by obese mice seem indicate that there is a downregulation of lipolysis.

Another indicator of the high presence and accumulation of lipids in the liver of obese mice is the large amount of fatty acid synthase observed by mass spectrometry in this experimental group. In addition, obese mice also exhibited higher PPARα mRNA levels, an essential transcription factor in the induction of fatty acid beta oxidation, and the increment in PPARγ mRNA levels which plays a key role in the adipocyte differentiation and lipogenic pathways. Taken together, these results indicate that lipogenesis and adipogenesis are enhanced, contributing to the adipogenic steatosis observed in the liver of obese mice.

On the other hand, despite ObM mice had further reduced autophagic activity, and enhanced perilpin content, also exhibited increased LAL expression, suggesting that in obese mice, melatonin promotes the lipid droplet turnover, which is associated with an improvement in liver steatosis.

In addition, melatonin treatment led to a decline in levels of fatty acid synthase, PPARα and PPARγ, pointing to a lower lipid content in the liver of treated obese mice. Furthermore, it is noteworthy that obese mice subjected to both short and long treatment showed higher levels of p62 than untreated mice. In addition to its role as marker of organelles and protein aggregates for autophagic degradation, p62 has also been implicated in various signal transduction pathways associated with obesity, such as the control of energy homeostasis and adipogenesis (Lee, Pfluger et al. 2010). Specifically, p62-knockout mice showed alterations in energy expenditure and increased PPARγ mRNA levels, increasing adipogenesis and leading to the development of obesity and insulin and

leptin resistance (Rodriguez, Duran et al. 2006). In light of this background, our results suggest that p62 acts as a negative regulator of PPARγ (Rodriguez, Duran et al. 2006), that besides being crucial in the formation and maturation of adipose tissue, has also been described as an inductor of adipogenic transformation of hepatocytes (Yu, Matsusue et al. 2003). Our results are consistent with the results of Dr. Rodriguez, as PPARγ exhibited antagonistic effects toward p62 in both ObC and ObM groups, significantly associated with decreased body or WAT weight in obese animals after melatonin treatment. The reduced PPARγ levels observed in both short and long melatonin treatments are consistent with in vitro studies, showing of the association of melatonin treatment with the suppression PPARγ expression during the early stages of adipogenesis (Alonso-Vale, Peres et al. 2009; Zhang, Su et al. 2010). These data imply that this hormone could act as a direct inhibitor of adipocyte differentiation, showing potential as a therapeutic agent for adipogenesis.

Although at first glance no differences were found between optical microscopic sections of ObC vs ObM mice, recently Stacchiotti and colleagues have reported that melatonin supplementation causes a partial conversion of macrosteatosis to microsteatosis in the liver of our experimental model (Stacchiotti, Favero et al. 2016).

The apparent lack of visually differences between ObC and ObM liver respect to Stacchiotti's work, could be due to the short duration of our treatment, along with the low daily administration of melatonin and the method of its administration compared to their study.

Summarizing what we have discussed so far, melatonin reduces autophagy processes through reducing ROS levels characteristic of obesity through scavenging free radicals, and stimulating antioxidant enzymatic

activity. This reduced autophagic activity implicates p62 accumulation in the down regulation of adipogenic pathways, accompanied by an eventual reduction in the body weight (Fig. 46). Therefore, in this first part of the study, we were not only able to describe the beneficial effects of reducing the body or WAT weight of obese animals under melatonin treatment, but we also revealed which mechanisms are modulated through melatonin induce this effect.

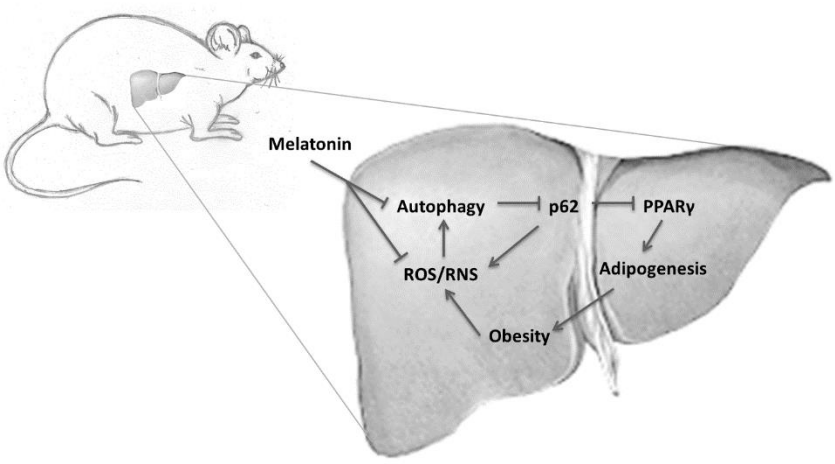

Figure 46. Melatonin administration reduced oxidative stress and autophagy levels in the liver, leading to the accumulation of p62, responsible for inactivating of the adipogenic gene PPARγ, and a decrease in body weight. ROS- reactive oxygen species; RNS- reactive nitrogen species; PPARγ –peroxisome proliferator-activated receptor gamma.

Our results clearly show that the efficiency of protein turnover is affected in the liver of obese animals. All of the UPR proteins were increased in the ObC mice as result of ER stress (Fig. 47), contributing to metabolic dysfunction and hepatic steatosis (Rutkowski and Kaufman 2007). A relationship between defective autophagy and the UPR, whichever is the inductor, has been described in other different pathologies (Sir, Chen et al. 2008). The deficiency in autophagy activity in

the ObC group led to the accumulation of damaged proteins and disturbed the ER function, which prevented the correct folding and maturation of proteins. Valko and colleagues reported that misfolded proteins are more susceptible to oxidative damage than intact proteins, so ER stress contributes to oxidative stress, resulting in a positive feedback loop (Valko, Leibfritz et al. 2007).

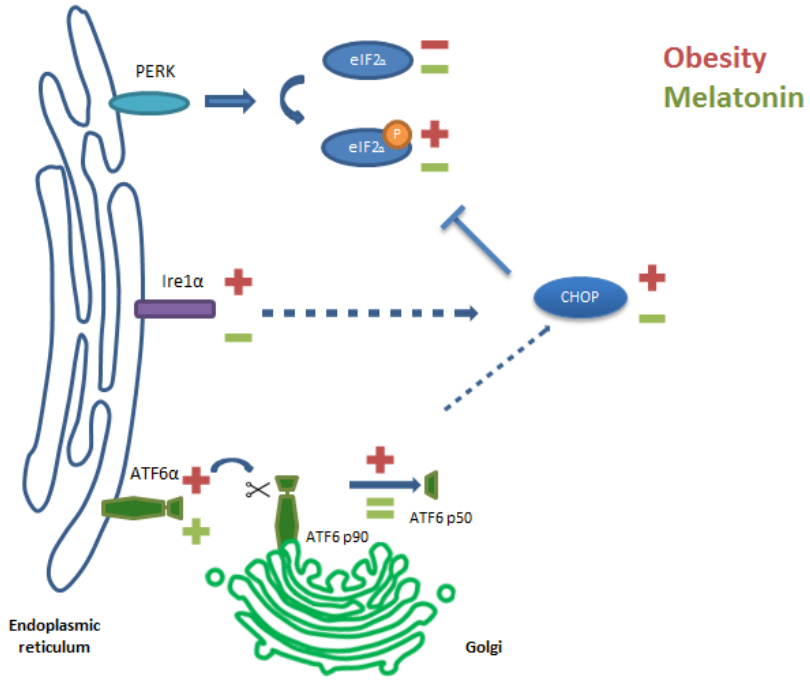

Figure 47. Effect of obesity and melatonin treatment in the hepatic unfolded protein response (UPR). Obesity (in red) activates (plus) the three main branches of the UPR: PERK, represented by the activation of eIF2α, Ire1α, and ATF6α, and CHOP as a point of confluence of the three UPR ways. Melatonin treatment (in green) significantly reduces (minus) endoplasmic reticulum stress in the liver of leptin deficient mice. ATF6α, activating transcription factor-6-α (90 kDa ATF6α – inactive form and 50 kDa ATF6α –active form); eIF2α, α-subunit of the eukaryotic initiation factor; peIF2α, eIF2α phosphorylated activated form; Ire1α, inositol-requiring enzyme-1; CHOP, C/EBP homologous protein.

However, short half-life proteins degradation through proteasome activity, and the removal of specific proteins by CMA, are properly carried out in the liver of obese mice. Although we did not seen changes in LAMP2A expression after short melatonin treatment, after four weeks melatonin treatment, both proteasome degradation, and CMA were less activated, probably due to less need for activation rather than a blockade, as we had seen in the case of autophagy. In agreement with our findings, the relationship between melatonin and proteasome inhibition has been recently described in human renal cancer cells (Vriend and Reiter 2014).

Despite the autophagy blockage, the results of the ER stress markers suggests that there was an improvement in ER state after melatonin supplementation. Thus, the phosphorylation of eIF2α as a PERK pathway marker, and the expression of Ire1α, and CHOP were all significantly decreased in the liver of ObM group. These results, and especially the decrease in Ire1α expression, not only indicate that melatonin protects against ER stress and hepatic steatosis, but also reduce the risk for developing other major disorders that are associated with obesity, including insulin resistance and type 2 diabetes. Ire1α is a point of confluence between ER stress and defective insulin signalling, so higher levels of this marker in the ObC group involve the activation of JNK, which can lead to insulin signalling disruption through inadequate phosphorylation of IRS-1 (Ozcan, Cao et al. 2004).

The observation that our obese mice show impairment in insulin signalling is supported by the results of Sirt1 protein expression and insulin receptor mRNA levels. Sirt1, is an important regulator of energy metabolism and glucose homeostasis, which also stimulate autophagic degradation (Salminen and Kaarniranta 2009), so low Sirt1 levels fit well with the decrease in autophagy activity showed in the liver of obese mice.

Sirt1 deficiency is involved in hepatic glucose overproduction, chronic hyperglycemia and the development of hepatic insulin resistance (Lagouge, Argmann et al. 2006; Wang, Kim et al. 2011; Chen, Lai et al. 2013; Favero, Franceschetti et al. 2015), thus lower Sirt1 levels observed in the ObC mice support the finding of a decline in insulin signalling. Moreover, the deficient insulin signalling of obese animals aims to be alleviated by increasing the expression of insulin receptor, as its higher mRNA levels indicate.

Similar to ER stress, insulin signalling was also improved in the liver of obese mice after melatonin treatment, as indicate the Ire1α reduction and the increase in hepatic Sirt1 levels in ObM mice. Melatonin enhancement of insulin signaling is supported by other studies conducted in rats where melatonin administration led to an enhancement in insulin function (Agil, Reiter et al. 2013; Faria, Kinote et al. 2013; Zanuto, Siqueira-Filho et al. 2013). Besides, melatonin role as improver of insulin signalling through increasing Sirt1 had been previously observed in the pancreas of mice with accelerated senescence, where insulin physiology and glucose metabolism improved after one month of melatonin treatment (Cuesta, Kireev et al. 2013). In addition, the levels of insulin receptor mRNA were decreased nearly 30% in ObM animals, supporting that insulin signalling was more efficient in this group.

Some of the results from our study must be interpreted with caution. Obese mice exhibited significantly higher levels of PI3K and p-Akt compared to WC mice. This effect is directly related to the increase in food intake in these animals, but not necessarily to an improvement in insulin pathway. We should consider that, as they intake much more food, obese mice require a greater response to insulin compared to the WC mice. However, in basis of our shown results, it is not 100% satisfied. Besides,

p62 over-expression has been related to an increasing in the insulin signalling pathway by interacting with IRS-1 and enhancing Akt phosphorylation (Manley, Williams et al. 2013). Thus, higher levels of IRS-1 downstream targets such as PI3K and Akt observed in obese mice could be due, at least in part, to the p62 positive role in insulin signaling.

Likewise, it is necessary to highlight the higher food intake observed in the ObM mice (more than 20%) compared with the ObC mice, which was also associated with a significant increase in PI3K and p-Akt. This finding emphasizes the beneficial role of melatonin in increasing the efficiency of metabolic processes. Moreover, other studies have reported that melatonin may mimic the action of leptin and insulin through the specifically activation of PI3K/Akt intracellular pathway (Slominski, Reiter et al. 2012; Szewczyk-Golec, Wozniak et al. 2015). This melatonin mechanism is consistent with the results from our WM group, which also showed an increase in the expression of these proteins. The PI3K/Akt pathway ends with mTOR phosphorylation, which showed an abrupt increase in the ObC animals, and correlates to the hepatic autophagy blockage associated with obesity. The significant reduction of p-mTOR in obese animals after melatonin treatment, even when PI3K and p-Akt expression was higher than in the ObC animals, directly correlated with a higher amino acid intake and is supported by the role of melatonin in insulin pathway activation. This observation opens up the possibility that the reduction in autophagy observed in the ObM group was not due to a blockage but rather to a reduction in misfolded proteins and oxidative stress that was induced by melatonin. In fact, WM mice also showed a significant decrease in the expression of p-mTOR compared to WC animals.

High levels of both AdipoR1 and AdipoR2 in the liver of obese mice provide an indirect measure of circulating adiponectin levels produced by WAT adipocytes. The need to improve adiponectin signalling is reflected in the high levels of mRNA of both receptors in the liver of obese mice. Besides, and as it is described by the literature, the obese mice, that exhibited higher levels of WAT, also would have adiponectin levels far below those of wild-type mice. The relationship between adiponectin and the amelioration of insulin sensitivity has been established many times, (Tomita, Oike et al. 2008; Combs and Marliss 2014; Fasshauer and Bluher 2015), so defective adiponectin signalling in obese mice supports the impairment in insulin signalling in the liver of these mice. On the other hand, melatonin treatment, in addition to reducing the amount of WAT in ObM, also reduced the expression of AdipoR1 and AdipoR2 in both phenotypes, suggesting that melatonin ameliorates adiponectin signalling and, again, supporting the fact that melatonin treatment leads to an improvement in insulin action. These findings are agree other studies in mice, other animal models of obesity and even in humans with NASH associated insulin resistance, where melatonin mediated an improvement in adipocyte metabolism together with risen adiponectin secretion and better insulin situation (Agil, Rosado et al. 2012; Gonciarz, Bielanski et al. 2013; Favero, Stacchiotti et al. 2015).

Yamauchi and colleagues have proved the role of adiponectin receptors in the activation of different signaling pathways. AdipoR1 is mainly involved in the coupling of inhibition of hepatic glucose production with the increasing of fatty acid oxidation, through the AMPK pathway, whereas AdipoR2 is more tightly linked to promotion the fatty acid oxidation through the activation of the PPARα pathway (Yamauchi, Kamon

et al. 2003). They also described that the expression levels of AdipoR1 and AdipoR2 are controlled by insulin/PI3K/Foxo1 axis, pointing that this pathway has an important role in the control of adiponectin sensitivity (Yamauchi, Kamon et al. 2003).

In addition, the activation of adiponectin/AMPK axis has been related with the suppression of the ER stress response to protect against steatosis and insulin resistance (Li, Choi et al. 2014). ObM mice, that showed better adiponectin signaling, also exhibited an enhanced AMPK phosphorylation, so melatonin maybe have improved these obesity related pathologies through activation of adiponectin/AMPK axis.

In obesity, WAT hypertrophy in addition to stimulate an adverse adipokines secretion pattern also predisposes to immune cell infiltration and inflammation (Fasshauer and Bluher 2015). Numerous studies have established a link between obesity, obesity-related diseases and inflammation based on ER stress activation (Boden, Duan et al. 2008; Manley, Williams et al. 2013; Park, Kim et al. 2014), and it is well recognized that inflammation is key player in the progression of the severity of liver complications (McCarty 2011; Bechmann, Hannivoort et al. 2012; Lavallard and Gual 2014). Our results support this background, as obese mice showed an exacerbated inflammatory liver response, through significant increment in NF-κB p65 phosphorylation of p65 and IL-6 and TNF-α levels.

As expected, based on the anti-inflammatory properties of melatonin (Cuzzocrea and Reiter 2002; Korkmaz, Reiter et al. 2009; Boga, Coto-Montes et al. 2012), these inflammatory markers are diminished in ObM animals. Our results on the effect of melatonin on ER stress and

inflammation are consistent with the work of Kim and colleagues, who showed that melatonin improves tunicamycin-induced hepatic steatosis by decreasing ER stress and the inflammatory response through regulating miR-23a (Kim, Kang et al. 2015).

Moreover, Kotas and colleagues have recently reviewed the role of Sirt1 in the repression of inflammation. They describe that Sirt1 opposes inflammation in metabolic tissues, such as the liver, by reducing TNF-α and IL-6 expression, while the specific deletion of Sirt1 increases NF-κB activity (Kotas, Gorecki et al. 2013). The anti-inflammatory property of melatonin is also consistent with the increase of Sirt1 levels that were observed in the ObM group and supports other studies that link melatonin anti-inflammatory effects with Sirt1 (Lim, Kim et al. 2012).

As a major site of energy production and lipid metabolism, mitochondria are intimately linked with the liver, and mitochondrial disorders actively participate in hepatic pathogenesis and development of steatosis and insulin resistance (Agil, El-Hammadi et al. 2015).

The oxygen consumption assays showed that the mitochondria of obese mice were slightly uncoupled respect to wild-type, reflected in the higher levels of the respiration state 4 and the reduced RCR obtained after glutamate/malate energization. This uncoupling clearly affected mitochondria phosphorylation capacity of ObC mice, since ADP/O ratio, and therefore the efficiency of oxidative phosphorylation was also decreased. In addition, the ATP produced after complex I supplementation was also significantly lower, supporting that oxidative phosphorylation is not occurring optimally in the liver of obese mice.

Due to the ability of mitochondria to accumulate melatonin, numerous studies have identified that melatonin can influence mitochondrial homeostasis (Reiter, Paredes et al. 2008; Paradies, Petrosillo et al. 2010). Thus, despite melatonin treatment did not change the ATP synthase content in ObM, the efficiency of oxidative phosphorylation associated with the complex I was greatly increased in these mice, although it was insufficient to significantly increase ATP production.

Regarding to the complex II related oxygen consumption assays (i.e. using succinate as substrate respiration and inhibiting complex I with rotenone), we showed that maximal O_2 consumption rate in the presence of ADP was increased in the liver of obese mice, but neither state 4 nor RCR were significantly altered. However, there was an inefficient oxidative phosphorylation, and a clear downward trend in the ATP production associated with succinate energization, that could be influenced by reduced hepatic SDHB complex II subunit levels observed in obese mice.

Again, melatonin treatment did not alter any of the respiratory related parameters in this electron transport chain supplementation. However, melatonin administration led to a greatly increment in the expression of SDHB complex II subunit in obese mice, which can be interpreted as an attempt to alleviate the low efficiency of oxidative phosphorylation associated with the use of succinate as a substrate for electron transport chain.

Both ATP produced during oxygen consumption assays, as basal ATP contained in isolated mitochondria indicate that obese mice, despite exhibited an exacerbated appetite, have a deficient capacity of oxidative

phosphorylation. Thus, there is a hepatic mitochondrial dysfunction associated with obesity, responsible for a lower energy production. Considering that obesity did not alter the expression levels of complex I, III and IV, we can say that, the decreased efficiency of oxidative phosphorylation, and the low ATP production is due to the drop of complex II expression levels, together with the lower ATP synthase content in the liver of ObC mice. This result is supported by Wang and colleagues study, where they described a reduction in energy production associated with a decrease in ATP synthase expression in the liver of diabetic mice (Wang, Chen et al. 2014).

On the other hand, although melatonin treatment did not alter most respiratory parameters, it resulted in higher ATP production in the liver of ObM mice. In addition, it is noteworthy the melatonin effect, by increasing the expression of the complex III and IV, in both wild-type and obese mice. This is consistent with other in vitro and in vivo experiments, were melatonin was able to maintain the efficiency and ATP synthesis through the increment of complex I, III and IV activities (Lopez, Garcia et al. 2009; Agil, El-Hammadi et al. 2015). Taken together, this results indicate that melatonin improves mitochondrial function by increasing the expression of these complexes, and ultimately enhancing the activity of the electron transport chain and oxidative phosphorylation. Melatonin treatment also improved obesity associated energy production deficit, although ObM ATP production are still far from basal ATP levels in wild-type mice.

In addition to ATP production carried out by the mitochondria, we also analysed the differences in cytosolic ATP content, to check the overall energy state of the liver cells of obese animals compared with wild-type

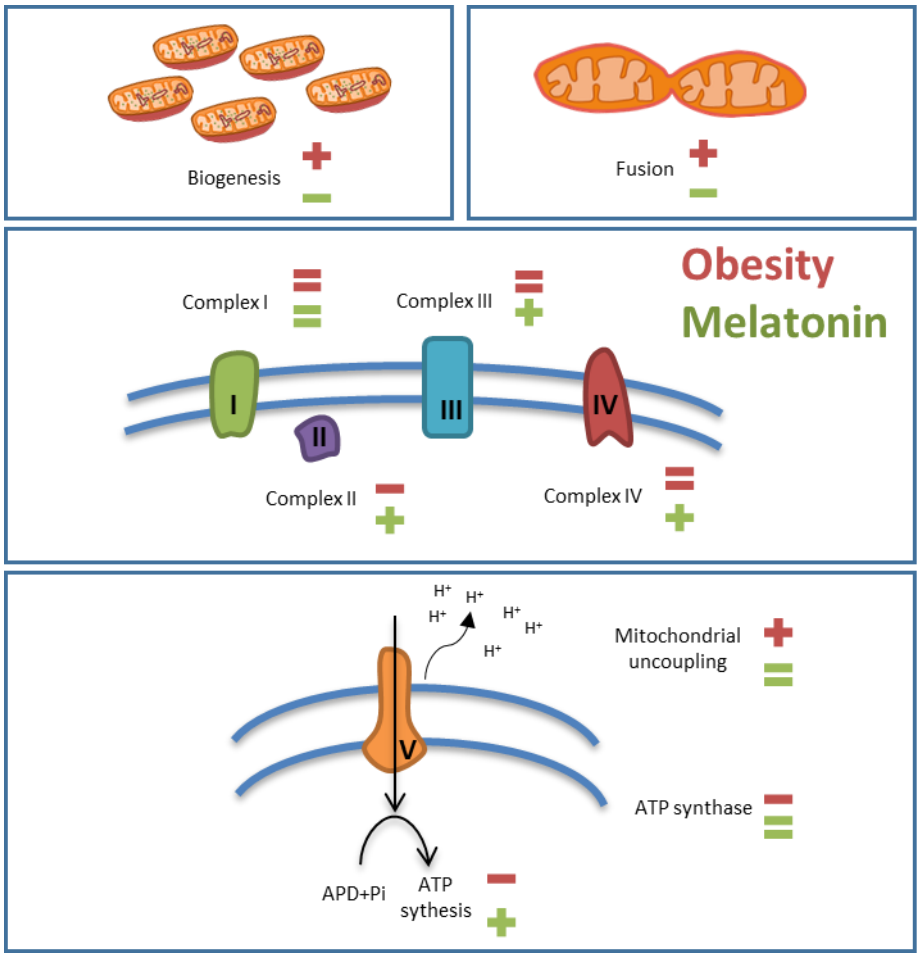

Figure 48. Effect of obesity and melatonin treatment in the hepatic mitochondrial function. Obesity (in red) is associated with liver mitochondrial dysfunction. Thus, obese mice show reduced (minus) SDHB complex II subunit and ATP5A subunit, together with decreased ATP production and increased mitochondrial uncoupling. The increase in mitochondrial fusion and biogenesis involve hepatic defence mechanisms against worse mitochondrial function as a result of obesity. Melatonin treatment (in green) significantly increases SDHB complex II subunit, UQCRC2 complex III subunit and MTCO1 complex IV subunit. Besides, despite melatonin treatment did not alter neither obesity mitocondrial uncoupling not ATP5A ATP synthase subunit, melatonin treated animals produced higher ATP amount. In addition, both biogenesis and mitochondrial fusion were reduced after melatonin treatment. NDUFB8- NADH dehydrogenase (ubiquinone) 1 b subcomplex 8 from complex I; SDHB - iron-sulfur complex II subunit; UQCRC2 - ubiquinol-cytochrome c reductase core protein II from complex III; MTCO1- cytochrome c oxidase subunit I from complex IV; ATP5A -ATP synthase subunit α; ADP- adenosine biphosphate; ATP: adenosine triphosphate.

mice. Thus, the greater amount of cytosolic ATP found in obese mice compared to wild-type points to a higher substrate-level phosphorylation associated with obesity. This makes sense if we consider the greatest amount of food ingested by obese mice. Maldi-toff analysis supports this idea, since ObC exhibited significant higher levels of the glycolytic enzyme, aldolase 2, compared with WC.

Obesity associated insulin resistance is related to the inability of insulin to suppress hepatic gluconeogenesis and promote glycolysis (Matsumoto, Han et al. 2006). Our obese melatonin treated animals have exhibited higher levels of aldolase 2, and even more cytosolic ATP than untreated mice, supporting the melatonin associated insulin signaling improvement saw above.

Many murine models of obesity and diabetes, including mice with genetic modifications and high-fat diet fed, extensively described an association between obesity and mitochondrial properties (Lacraz, Couturier et al. 2008; Perfield, Ortinau et al. 2013; Agil, El-Hammadi et al. 2015). Thus, defects in mitochondrial respiration and ATP production observed in our ObC mice were associated with changes in mitochondrial biogenesis and dynamism.

The mitochondrial dysfunction observed in obese mice would increase the AMP/ ATP ratio, leading to higher AMPK activation showed in these animals. This energy sensor is involved in many physiological functions, that include the promotion of mitochondrial biogenesis (Zhang, Zhou et al. 2009). TFAM is a key activator of mitochondrial transcription and it participates in mitochondrial genome replication, so its higer mRNA expression indicates that obese mice have enhanced mitochondrial

biogenesis. Besides, the liver of obese mice also expressed increased levels of porin, which as a mitochondrial mass marker, confirms this result.

This promotion of mitochondrial mass could be acting as a defence mechanism to try to alleviate the shortage of ATP observed in ObC mice. This higher expression of mitochondria in obesity have been previously seen by Marciniak and colleagues in heart tissue of high-fat diet fed mice, which exhibited an increased mitochondrial biogenesis, although the mitochondrial oxygen consumption was reduced (Marciniak, Marechal et al. 2014).

Otherwise, melatonin treatment resulted in a reduction in TFAM levels in both obese and wild-type treated animals, but whereas ObM mice exhibited lower levels of porin, WM did not change the content of this indicator of mitochondrial mass respect to WC. This discrepancy between TFAM and porin levels in WM mice could be due to a protective effect of melatonin for mitochondria. Thus, despite producing fewer mitochondria, they would be in better condition and their turnover would be decreased, so WM have the same amount of mitochondria than WC. Meanwhile, the decrease in ObM in both mitochondrial biogenesis and mass markers suggests that their mitochondria are more effective than obese untreated mice, so the need of this organelle is lower and its biogenesis is decreased, so this supports the beneficial role of melatonin in mitochondrial function in obesity.

Fission has been described as a factor related with nutrient excess and cellular dysfunction (Wai and Langer 2016) however, our obese animals exhibited higher levels of the fusion marker (Mfn2), and lower fission related protein (Drp1) content, compared to wild-type ones,

suggesting mitochondria of our obese mice are more aggregated than wild-type mitochondria. This result can be explained if we take into account the autophagy blocking and the mitochondrial dysfunction observed in the liver of the ObC mice. Hepatic cells have to remove damaged and non-functional mitochondria to maintain a metabolically healthy environment. However, as the obese mice have interrupted the mitochondria turnover system, this organelle is fused to optimize the resources and recover the activity of damaged or depolarised mitochondrial membranes.

Taken together, the increase in mitochondrial fusion and biogenesis involve hepatic defence mechanisms against worse mitochondrial function as a result of obesity.

Regarding the effect of melatonin in mitochondrial dynamics, obese treated mice reduced significantly both Drp1 and Mfn2 levels. Therefore, to interpret this result we must take into account the Mfn2/Drp1 ratio that points that melatonin treatment promotes mitochondrial fission in the liver of obese mice.

Considering that despite ObM mice had less mitochondrial mass and less aggregated, their ATP production was enhanced, our results suggested that melatonin treatment led to an improvement in mitochondria function in the liver of obese mice.

Under physiological condition, the MIM is impermeable to almost ions and metabolites, and it is the responsible to generate the proton-motive force to produce ATP. However, in stress conditions, specially associated with increased ROS production and low adenine nucleotide concentrations, pore opens disrupting the permeability barrier of the MIM (Paradies, Petrosillo et al. 2010). The results of the study of Bcl2 family

proteins point to an increased permeabilization of the MOM in the liver of obese mice. Besides, porin and cyclosporine D, two of the mPTP components, were also enhanced in obese mice, suggesting that the liver of obese animals is predisposed to undergo programmed cell death mechanisms. This result is supported by increased CHOP levels exhibited by ObC mice compared to wild-type. Excess free radicals and oxidative stress may contribute to increased permeability of the MOM and MIM described in obese mice, since several studies have demonstrated that ROS production and mitochondrial dysfunction are important indicators of apoptosis (Valko, Leibfritz et al. 2007; Brenner, Galluzzi et al. 2013; Wang, Li et al. 2015).

However, although MOMP and mPTP have traditionally been associated with apoptosis regulation, it has also been reported that the proteins that comprise both pores are involved in mitochondrial morphological changes in healthy cells (Karbowski, Norris et al. 2006; Wang, Li et al. 2015). Thus, Bax is necessary to the induction of mitochondrial fusion through the activation of Mfn2 (Karbowski, Norris et al. 2006), while the over-expression of the porin and cyclophilin D alters the mitochondrial morphology during early ageing in elm seeds (Wang, Li et al. 2015).

Melatonin effects in cell death mechanisms were different depending on the mouse phenotype. In this manner, apoptosis markers Bax and CHOP were decreased in obese animals after melatonin treatment. This melatonin protective effect against apoptosis has already seen in the liver of Zucker rats after ischemia/reperfusion (Kireev, Bitoun et al. 2013), and correlates well with the lower mitochondrial fusion observed in the liver of obese mice.

However, although the levels of the pro-apoptotic protein Bax were decreased after treatment in wild-type mice, the amount of anti-apoptotic Bcl2 marker was also lower. So, when we analyzed the Bax/ Bcl2 ratio we saw that, as happened with the expression of CHOP, these apoptotic markers were increased.

On the other hand, although melatonin treatment did not alter cyclophilin D levels in WM mice, it was increased in ObM. Cyclophilin D is a key regulatory component of the mPTP (Loureiro, Mesquita et al. 2013) and it has been proposed that it suppresses apoptotic cell death in a hexokinase II-dependent way in cancer cells (Machida, Ohta et al. 2006). Consequently, this higher expression of cyclophilin D in the liver of obese treated mice may be due to a greater ability to open and close the pore, rather than higher levels of apoptosis.

Although obesity is a multifactorial disorder, a reduction in plasmatic leptin levels and/or leptin resistance plays a role in the development of common forms of obesity that usually lead to extreme obesity. Therefore, using a leptin-deficient animal model, we characterized the effect of melatonin on hepatic protein and lipid metabolism, together with hepatic mitochondrial function, as major site of energy production and lipid metabolism.

The role of melatonin in the regulation of leptin, and therefore, obesity, has been previously demonstrated (Alonso-Vale, Andreotti et al. 2005; Banerjee, Udin et al. 2011). However, our study provides a substantial amount of evidence to support the potential of melatonin as a therapeutic agent for ameliorating and preventing the deleterious hepatic cellular effects that are caused by leptin deficiency or resistance. Our use of an animal model based on the common causes of obesity emphasizes the relevance of our findings.

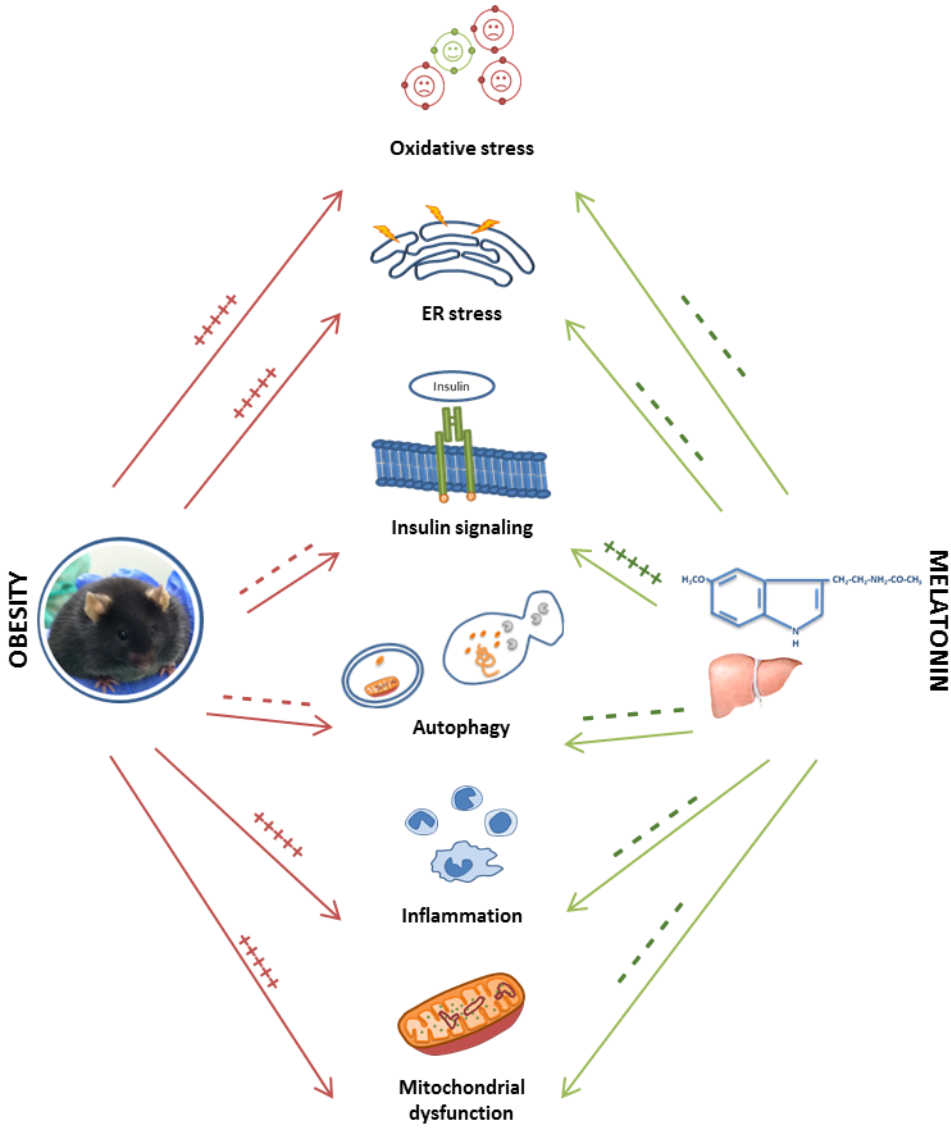

Figure. 49. Global effect of obesity and melatonin treatment in the liver of leptin-deficient mice (ob/ob). The liver of ob/ob mice (in red) exhibits enhanced (plus) oxidative and endoplasmic reticulum (ER) stress, impaired (minor) insulin signalling, blockage of autophagy, an exacerbated inflammatory response and mitochondrial dysfunction. Melatonin treatment (in green) acts as a therapeutic agent that ameliorated hepatic homeostasis by reducing oxidative and ER stress, increasing insulin signalling and decreasing inflammation and mitochondrial dysfunction. However, however, melatonin instead of reverse blocking autophagy further reduces their activity levels. ER- endoplasmic reticulum.

CONCLUSIONS

CONCLUSIONS

The liver of leptin-deficient mice presented evident alterations in lipid and glucose metabolism, mitochondrial function, oxidative and inflammatory status, and cellular quality control systems as unfolded protein response and autophagy activity. From the results obtained during the development of this PhD thesis we can conclude that:

1. Excessive appetite motivated by the absence of leptin leads to increased body and white adipose tissue weight in ob/ob mice.
2. Carbohydrate and lipid metabolism are altered in the liver of leptin-deficient mice leading to lipid droplets accumulation and hepatic steatosis development.
3. Leptin deficiency causes mitochondrial dysfunction in the liver of ob/ob mice characterized by remodelling the electron transport chain constituents, reduced oxidative phosphorylation efficiency, lower ATP production and increased permeabilization of mitochondrial outer membrane.
4. Hepatocytes of leptin-deficient mice presents exacerbated oxidative stress and blocking autophagy that lead to misfolded proteins accumulation, endoplasmic reticulum stress and triggering inflammatory response.
5. Melatonin exerts different effects in mice according to the presence or absence of leptin.
6. Melatonin treatment exacerbates appetite caused by the absence of leptin in ob/ob mice, without increasing body weight and reducing white adipose tissue content. Although melatonin treatment does not affect macroscopic parameters and the histological aspects of liver from ob/ob mice, melatonin improves

hepatic carbohydrate, lipid and mitochondrial metabolism associated with leptin deficiency. Wild-type treated mice suffer a metabolic readjustment as a result of the continued presence of an antioxidant such as melatonin, since neither food intake, body weight, or fat content are affected by melatonin treatment.

7. Melatonin treatment improves mitochondrial function in the liver of ob/ob mice by increasing oxidative phosphorylation efficiency and ATP production.
8. Melatonin treatment reduces hepatic oxidative stress and inflammatory response in leptin-deficient mice so, despite increasing autophagy blocking associated with leptin deficiency, endoplasmic reticulum stress are decreased in the liver of ob/ob melatonin treated mice.

CONCLUSIONES

El hígado de los ratones deficientes en leptina presentó alteraciones claras en el metabolismo de lípidos y de glucosa, en la función mitocondrial, en los estados oxidativo e inflamatorio y en los sistemas de control de calidad celular como la respuesta a proteínas mal plegadas y la actividad autofágica. De los resultados obtenidos a lo largo de la presente tesis doctoral, podemos concluir que:

1. El excesivo apetito motivado por la ausencia de leptina conduce a un incremento en el peso corporal y en el contenido de tejido adiposo blanco en los ratones ob/ob.
2. El metabolismo de carbohidratos y lípidos está alterado en el hígado de los ratones deficientes en leptina, dando lugar a la acumulación de gotas lipídicas y al desarrollo de esteatosis hepática.
3. La deficiencia en leptina causa disfunción mitocondrial en el hígado de los ratones ob/ob caracterizada por la remodelación de los componentes de la cadena de transporte de electrones, la disminución de la eficiencia de la fosforilación oxidativa, la menor producción de ATP y el incremento en la permeabilización de la membrana mitocondrial externa.
4. Los hepatocitos de los ratones deficientes en leptina presentan un estrés oxidativo exacerbado y un bloqueo de la autofagia que conducen a la acumulación de proteínas mal plegadas, estrés del retículo endoplásmico y al disparo de la respuesta inflamatoria.
5. La melatonina ejerce diferentes efectos en los ratones dependiendo de la presencia o ausencia de leptina.

6. El tratamiento con melatonina exacerba el apetito causado por la ausencia de leptina en los ratones ob/ob, sin incrementar el peso corporal y reduciendo el contenido del tejido adiposo blanco. Aunque el tratamiento con melatonina no afectó a los parámetros macroscópicos ni a los aspectos histológicos del hígado de los ratones ob/ob, la melatonina mejoró el metabolismo de carbohidratos, lipídico y mitocondrial asociado con la deficiencia en leptina. Los ratones wild-type tratados sufren un reajuste metabólico como resultado de la presencia continua de un antioxidante como la melatonina, ya que el tratamiento no afectó a los niveles de alimentos ingeridos, al peso corporal o a la cantidad de grasa.
7. El tratamiento con melatonina mejora la función mitocondrial en el hígado de los ratones ob/ob incrementando la eficiencia de la fosforilación oxidativa y la producción de ATP.
8. El tratamiento con melatonina reduce el estrés oxidativo hepático, y la respuesta inflamatoria en el hígado de los ratones deficientes en leptina ya que, a pesar de incrementar el bloqueo autofágico asociado con la deficiencia en leptina, se redujo el estrés del retículo endoplásmico en el hígado de los ratones ob/ob sometidos a tratamiento.

BIBLIOGRAPHY

(2013). "Obesity and overweight.", pp.311.
Adams, J. (2003). "The proteasome: structure, function, and role in the cell." Cancer Treat Rev **29 Suppl 1**: 3-9.
Aghajan, M., N. Li, et al. (2012). "Obesity, autophagy and the pathogenesis of liver and pancreatic cancers." J Gastroenterol Hepatol **27 Suppl 2**: 10-14.
Agil, A., M. El-Hammadi, et al. (2015). "Melatonin reduces hepatic mitochondrial dysfunction in diabetic obese rats." J Pineal Res **59**(1): 70-79.
Agil, A., R. J. Reiter, et al. (2013). "Melatonin ameliorates low-grade inflammation and oxidative stress in young Zucker diabetic fatty rats." J Pineal Res **54**(4): 381-388.
Agil, A., I. Rosado, et al. (2012). "Melatonin improves glucose homeostasis in young Zucker diabetic fatty rats." J Pineal Res **52**(2): 203-210.
Alonso-Vale, M. I., S. Andreotti, et al. (2006). "Intermittent and rhythmic exposure to melatonin in primary cultured adipocytes enhances the insulin and dexamethasone effects on leptin expression." J Pineal Res **41**(1): 28-34.
Alonso-Vale, M. I., S. Andreotti, et al. (2005). "Melatonin enhances leptin expression by rat adipocytes in the presence of insulin." Am J Physiol Endocrinol Metab **288**(4): E805-812.
Alonso-Vale, M. I., S. B. Peres, et al. (2009). "Adipocyte differentiation is inhibited by melatonin through the regulation of C/EBPbeta transcriptional activity." J Pineal Res **47**(3): 221-227.
Andreeva, L., R. Heads, et al. (1999). "Cyclophilins and their possible role in the stress response." Int J Exp Pathol **80**(6): 305-315.
Arnao MB, C. A., Acosta M (2001). "The hydrophilic and lipophilic contribution to total antioxidant activity." Food Chemistry **73**: 239-244.
Aronson, D. and E. J. Rayfield (2002). "How hyperglycemia promotes atherosclerosis: molecular mechanisms." Cardiovasc Diabetol **1**: 1.
Axe, E. L., S. A. Walker, et al. (2008). "Autophagosome formation from membrane compartments enriched in phosphatidylinositol 3-phosphate and dynamically connected to the endoplasmic reticulum." J Cell Biol **182**(4): 685-701.
Banerjee, A., S. Udin, et al. (2011). "Regulation of leptin synthesis in white adipose tissue of the female fruit bat, Cynopterus sphinx: role of melatonin with or without insulin." Exp Physiol **96**(2): 216-225.

Baratta, F., D. Pastori, et al. (2015). "Does Lysosomial Acid Lipase Reduction Play a Role in Adult Non-Alcoholic Fatty Liver Disease?" Int J Mol Sci **16**(12): 28014-28021.

Bardag-Gorce, F. (2010). "Effects of ethanol on the proteasome interacting proteins." World J Gastroenterol **16**(11): 1349-1357.

Barlow, A. D. and D. C. Thomas (2015). "Autophagy in diabetes: beta-cell dysfunction, insulin resistance, and complications." DNA Cell Biol **34**(4): 252-260.

Bechmann, L. P., R. A. Hannivoort, et al. (2012). "The interaction of hepatic lipid and glucose metabolism in liver diseases." J Hepatol **56**(4): 952-964.

Beltowski, J., G. Wojcicka, et al. (2000). "The effect of dietary-induced obesity on lipid peroxidation, antioxidant enzymes and total plasma antioxidant capacity." J Physiol Pharmacol **51**(4 Pt 2): 883-896.

Bijland, S., S. J. Mancini, et al. (2013). "Role of AMP-activated protein kinase in adipose tissue metabolism and inflammation." Clin Sci (Lond) **124**(8): 491-507.

Boden, G., X. Duan, et al. (2008). "Increase in endoplasmic reticulum stress-related proteins and genes in adipose tissue of obese, insulin-resistant individuals." Diabetes **57**(9): 2438-2444.

Boga, J. A., A. Coto-Montes, et al. (2012). "Beneficial actions of melatonin in the management of viral infections: a new use for this "molecular handyman"?" Rev Med Virol **22**(5): 323-338.

Bouloumie, A., T. Marumo, et al. (1999). "Leptin induces oxidative stress in human endothelial cells." FASEB J **13**(10): 1231-1238.

Bradford, M. M. (1976). "A rapid and sensitive method for the quantitation of microgram quantities of protein utilizing the principle of protein-dye binding." Anal Biochem **72**: 248-254.

Brenner, C., L. Galluzzi, et al. (2013). "Decoding cell death signals in liver inflammation." J Hepatol **59**(3): 583-594.

Carr, R. M. and R. S. Ahima (2015). "Pathophysiology of lipid droplet proteins in liver diseases." Exp Cell Res.

Carr, R. M. and J. Correnti (2015). "Insulin resistance in clinical and experimental alcoholic liver disease." Ann N Y Acad Sci.

Carrillo-Vico, A., J. M. Guerrero, et al. (2005). "A review of the multiple actions of melatonin on the immune system." Endocrine **27**(2): 189-200.

Cipolla-Neto, J., F. G. Amaral, et al. (2014). "Melatonin, energy metabolism, and obesity: a review." J Pineal Res **56**(4): 371-381.

Cizza, G., M. Requena, et al. (2011). "Chronic sleep deprivation and seasonality: implications for the obesity epidemic." J Endocrinol Invest **34**(10): 793-800.
Combs, T. P. and E. B. Marliss (2014). "Adiponectin signaling in the liver." Rev Endocr Metab Disord **15**(2): 137-147.
Coto-Montes, A., J. A. Boga, et al. (2012). "Role of melatonin in the regulation of autophagy and mitophagy: a review." Mol Cell Endocrinol **361**(1-2): 12-23.
Coto-Montes, A. and R. Hardeland (1999). "Antioxidative effects of melatonin in Drosophila melanogaster: antagonization of damage induced by the inhibition of catalase." J Pineal Res **27**(3): 154-158.
Couillard, C., P. Mauriege, et al. (2000). "Hyperleptinemia is more closely associated with adipose cell hypertrophy than with adipose tissue hyperplasia." Int J Obes Relat Metab Disord **24**(6): 782-788.
Craigen, W. J. (2010). Mitocondrial disorders.
Crompton, M. (2000). "Mitochondrial intermembrane junctional complexes and their role in cell death." J Physiol **529 Pt 1**: 11-21.
Cuervo, A. M. (2004). "Autophagy: many paths to the same end." Mol Cell Biochem **263**(1-2): 55-72.
Cuervo, A. M. and E. Wong (2014). "Chaperone-mediated autophagy: roles in disease and aging." Cell Res **24**(1): 92-104.
Cuesta, S., R. Kireev, et al. (2013). "Melatonin can improve insulin resistance and aging-induced pancreas alterations in senescence-accelerated prone male mice (SAMP8)." Age (Dordr) **35**(3): 659-671.
Cuzzocrea, S. and R. J. Reiter (2002). "Pharmacological actions of melatonin in acute and chronic inflammation." Curr Top Med Chem **2**(2): 153-165.
Czaja, M. J. (2010). "Autophagy in health and disease. 2. Regulation of lipid metabolism and storage by autophagy: pathophysiological implications." Am J Physiol Cell Physiol **298**(5): C973-978.
Chen, Y. R., Y. L. Lai, et al. (2013). "SIRT1 interacts with metabolic transcriptional factors in the pancreas of insulin-resistant and calorie-restricted rats." Mol Biol Rep **40**(4): 3373-3380.
Davi, G., M. T. Guagnano, et al. (2002). "Platelet activation in obese women: role of inflammation and oxidant stress." JAMA **288**(16): 2008-2014.
de Brito, O. M. and L. Scorrano (2008). "Mitofusin 2 tethers endoplasmic reticulum to mitochondria." Nature **456**(7222): 605-610.

de Gonzalo-Calvo, D., K. Neitzert, et al. (2010). "Differential inflammatory responses in aging and disease: TNF-alpha and IL-6 as possible biomarkers." Free Radic Biol Med **49**(5): 733-737.
Ding, B., G. Zhang, et al. (2014). "Phosphoprotein of human parainfluenza virus type 3 blocks autophagosome-lysosome fusion to increase virus production." Cell Host Microbe **15**(5): 564-577.
Ding, L., G. Ma, et al. (2015). "Autophagy Blockage Enhances Radiosensitivity of Osteosarcoma MG-63 Cells In Vitro." Clin Lab **61**(10): 1365-1372.
Egan, B. M., E. L. Greene, et al. (2001). "Insulin resistance and cardiovascular disease." Am J Hypertens **14**(6 Pt 2): 116S-125S.
Esterbauer, H., R. J. Schaur, et al. (1991). "Chemistry and biochemistry of 4-hydroxynonenal, malonaldehyde and related aldehydes." Free Radic Biol Med **11**(1): 81-128.
Fan, L., G. Sun, et al. (2013). "Melatonin reverses tunicamycin-induced endoplasmic reticulum stress in human hepatocellular carcinoma cells and improves cytotoxic response to doxorubicin by increasing CHOP and decreasing survivin." J Pineal Res **55**(2): 184-194.
Faria, J. A., A. Kinote, et al. (2013). "Melatonin acts through MT1/MT2 receptors to activate hypothalamic Akt and suppress hepatic gluconeogenesis in rats." Am J Physiol Endocrinol Metab **305**(2): E230-242.
Fasshauer, M. and M. Bluher (2015). "Adipokines in health and disease." Trends Pharmacol Sci **36**(7): 461-470.
Favero, G., L. Franceschetti, et al. (2015). "Sirtuins, aging, and cardiovascular risks." Age (Dordr) **37**(4): 9804.
Favero, G., A. Stacchiotti, et al. (2015). "Melatonin reduces obesity and restores adipokine patterns and metabolism in obese (ob/ob) mice." Nutr Res **35**(10): 891-900.
Fernandez-Real, J. M., M. Broch, et al. (2003). "Insulin resistance, inflammation, and serum fatty acid composition." Diabetes Care **26**(5): 1362-1368.
Fidaleo, M., S. Arnauld, et al. (2011). "A role for the peroxisomal 3-ketoacyl-CoA thiolase B enzyme in the control of PPARalpha-mediated upregulation of SREBP-2 target genes in the liver." Biochimie **93**(5): 876-891.
Frezza, C., S. Cipolat, et al. (2006). "OPA1 controls apoptotic cristae remodeling independently from mitochondrial fusion." Cell **126**(1): 177-189.

Fu, S., S. M. Watkins, et al. (2012). "The role of endoplasmic reticulum in hepatic lipid homeostasis and stress signaling." Cell Metab **15**(5): 623-634.
Fu, Y., N. Luo, et al. (2005). "Adiponectin promotes adipocyte differentiation, insulin sensitivity, and lipid accumulation." J Lipid Res **46**(7): 1369-1379.
Garcia-Cazarin, M. L., N. N. Snider, et al. (2011). "Mitochondrial isolation from skeletal muscle." J Vis Exp(49).
Geetha, T., C. Zheng, et al. (2012). "Sequestosome 1/p62, a scaffolding protein, is a newly identified partner of IRS-1 protein." J Biol Chem **287**(35): 29672-29678.
Gerstner, J. R. and J. C. Yin (2010). "Circadian rhythms and memory formation." Nat Rev Neurosci **11**(8): 577-588.
Gimenez-Xavier, P., R. Francisco, et al. (2008). "LC3-I conversion to LC3-II does not necessarily result in complete autophagy." Int J Mol Med **22**(6): 781-785.
Goldman, S., Y. Zhang, et al. (2010). "Autophagy and adipogenesis: implications in obesity and type II diabetes." Autophagy **6**(1): 179-181.
Gonciarz, M., W. Bielanski, et al. (2013). "Plasma insulin, leptin, adiponectin, resistin, ghrelin, and melatonin in nonalcoholic steatohepatitis patients treated with melatonin." J Pineal Res **54**(2): 154-161.
Gotoh, T., M. Endo, et al. (2011). "Endoplasmic reticulum stress-related inflammation and cardiovascular diseases." Int J Inflam **2011**: 259462.
Groll, M. and B. C. Potts (2011). "Proteasome structure, function, and lessons learned from beta-lactone inhibitors." Curr Top Med Chem **11**(23): 2850-2878.
Gustafson, B., S. Hedjazifar, et al. (2015). "Insulin resistance and impaired adipogenesis." Trends Endocrinol Metab **26**(4): 193-200.
Hardeland, R. (2009). "Melatonin: signaling mechanisms of a pleiotropic agent." Biofactors **35**(2): 183-192.
Hardeland, R. (2013). "Melatonin and the theories of aging: a critical appraisal of melatonin's role in antiaging mechanisms." J Pineal Res **55**(4): 325-356.
Havlis, J., H. Thomas, et al. (2003). "Fast-response proteomics by accelerated in-gel digestion of proteins." Anal Chem **75**(6): 1300-1306.
Hayashi-Nishino, M., N. Fujita, et al. (2009). "A subdomain of the endoplasmic reticulum forms a cradle for autophagosome formation." Nat Cell Biol **11**(12): 1433-1437.

Holmstrom, M. H., R. Z. Tom, et al. (2013). "Effect of leptin treatment on mitochondrial function in obese leptin-deficient ob/ob mice." Metabolism **62**(9): 1258-1267.
Hoyer-Hansen, M. and M. Jaattela (2007). "Connecting endoplasmic reticulum stress to autophagy by unfolded protein response and calcium." Cell Death Differ **14**(9): 1576-1582.
Huo, J., Y. Ma, et al. (2016). "Loss of Fas apoptosis inhibitory molecule leads to spontaneous obesity and hepatosteatosis." Cell Death Dis **7**: e2091.
Jami, M. S., C. Barreiro, et al. (2010). "Proteome analysis of the penicillin producer Penicillium chrysogenum: characterization of protein changes during the industrial strain improvement." Mol Cell Proteomics **9**(6): 1182-1198.
Ji, C. and N. Kaplowitz (2006). "ER stress: can the liver cope?" J Hepatol **45**(2): 321-333.
Jo, Y. H. and C. Buettner (2014). "Why leptin keeps you warm." Mol Metab **3**(8): 779-780.
Jung, U. J. and M. S. Choi (2014). "Obesity and its metabolic complications: the role of adipokines and the relationship between obesity, inflammation, insulin resistance, dyslipidemia and nonalcoholic fatty liver disease." Int J Mol Sci **15**(4): 6184-6223.
Karbowski, M., K. L. Norris, et al. (2006). "Role of Bax and Bak in mitochondrial morphogenesis." Nature **443**(7112): 658-662.
Kasim-Karakas, S. E., H. Vriend, et al. (1996). "Effects of dietary carbohydrates on glucose and lipid metabolism in golden Syrian hamsters." J Lab Clin Med **128**(2): 208-213.
Kim, S. J., H. S. Kang, et al. (2015). "Melatonin ameliorates ER stress-mediated hepatic steatosis through miR-23a in the liver." Biochem Biophys Res Commun **458**(3): 462-469.
Kim, T. W., J. H. Jeong, et al. (2015). "The impact of sleep and circadian disturbance on hormones and metabolism." Int J Endocrinol **2015**: 591729.
Kireev, R., S. Bitoun, et al. (2013). "Melatonin treatment protects liver of Zucker rats after ischemia/reperfusion by diminishing oxidative stress and apoptosis." Eur J Pharmacol **701**(1-3): 185-193.
Kirsz, K., M. Szczesna, et al. (2014). "Influence of season and nutritional status on the direct effects of leptin, orexin-A and ghrelin on luteinizing hormone and growth hormone secretion in the ovine pituitary explant model." Domest Anim Endocrinol **48**: 69-76.
Klemm, D. J., J. W. Leitner, et al. (2001). "Insulin-induced adipocyte differentiation. Activation of CREB rescues adipogenesis from the

arrest caused by inhibition of prenylation." J Biol Chem **276**(30): 28430-28435.
Komatsu, M. (2011). "Potential role of p62 in tumor development." Autophagy **7**(9): 1088-1090.
Korkmaz, A., R. J. Reiter, et al. (2009). "Melatonin: an established antioxidant worthy of use in clinical trials." Mol Med **15**(1-2): 43-50.
Kotas, M. E., M. C. Gorecki, et al. (2013). "Sirtuin-1 is a nutrient-dependent modulator of inflammation." Adipocyte **2**(2): 113-118.
Kus, I., M. Sarsilmaz, et al. (2004). "Pinealectomy increases and exogenous melatonin decreases leptin production in rat anterior pituitary cells: an immunohistochemical study." Physiol Res **53**(4): 403-408.
Lacraz, G., K. Couturier, et al. (2008). "Liver mitochondrial properties from the obesity-resistant Lou/C rat." Int J Obes (Lond) **32**(4): 629-638.
Lagouge, M., C. Argmann, et al. (2006). "Resveratrol improves mitochondrial function and protects against metabolic disease by activating SIRT1 and PGC-1alpha." Cell **127**(6): 1109-1122.
Lavallard, V. J. and P. Gual (2014). "Autophagy and non-alcoholic fatty liver disease." Biomed Res Int **2014**: 120179.
Lavallard, V. J., A. J. Meijer, et al. (2012). "Autophagy, signaling and obesity." Pharmacol Res **66**(6): 513-525.
Lee, S. J., P. T. Pfluger, et al. (2010). "A functional role for the p62-ERK1 axis in the control of energy homeostasis and adipogenesis." EMBO Rep **11**(3): 226-232.
Levine, R. L., D. Garland, et al. (1990). "Determination of carbonyl content in oxidatively modified proteins." Methods Enzymol **186**: 464-478.
Li, X., Y. Choi, et al. (2014). "Piperonal prevents high-fat diet-induced hepatic steatosis and insulin resistance in mice via activation of adiponectin/AMPK pathway." Int J Obes (Lond) **38**(1): 140-147.
Liang, F., S. Kume, et al. (2009). "SIRT1 and insulin resistance." Nat Rev Endocrinol **5**(7): 367-373.
Lim, H. D., Y. S. Kim, et al. (2012). "Cytoprotective and anti-inflammatory effects of melatonin in hydrogen peroxide-stimulated CHON-001 human chondrocyte cell line and rabbit model of osteoarthritis via the SIRT1 pathway." J Pineal Res **53**(3): 225-237.
Lin, Z., F. Wu, et al. (2014). "Adiponectin protects against acetaminophen-induced mitochondrial dysfunction and acute

liver injury by promoting autophagy in mice." J Hepatol **61**(4): 825-831.
Ling, D. and P. M. Salvaterra (2009). "A central role for autophagy in Alzheimer-type neurodegeneration." Autophagy **5**(5): 738-740.
Lopez-Erauskin, J., J. Galino, et al. (2012). "Oxidative stress modulates mitochondrial failure and cyclophilin D function in X-linked adrenoleukodystrophy." Brain **135**(Pt 12): 3584-3598.
Lopez, A., J. A. Garcia, et al. (2009). "Melatonin protects the mitochondria from oxidative damage reducing oxygen consumption, membrane potential, and superoxide anion production." J Pineal Res **46**(2): 188-198.
Loschen, G., A. Azzi, et al. (1974). "Superoxide radicals as precursors of mitochondrial hydrogen peroxide." FEBS Lett **42**(1): 68-72.
Loureiro, R., S. Magalhaes-Novais, et al. (2015). "Melatonin antiproliferative effects require active mitochondrial function in embryonal carcinoma cells." Oncotarget **6**(19): 17081-17096.
Loureiro, R., K. A. Mesquita, et al. (2013). "Mitochondria in cancer stem cells: a target for therapy." Recent Pat Endocr Metab Immune Drug Discov **7**(2): 102-114.
Lubinsky, S. and G. C. Bewley (1979). "Genetics of Catalase in DROSOPHILA MELANOGASTER: Rates of Synthesis and Degradation of the Enzyme in Flies Aneuploid and Euploid for the Structural Gene." Genetics **91**(4): 723-742.
Machida, K., Y. Ohta, et al. (2006). "Suppression of apoptosis by cyclophilin D via stabilization of hexokinase II mitochondrial binding in cancer cells." J Biol Chem **281**(20): 14314-14320.
Malhi, H. and R. J. Kaufman (2011). "Endoplasmic reticulum stress in liver disease." J Hepatol **54**(4): 795-809.
Malik, S. A., G. Marino, et al. (2011). "Neuroendocrine regulation of autophagy by leptin." Cell Cycle **10**(17): 2917-2923.
Manley, S., J. A. Williams, et al. (2013). "Role of p62/SQSTM1 in liver physiology and pathogenesis." Exp Biol Med (Maywood) **238**(5): 525-538.
Mantele, S., D. T. Otway, et al. (2012). "Daily rhythms of plasma melatonin, but not plasma leptin or leptin mRNA, vary between lean, obese and type 2 diabetic men." PLoS One **7**(5): e37123.
Marciniak, C., X. Marechal, et al. (2014). "Cardiac contractile function and mitochondrial respiration in diabetes-related mouse models." Cardiovasc Diabetol **13**: 118.
Marciniak, S. J., C. Y. Yun, et al. (2004). "CHOP induces death by promoting protein synthesis and oxidation in the stressed endoplasmic reticulum." Genes Dev **18**(24): 3066-3077.

Mari, M., S. A. Tooze, et al. (2011). "The puzzling origin of the autophagosomal membrane." F1000 Biol Rep **3**: 25.
Martin, J. P., Jr., M. Dailey, et al. (1987). "Negative and positive assays of superoxide dismutase based on hematoxylin autoxidation." Arch Biochem Biophys **255**(2): 329-336.
Matas, J., N. T. Young, et al. (2009). "Increased expression and intramitochondrial translocation of cyclophilin-D associates with increased vulnerability of the permeability transition pore to stress-induced opening during compensated ventricular hypertrophy." J Mol Cell Cardiol **46**(3): 420-430.
Mathew, R., C. M. Karp, et al. (2009). "Autophagy suppresses tumorigenesis through elimination of p62." Cell **137**(6): 1062-1075.
Matsumoto, M., S. Han, et al. (2006). "Dual role of transcription factor FoxO1 in controlling hepatic insulin sensitivity and lipid metabolism." J Clin Invest **116**(9): 2464-2472.
McCarty, M. F. (2011). "Full-spectrum antioxidant therapy featuring astaxanthin coupled with lipoprivic strategies and salsalate for management of non-alcoholic fatty liver disease." Med Hypotheses **77**(4): 550-556.
Mizushima, N. and T. Yoshimori (2007). "How to interpret LC3 immunoblotting." Autophagy **3**(6): 542-545.
Montgomery, M. K. and N. Turner (2015). "Mitochondrial dysfunction and insulin resistance: an update." Endocr Connect **4**(1): R1-R15.
Muriach, M., M. Flores-Bellver, et al. (2014). "Diabetes and the brain: oxidative stress, inflammation, and autophagy." Oxid Med Cell Longev **2014**: 102158.
Nunn, A. V., J. Bell, et al. (2007). "The integration of lipid-sensing and anti-inflammatory effects: how the PPARs play a role in metabolic balance." Nucl Recept **5**(1): 1.
Ohrvall, M., S. Tengblad, et al. (1993). "Lower tocopherol serum levels in subjects with abdominal adiposity." J Intern Med **234**(1): 53-60.
Oliván, M., V. Fernández-Suárez, et al. (2016). "Identification of Biomarkers of Stress in Meat of Pigs Managed under Different Mixing Treatments." British Biotechnology Journal **11**(1): 1-13.
Ozcan, L., J. Cristina de Souza, et al. (2013). "Activation of calcium/calmodulin-dependent protein kinase II in obesity mediates suppression of hepatic insulin signaling." Cell Metab **18**(6): 803-815.
Ozcan, U., Q. Cao, et al. (2004). "Endoplasmic reticulum stress links obesity, insulin action, and type 2 diabetes." Science **306**(5695): 457-461.

Paradies, G., V. Paradies, et al. (2014). "Oxidative stress, cardiolipin and mitochondrial dysfunction in nonalcoholic fatty liver disease." World J Gastroenterol **20**(39): 14205-14218.

Paradies, G., G. Petrosillo, et al. (2010). "Melatonin, cardiolipin and mitochondrial bioenergetics in health and disease." J Pineal Res **48**(4): 297-310.

Park, M. H., D. H. Kim, et al. (2014). "Age-related inflammation and insulin resistance: a review of their intricate interdependency." Arch Pharm Res **37**(12): 1507-1514.

Pearson, G. L., N. Mellett, et al. (2014). "Lysosomal acid lipase and lipophagy are constitutive negative regulators of glucose-stimulated insulin secretion from pancreatic beta cells." Diabetologia **57**(1): 129-139.

Perez-Carreras, M., P. Del Hoyo, et al. (2003). "Defective hepatic mitochondrial respiratory chain in patients with nonalcoholic steatohepatitis." Hepatology **38**(4): 999-1007.

Perfield, J. W., 2nd, L. C. Ortinau, et al. (2013). "Altered hepatic lipid metabolism contributes to nonalcoholic fatty liver disease in leptin-deficient Ob/Ob mice." J Obes **2013**: 296537.

Pfluger, P. T., D. Herranz, et al. (2008). "Sirt1 protects against high-fat diet-induced metabolic damage." Proc Natl Acad Sci U S A **105**(28): 9793-9798.

Picard, F., M. Kurtev, et al. (2004). "Sirt1 promotes fat mobilization in white adipocytes by repressing PPAR-gamma." Nature **429**(6993): 771-776.

Puigserver, P. and B. M. Spiegelman (2003). "Peroxisome proliferator-activated receptor-gamma coactivator 1 alpha (PGC-1 alpha): transcriptional coactivator and metabolic regulator." Endocr Rev **24**(1): 78-90.

Purushotham, A., T. T. Schug, et al. (2009). "Hepatocyte-specific deletion of SIRT1 alters fatty acid metabolism and results in hepatic steatosis and inflammation." Cell Metab **9**(4): 327-338.

Putti, R., R. Sica, et al. (2015). "Diet impact on mitochondrial bioenergetics and dynamics." Front Physiol **6**: 109.

Ramis, M. R., S. Esteban, et al. (2015). "Caloric restriction, resveratrol and melatonin: Role of SIRT1 and implications for aging and related-diseases." Mech Ageing Dev **146-148**: 28-41.

Reiter, R. J., S. D. Paredes, et al. (2008). "Melatonin combats molecular terrorism at the mitochondrial level." Interdiscip Toxicol **1**(2): 137-149.

Reiter, R. J., D. X. Tan, et al. (2010). "Melatonin: a multitasking molecule." Prog Brain Res **181**: 127-151.

Reiter, R. J., D. X. Tan, et al. (2012). "Obesity and metabolic syndrome: association with chronodisruption, sleep deprivation, and melatonin suppression." Ann Med **44**(6): 564-577.
Reiter, R. J., D. X. Tan, et al. (2003). "Melatonin as an antioxidant: biochemical mechanisms and pathophysiological implications in humans." Acta Biochim Pol **50**(4): 1129-1146.
Rivara, S., D. Pala, et al. (2015). "Therapeutic uses of melatonin and melatonin derivatives: a patent review (2012 - 2014)." Expert Opin Ther Pat: 1-17.
Rodgers, J. T., C. Lerin, et al. (2005). "Nutrient control of glucose homeostasis through a complex of PGC-1alpha and SIRT1." Nature **434**(7029): 113-118.
Rodriguez, A., A. Duran, et al. (2006). "Mature-onset obesity and insulin resistance in mice deficient in the signaling adapter p62." Cell Metab **3**(3): 211-222.
Ros Perez, M. and G. Medina-Gomez (2011). "[Obesity, adipogenesis and insulin resistance]." Endocrinol Nutr **58**(7): 360-369.
Rui, L. (2014). "Energy metabolism in the liver." Compr Physiol **4**(1): 177-197.
Rutkowski, D. T. and R. J. Kaufman (2007). "That which does not kill me makes me stronger: adapting to chronic ER stress." Trends Biochem Sci **32**(10): 469-476.
Sainz, N., A. Rodriguez, et al. (2010). "Leptin administration downregulates the increased expression levels of genes related to oxidative stress and inflammation in the skeletal muscle of ob/ob mice." Mediators Inflamm **2010**: 784343.
Saito, I., K. Yonemasu, et al. (2003). "Association of body mass index, body fat, and weight gain with inflammation markers among rural residents in Japan." Circ J **67**(4): 323-329.
Salminen, A. and K. Kaarniranta (2009). "SIRT1: regulation of longevity via autophagy." Cell Signal **21**(9): 1356-1360.
Saltiel, A. R. and J. E. Pessin (2002). "Insulin signaling pathways in time and space." Trends Cell Biol **12**(2): 65-71.
Salvi, M., V. Battaglia, et al. (2007). "Catalase takes part in rat liver mitochondria oxidative stress defense." J Biol Chem **282**(33): 24407-24415.
Scatena, R., P. Bottoni, et al. (2007). "The role of mitochondria in pharmacotoxicology: a reevaluation of an old, newly emerging topic." Am J Physiol Cell Physiol **293**(1): C12-21.
Scherz-Shouval, R. and Z. Elazar (2011). "Regulation of autophagy by ROS: physiology and pathology." Trends Biochem Sci **36**(1): 30-38.

Schroder, M. and R. J. Kaufman (2005). "ER stress and the unfolded protein response." Mutat Res **569**(1-2): 29-63.
Shoelson, S. E., J. Lee, et al. (2003). "Inflammation and the IKK beta/I kappa B/NF-kappa B axis in obesity- and diet-induced insulin resistance." Int J Obes Relat Metab Disord **27 Suppl 3**: S49-52.
Silva, A. M. and P. J. Oliveira (2012). "Evaluation of respiration with clark type electrode in isolated mitochondria and permeabilized animal cells." Methods Mol Biol **810**: 7-24.
Singh, R. and A. M. Cuervo (2012). "Lipophagy: connecting autophagy and lipid metabolism." Int J Cell Biol **2012**: 282041.
Singh, R., S. Kaushik, et al. (2009). "Autophagy regulates lipid metabolism." Nature **458**(7242): 1131-1135.
Singh, R., Y. Xiang, et al. (2009). "Autophagy regulates adipose mass and differentiation in mice." J Clin Invest **119**(11): 3329-3339.
Sir, D., W. L. Chen, et al. (2008). "Induction of incomplete autophagic response by hepatitis C virus via the unfolded protein response." Hepatology **48**(4): 1054-1061.
Skop, V., M. Cahova, et al. (2012). "Autophagy-lysosomal pathway is involved in lipid degradation in rat liver." Physiol Res **61**(3): 287-297.
Slominski, R. M., R. J. Reiter, et al. (2012). "Melatonin membrane receptors in peripheral tissues: distribution and functions." Mol Cell Endocrinol **351**(2): 152-166.
Speakman, J., C. Hambly, et al. (2007). "Animal models of obesity." Obes Rev **8 Suppl 1**: 55-61.
Stacchiotti, A., G. Favero, et al. (2016). "Hepatic Macrosteatosis Is Partially Converted to Microsteatosis by Melatonin Supplementation in ob/ob Mice Non-Alcoholic Fatty Liver Disease." PLoS One **11**(1): e0148115.
Stadtman, E. R. (2004). "Role of oxidant species in aging." Curr Med Chem **11**(9): 1105-1112.
Szewczyk-Golec, K., A. Wozniak, et al. (2015). "Inter-relationships of the chronobiotic, melatonin, with leptin and adiponectin: implications for obesity." J Pineal Res **59**(3): 277-291.
Taddeo, E. P., R. C. Laker, et al. (2014). "Opening of the mitochondrial permeability transition pore links mitochondrial dysfunction to insulin resistance in skeletal muscle." Mol Metab **3**(2): 124-134.
Tan, D. X., L. C. Manchester, et al. (2011). "Significance and application of melatonin in the regulation of brown adipose tissue metabolism: relation to human obesity." Obes Rev **12**(3): 167-188.

Tan, X., X. Sun, et al. (2012). "Leptin deficiency contributes to the pathogenesis of alcoholic fatty liver disease in mice." Am J Pathol **181**(4): 1279-1286.
Tomás-Zapico, C. (2005). "Muerte celular por autofagia como mecanismo de supervivencia ante el estrés oxidativo fisiológico en la glándula de Harder del hámster sirio." PhD thesis.
Tomita, K., Y. Oike, et al. (2008). "Hepatic AdipoR2 signaling plays a protective role against progression of nonalcoholic steatohepatitis in mice." Hepatology **48**(2): 458-473.
Valko, M., D. Leibfritz, et al. (2007). "Free radicals and antioxidants in normal physiological functions and human disease." Int J Biochem Cell Biol **39**(1): 44-84.
Vega-Naredo, I. (2010). "Modulación redox de la autofagia en la glándula de Harder de hámster Sirio." PhD thesis.
Vega-Naredo, I., B. Caballero, et al. (2012). "Melatonin modulates autophagy through a redox-mediated action in female Syrian hamster Harderian gland controlling cell types and gland activity." J Pineal Res **52**(1): 80-92.
Vernon, G., A. Baranova, et al. (2011). "Systematic review: the epidemiology and natural history of non-alcoholic fatty liver disease and non-alcoholic steatohepatitis in adults." Aliment Pharmacol Ther **34**(3): 274-285.
Videla, L. A. and P. Pettinelli (2012). "Misregulation of PPAR Functioning and Its Pathogenic Consequences Associated with Nonalcoholic Fatty Liver Disease in Human Obesity." PPAR Res **2012**: 107434.
Vincent, H. K., K. E. Innes, et al. (2007). "Oxidative stress and potential interventions to reduce oxidative stress in overweight and obesity." Diabetes Obes Metab **9**(6): 813-839.
Vincent, H. K., J. W. Morgan, et al. (2004). "Obesity exacerbates oxidative stress levels after acute exercise." Med Sci Sports Exerc **36**(5): 772-779.
Vincent, H. K., S. K. Powers, et al. (2001). "Mechanism for obesity-induced increase in myocardial lipid peroxidation." Int J Obes Relat Metab Disord **25**(3): 378-388.
Vincent, H. K. and A. G. Taylor (2006). "Biomarkers and potential mechanisms of obesity-induced oxidant stress in humans." Int J Obes (Lond) **30**(3): 400-418.
Vriend, J. and R. J. Reiter (2014). "Melatonin as a proteasome inhibitor. Is there any clinical evidence?" Life Sci **115**(1-2): 8-14.
Wai, T. and T. Langer (2016). "Mitochondrial Dynamics and Metabolic Regulation." Trends Endocrinol Metab.

Wallstrom, P., E. Wirfalt, et al. (2001). "Serum concentrations of beta-carotene and alpha-tocopherol are associated with diet, smoking, and general and central adiposity." Am J Clin Nutr **73**(4): 777-785.
Wang, C., Z. Chen, et al. (2014). "Hepatic overexpression of ATP synthase beta subunit activates PI3K/Akt pathway to ameliorate hyperglycemia of diabetic mice." Diabetes **63**(3): 947-959.
Wang, C. W. and D. J. Klionsky (2003). "The molecular mechanism of autophagy." Mol Med **9**(3-4): 65-76.
Wang, R. H., H. S. Kim, et al. (2011). "Hepatic Sirt1 deficiency in mice impairs mTorc2/Akt signaling and results in hyperglycemia, oxidative damage, and insulin resistance." J Clin Invest **121**(11): 4477-4490.
Wang, Y., Y. Li, et al. (2015). "Reactive oxygen species-provoked mitochondria-dependent cell death during ageing of elm (Ulmus pumila L.) seeds." Plant J **81**(3): 438-452.
Westermann, B. (2012). "Bioenergetic role of mitochondrial fusion and fission." Biochim Biophys Acta **1817**(10): 1833-1838.
Wheatcroft, S. B., I. L. Williams, et al. (2003). "Pathophysiological implications of insulin resistance on vascular endothelial function." Diabet Med **20**(4): 255-268.
Witt-Enderby, P. A., N. M. Radio, et al. (2006). "Therapeutic treatments potentially mediated by melatonin receptors: potential clinical uses in the prevention of osteoporosis, cancer and as an adjuvant therapy." J Pineal Res **41**(4): 297-305.
Wree, A., A. Kahraman, et al. (2011). "Obesity affects the liver - the link between adipocytes and hepatocytes." Digestion **83**(1-2): 124-133.
Yamauchi, T., J. Kamon, et al. (2003). "Cloning of adiponectin receptors that mediate antidiabetic metabolic effects." Nature **423**(6941): 762-769.
Yazdi, P. G., H. Moradi, et al. (2013). "Skeletal muscle mitochondrial depletion and dysfunction in chronic kidney disease." Int J Clin Exp Med **6**(7): 532-539.
Ye, J. (2013). "Mechanisms of insulin resistance in obesity." Front Med **7**(1): 14-24.
Yla-Anttila, P., H. Vihinen, et al. (2009). "3D tomography reveals connections between the phagophore and endoplasmic reticulum." Autophagy **5**(8): 1180-1185.
Yoo, Y. M. (2013). "Melatonin-mediated insulin synthesis during endoplasmic reticulum stress involves HuD expression in rat insulinoma INS-1E cells." J Pineal Res **55**(2): 207-220.

Yoshida, H., T. Matsui, et al. (2003). "A time-dependent phase shift in the mammalian unfolded protein response." Dev Cell **4**(2): 265-271.
Yu, S., K. Matsusue, et al. (2003). "Adipocyte-specific gene expression and adipogenic steatosis in the mouse liver due to peroxisome proliferator-activated receptor gamma1 (PPARgamma1) overexpression." J Biol Chem **278**(1): 498-505.
Zanuto, R., M. A. Siqueira-Filho, et al. (2013). "Melatonin improves insulin sensitivity independently of weight loss in old obese rats." J Pineal Res **55**(2): 156-165.
Zephy, D. and J. Ahmad (2014). "Type 2 diabetes mellitus: Role of melatonin and oxidative stress." Diabetes Metab Syndr.
Zhang, B. B., G. Zhou, et al. (2009). "AMPK: an emerging drug target for diabetes and the metabolic syndrome." Cell Metab **9**(5): 407-416.
Zhang, L., P. Su, et al. (2010). "Melatonin inhibits adipogenesis and enhances osteogenesis of human mesenchymal stem cells by suppressing PPARgamma expression and enhancing Runx2 expression." J Pineal Res **49**(4): 364-372.
Zhang, N., M. M. Cao, et al. (2015). "Autophagy regulates insulin resistance following endoplasmic reticulum stress in diabetes." J Physiol Biochem.
Zhang, Y., S. Goldman, et al. (2009). "Adipose-specific deletion of autophagy-related gene 7 (atg7) in mice reveals a role in adipogenesis." Proc Natl Acad Sci U S A **106**(47): 19860-19865.
Zhang, Y., L. Yu, et al. (2014). "Protopanaxatriol, a novel PPARgamma antagonist from Panax ginseng, alleviates steatosis in mice." Sci Rep **4**: 7375.
Zieba, D. A., M. Szczesna, et al. (2008). "Leptin as a nutritional signal regulating appetite and reproductive processes in seasonally-breeding ruminants." J Physiol Pharmacol **59 Suppl 9**: 7-18.

ANNEXE

J. Pineal Res. 2013
Doi:10.1111/jpi.12104

Journal of Pineal Research

Journal of Pineal Research
Molecular, Biological, Physiological and Clinical Aspects of Melatonin

Melatonin administration decreases adipogenesis in the liver of ob/ob mice through autophagy modulation

Abstract: Despite efforts to curb the incidence of obesity and its comorbidities, this condition remains the fifth leading cause of death worldwide. To identify ways to reduce this global effect, we investigated the actions of daily melatonin administration on oxidative stress parameters and autophagic processes as a possible treatment of obesity in ob/ob mice. The involvement of melatonin in many physiological functions, such as the regulation of seasonal body weight variation, glucose uptake, or adiposity, and the role of this indoleamine as an essential antioxidant, has become the focus of numerous anti-obesity studies. Here, we examined the oxidative status in the livers of obese melatonin-treated and untreated mice, observing a decrease in the oxidative stress levels through elevated catalase activity. ROS-mediated autophagy was downregulated in the liver of melatonin-treated animals and was accompanied by significant accumulation of p62. Autophagy is closely associated with adipogenesis; in this study, we report that melatonin-treated obese mice also showed reduced adiposity, as demonstrated by diminished body weight and reduced peroxisome proliferator-activated receptor gamma expression. Based on these factors, it is reasonable to assume that oxidative stress and autophagy play important roles in obesity, and therefore, melatonin could be an interesting target molecule for the development of a potential therapeutic agent to curb body weight.

Beatriz de Luxán-Delgado[1], Beatriz Caballero[1], Yaiza Potes[1], Adrian Rubio-González[1], Illán Rodríguez[1], José Gutiérrez-Rodríguez[2], Juan J. Solano[2] and Ana Coto-Montes[1]

[1]Department of Morphology and Cellular Biology, Faculty of Medicine, University of Oviedo, Oviedo, Spain; [2]Geriatrics Service, Monte Naranco Hospital, Oviedo, Spain

Key words: adipogenesis, autophagy, melatonin, obesity, oxidative stress

Address reprint requests to Beatriz de Luxán Delgado and Ana Coto Montes, Department of Morphology and Cellular Biology, Faculty of Medicine, University of Oviedo, C/ Julián Clavería s/n, 33006, Oviedo, Spain.
E-mails: b.luxandelgado@gmail.com and acoto@uniovi.es

Received July 26, 2013;
Accepted October 15, 2013.

Introduction

The frequency of obesity and its comorbidities has more than doubled in the last 20 yrs worldwide, reflecting sedentary lifestyles and increased caloric intake [1]. Thus, overweight and obesity are the fifth leading cause of global deaths, and the World Health Organization estimates that there are approximately 500 million obese people and 1.5 billion overweight individuals in the world [1].

Tremendous advances have been made in the recent decades in understanding the molecular mechanisms underlying the pathology of obesity to identify useful molecules for the treatment of this condition. The use of animal models to understand the regulation of food intake and energy expenditure is critical for the development of obesity treatments. Several animal models have been employed to study the environmental, physiological and genetic basis of obesity [2]. The adipocyte-derived cytokine, leptin, and its receptor were discovered 20 yrs ago [3, 4], representing a major advance in the knowledge of this disease. Subsequently, the leptin deficient mutant mouse, Lep^{ob}, was developed at Jackson Laboratories in the 1940s. This mouse, commonly referred to as ob/ob, carries a mutation in the leptin gene that generates a non-functional leptin protein [2]. As this protein plays a major role in food intake and energy expenditure, leptin deficiency or resistance leads to massive obesity, accompanied by type 2 diabetes and other obesity-related pathologies [5].

Obesity is a state of chronic oxidative stress, and this could be one of the most important mechanisms in the development of co-morbidities that accompany this disease [6]. Vincent and Taylor [7] reviewed several potential contributors to oxidative stress in obesity, including hyperglycaemia [8], increased muscle activity to carry excessive weight [9], elevated tissue lipid levels [10, 11], inadequate antioxidant defences [11–13], chronic inflammation, [14–16] endothelial reactive oxygen species (ROS) production [17, 18] and hyperleptinaemia [19]. In each of these cases, free radical production is directly increased or there is insufficient antioxidant capacity to attenuate free radical damage [6, 20].

Most organisms possess efficient enzymatic and non-enzymatic antioxidant systems to detoxify free radicals and prevent oxidative stress. As a natural antioxidant, melatonin and its metabolites play diverse roles in radical detoxification, reflecting the ubiquitous action of these compounds [21–23]. Melatonin (N-acetyl-5-methoxy tryptamine) is an indoleamine synthesised by the pineal gland and many other organs [24–26], which acts as a direct free radical scavenger and indirectly via stimulation of a set of antioxidant enzymes [27, 28]. This indoleamine is also involved in numerous physiological functions, such as the regulation of circadian rhythms, sleep promotion, tumour growth inhibition, immune defence, thermoregulation, and reproductive activity in seasonally reproductive animals [29–32]. In addition, melatonin has been associated with adiposity, body mass and both energy intake and expenditure [33–36], but these roles are not fully understood.

Numerous publications have confirmed the regulatory effects of melatonin on the cell cycle, triggering apoptosis in cancer cells that lead to cell death, and activation of autophagy as a survival mechanism [37–39]. As both processes have been associated with obesity [40, 41], increasing direct and indirect evidence suggests that melatonin is a potentially valuable target against excess weight gain. Apoptosis, the most important process in programmed cell death (PCD), is also referred to as PCD type I, and autophagy is referred to as PCD type II. However, rather than being a mechanism of cell death, autophagy is primarily a survival process [42]. Autophagy is a highly conserved process in which eukaryotic cells self-digest cytosolic components to degrade long-lived proteins and organelles in response to starvation and other stresses [39]. Three types of autophagy have been identified: microautophagy, chaperone-mediated autophagy (CMA) and macroautophagy (hereafter referred to as autophagy). Recent studies have shown that autophagy is involved in adipose tissue development and cytoplasmic remodelling [43, 44]. Goldman and colleagues [45] have described that autophagy-related 7 (atg7) knockout mice present much smaller adipose tissue deposits that their wild-type counterparts, and Younce and Kolattukudy [46] have demostrated that inhibition of autophagy by specific inhibitors decreased adipogenesis.

Similarly, melatonin-treated adipocytes significantly suppressed of a major gene involved in the regulation of adipogenesis, PPARγ (peroxisome proliferator-activated receptor gamma), in the early stages of adipocyte differentiation [47]. In addition, melatonin administration is associated with an improvement in overweight and obesity characteristics, as reduced body weight gain and increased antioxidant enzyme activity have been observed [33, 48]. Thus, the aim of this study was to characterise the relationship among three factors (oxidative stress, obesity and autophagy), and determine how melatonin, as a major antioxidant molecule, might act as a potential therapeutic target for this health problem. Hence, we employed ob/ob mice to investigate the effects of exogenous melatonin on oxidative stress and autophagic regulation as a possible obesity modulator.

Materials and methods

Animals

Eight six-week-old male leptin-deficient obese B6.V-Lep-ob/J (ob/ob) mice were purchased from Charles River Laboratory (Charles River Laboratories España, SA, Barcelona, Spain). The mice were housed two per cage under 12:12 hr dark-light cycle at 22 ± 2°C. The animals received tap water and a standard chow diet ad libitum. The experiment protocol was approved through the Oviedo University Animal Care and Use Committee. All experiments were performed according to the Spanish Government Guide and the European Community Guide for Animal Care (Council Directive 86/609/EEC).

After a 2-wk acclimatisation period, a randomised group of four obese mice were treated with melatonin for 2 wk, and the remaining four obese mice were maintained as a control group for same period. All the animals were weighed at the beginning (baseline) and the end of the experiment of the experiment. Differences in the initial body weight between the different groups were not significant.

At 2 hr after lights off, intraperitoneal injections of melatonin were administered daily at a dose of 500 μg/kg body weight (Sigma Aldrich, St Louis, MO, USA). The melatonin was dissolved in 0.1% absolute ethanol: saline. The animals in the control group received vehicle at a comparable dosage, route and treatment duration. The animals were sacrificed by decapitation, and the liver of each mouse was immediately removed and frozen at −80°C until further use.

The liver (0.1 g) of each mouse was homogenised using a Polytron homogeniser at 4°C in 2 mL of lysis buffer (50 mM phosphate buffer, pH 7.5, 1 mM NaF, 1 mM Na_3VO_4, and 0.1% Triton-X 100 (1:10 w/v)). The tissue homogenates were then subsequently centrifuged at 1500 g for 6 min at 4°C, and the supernatants were collected. The amount of protein in the supernatants was measured using the Bradford method [49].

Lipid oxidative damage (LPO)

The concentration of the end-products of the lipid peroxidation cascade, reactive aldehyde malondialdehyde (MDA) and 4-hydroxy-2-(E)-nonenal (4-HNE) was determined to measure lipid peroxidation. The MDA and 4-HNE content in the liver was determined using an LPO Assay Kit from Calbiochem (No. 437634, San Diego, CA, USA), based on the condensation of the chromogene 1-methyl-2-phenylindole with either MDA or 4-HNE. The results are expressed as nmol MDA+4-HNE/g protein.

Protein oxidative damage (PD)

The protein carbonyl concentrations were determined according to the methods of Levine [50], with modifications of Coto-Montes and Hardeland [51]. The data are presented as nmol carbonyl protein/mg protein.

Catalase activity

Catalase (CAT; EC 1.11.1.6) activity, which converts hydrogen peroxide (H_2O_2) into O_2 and H_2O, was assayed according to the previously described methods of Lubinsky and Bewley, using H_2O_2 as a substrate [52]. The data are expressed as μmol H_2O_2/min mg protein.

Superoxide dismutase activity

Superoxide dismutase (SOD; EC 1.15.1.1), which catalyses the dismutation of superoxide anion (O_2^-) to H_2O_2, was measured according to the previously described method of Martin and colleagues [53]. SOD inhibits haematoxylin auto-oxidation to the coloured compound haematein. The results are expressed as SOD units/mg protein.

Western blot immunoassay

The tissue homogenates (50 or 100 μg of protein per sample) were mixed with Laemmli sample buffer (BioRad

Laboratories, Inc., Hercules, CA, USA) and denatured by boiling at 100°C for 5 min. The samples were fractionated using SDS-polyacrylamide gel electrophoresis (PAGE) at 200 V and subsequently transferred onto a polyvinylidene fluoride sheets (PVDF) at 100 V (Immobilon TM-P; Millipore Corp., Bedford, MA, USA). The membranes were blocked for 1 hr at room temperature with 5 or 10% (w/v) skim milk dissolved in Tris-buffered saline containing Tween (TBS-T) (50 mm Tris/HCl, pH 7.5, 150 mm NaCl, and 0.05% Tween-20). Subsequently, the membranes were incubated with the respective primary antibodies: anti-LAMP2A (ab18528, Abcam, Cambridge, UK), anti-Beclin1 (sc-10086, Santa Cruz Biotechnology, Santa Cruz, CA, USA), anti-LC3 (PD014, Medical & Biological Laboratories CO., LTC, Naka-ku Nagoya, Japan), anti-p62 (H00008878-M01, Abnova, Walnut, CA, USA), anti-PPARγ (sc-7273, Santa Cruz Biotechnology) and anti-β-actin (AC-15 Sigma Aldrich), previously diluted in TBS-T buffer containing 1% (w/v) skin milk. After three 10 or 20 min washes in TBS-T, the membranes where incubated with the corresponding horseradish peroxidase-conjugated secondary antibody (Sigma Aldrich, Saint Louis, MO, USA) diluted in TBS-T buffer containing 1% (w/v) skin milk for 2 hr at room temperature, followed by three times for 10 or 20 min washes in TBS-T.

The membrane was developed using a chemiluminescent horseradish peroxidase substrate (WBKLS0500, Millipore Corporation, Billerica, USA) according to the manufacturer's protocol. All data presented are representatives from at least three separate experiments. The levels of proteins were quantitatively analyzed using Quantity One 5.5.1 software. The results were normalized to β-actin as a loading control.

Statistical analysis

The statistical software package SPSS 15.0 for Windows (SPSS Inc., Chicago, IL, USA) was used for all statistical analyses. The data are presented as the means values $\pm$ standard deviation of the mean (S.D.). The normality of the data was analyzed using the Kolmogorov-Smirnov test. The variables were compared between groups using Student's t test. The differences were considered statistically significant when $P < 0.05$.

Results

Although the analysis of the oxidative damage markers showed that LPO levels were similar in both study groups, non-significant downward trend of damaged lipids in the melatonin-treated group was observed (Fig. 1A). However, we saw a significant reduction in hepatic protein damage in the group treated with melatonin compared with the control group ($P < 0.05$) (Fig. 1B).

The CAT activity levels were significantly higher in the liver tissue of the melatonin treated mice compared with that of the control animals ($P < 0.01$) (Fig. 2A); thus, melatonin increased the antioxidant capacity in ob/ob mice. SOD activity was not changed in the liver of melatonin-supplemented animals (Fig. 2B).

LAMP2A (lysosome-associated membrane protein type 2A) is a lysosomal membrane chaperone which facilitates the internalisation of proteins and peptides containing the amino acid sequence KFERQ. The analysis of LAMP2A immunoblotting as a marker of CMA showed non-significant differences between the experimental groups (Fig. 3).

We performed western blot analysis using antibodies against Beclin1 and LC3 (microtubule-associated protein 1 light chain 3) to study lysosomal-related processes, such as macroautophagy, in the livers of ob/ob mice. Beclin1 is a class III phosphatidylinositol 3-kinase-interacting protein, which plays an essential role in promoting autophagy. The immunoblot analysis showed a significant decrease in Beclin1 protein expression in the melatonin-treated group compared with the control group ($P < 0.01$) (Fig. 4), suggesting that melatonin downregulates autophagy in the livers of ob/ob mice.

LC3 is an autophagosomal orthologue of yeast Atg8. The unprocessed form of LC3, pro-LC3, is proteolytically processed into LC3-I, a mature form lacking some amino acids from the C-terminus. LC3-I is subsequently modified into a phosphatidylethanolamine-conjugated form, LC3-II, associated with phagophores, autophagosomes and autophagolysosomes [54], which is considered an autophagosomal marker. The western blot analysis showed two bands corresponding to LC3-I and LC3-II (18 and 16 kDa, respectively) in the livers of ob/ob mice (Fig. 5A). No significant differences were observed between either group, or LC3-I and LC3-II (Fig. 5B and D). Nevertheless, the analysis of the immunoblot showed a significant increase in the LC3-II/LC3-I ratio in the melatonin-treated group compared with the control group ($P < 0.01$) (Fig. 5C).

Sequestosome 1, or p62, is a selective substrate for autophagy, which interacts with LC3 during autophagosome formation and subsequently is degraded in the lysosome with other selected substrates [55]. The immunoblot results showed a significant increase in p62 protein expression in the group treated with melatonin compared with the control group ($P < 0.01$) (Fig. 6).

PPARγ is a member of a nuclear hormone receptor superfamily, predominantly found in adipose tissue, but also expressed in liver and muscle tissue [56], and this protein plays an essential role in adipogenesis and fat storage [57]. Our analysis of PPARγ protein levels through western blotting showed a significant decrease in the expression of this protein after melatonin treatment compared with non-treated animals ($P < 0.05$) (Fig. 7). Moreover, after only 2 wk of exogenous melatonin treatment, the obese mice showed a significant reduction in body weight ($P < 0.05$) (Table 1).

Discussion

Obesity is a complex multi-factorial chronic disease associated with low-grade chronic oxidative stress [6]; thus, many studies have focused on the effects of melatonin, using antioxidant capacity as a potential treatment against obesity [33, 48, 58]. In the present study, melatonin-treated animals showed a reduction in oxidative stress, reflected in a significantly reduced protein damage. In addition, melatonin treatment was associated with a statistically significant rise

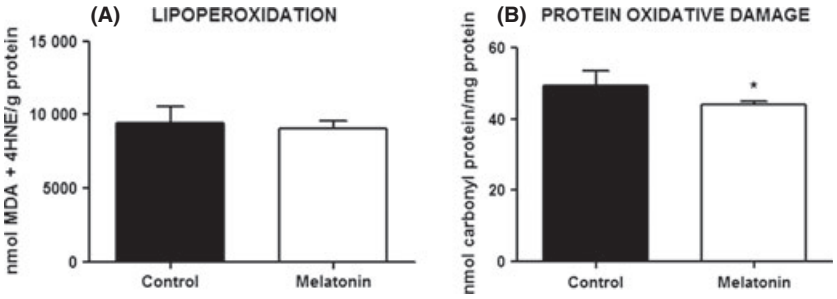

Fig. 1. Lipid and protein oxidative damage in the liver of ob/ob mice. (A) Liver's lipid peroxidation presented as nmol MDA+4-HNE/g protein. (B) Protein damage expressed as nmol carbonyl protein/mg protein. The data are expressed as the means ± S.D., calculated from at least three separate measurements performed in triplicate. $*P < 0.05$.

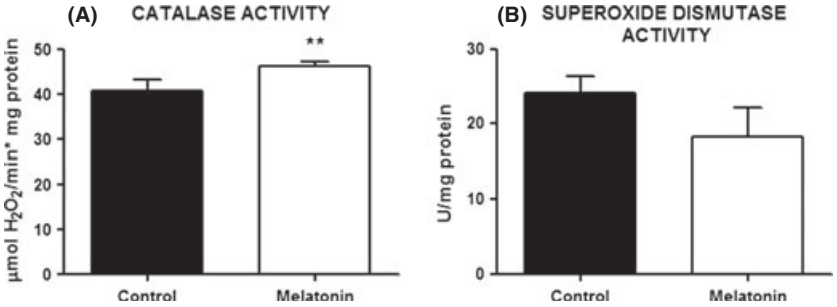

Fig. 2. Antioxidant enzyme assay in the liver of of ob/ob mice. (A) Catalase activity expressed as μmol H_2O_2/min mg protein. (B) Superoxide dismutase activity expressed as superoxide dismutase Units/mg protein. The data are expressed as the means ± S.D., calculated from at least three separate experiments performed in triplicate. $**P < 0.01$.

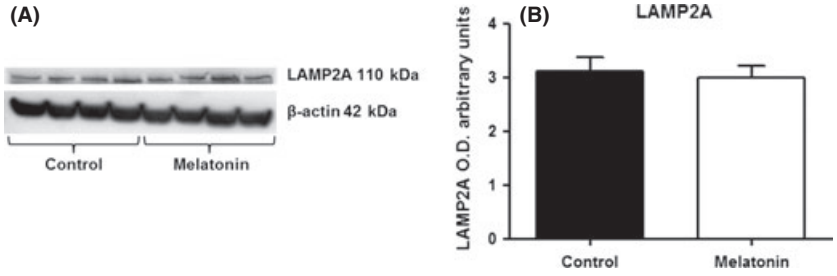

Fig. 3. (A) Western blot analysis of LAMP2A using 100 mg of protein from the livers of ob/ob mice. (B) Bar chart showing the semi-quantitative optical density (arbitrary units of blot bands) normalised to *β*-actin. The data are expressed as the means ± S.D., calculated from at least three separate experiments performed in triplicate.

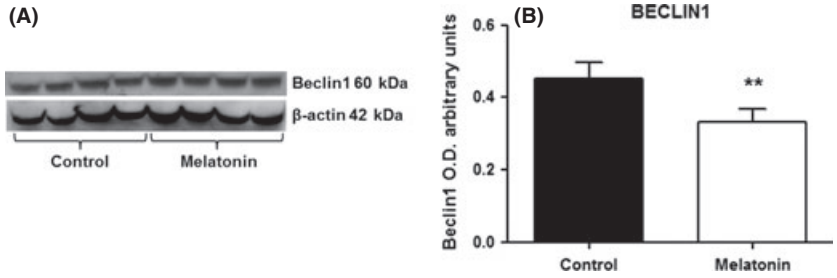

Fig. 4. (A) Western blot analysis of Beclin1 expression using 100 mg of protein from the livers of ob/ob mice. (B) Bar chart showing the semi-quantitative optical density (arbitrary units of blot bands) normalised to *β*-actin. The data are expressed as the means ± S.D., calculated from at least three separate experiments performed in triplicate. $**P < 0.01$.

in CAT activity levels compared with the control mice. Nevertheless, statistically significant differences were not observed in SOD activity after melatonin treatment. This data is, very probably, related to the melatonin's ability to scavenge free radicals [59]. Melatonin directly removes O_2^-, the SOD's substrate, thus, it is not necessary that melatonin increases SOD activity to counteract oxidative stress of obesity, contrary to what happens with the CAT activity. Taken together, these results suggest that exogenous melatonin acts as both a direct and indirect antioxidant for antioxidant defence regulation in ob/ob mice.

Melatonin has been characterised as a possible treatment for many diseases due to the lack of reported toxicity and no serious adverse effects [34]. Several studies have shown the antioxidant capacity of melatonin and its role in the circadian system; however, melatonin has also been implicated in a number of neuroendocrine and physiological processes [47]. Recently, changes in seasonal body weight, depending on photoperiod alterations and melatonin levels have been reported, supporting a potential role for melatonin in obesity regulation [34]. Moreover, this indoleamine promotes weight loss through the stimulation

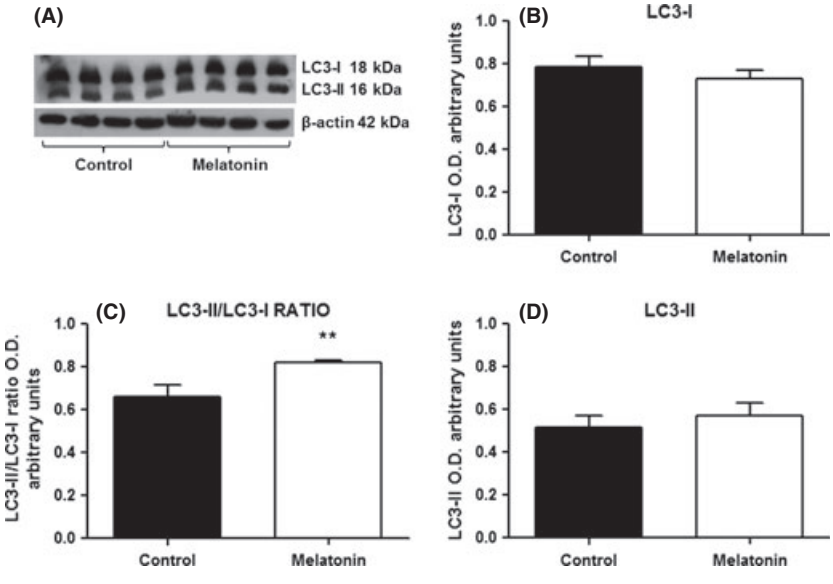

Fig. 5. Determination of autophagic flux in the liver of of ob/ob mice. (A) Western blot analysis of LC3-I and LC3-II using 50 mg of protein from the livers of ob/ob mice. Bar chart showing the semi-quantitative optical density (arbitrary units of blot bands) normalised to β-actin: (B) bar chart of LC3-I, (D) bar chart of LC3-II, (C) bar chart of the LC3-II/LC3-I ratio. The data are expressed as the means ± S.D., calculated from at least three separate experiments performed in triplicate. $^{**}P < 0.01$.

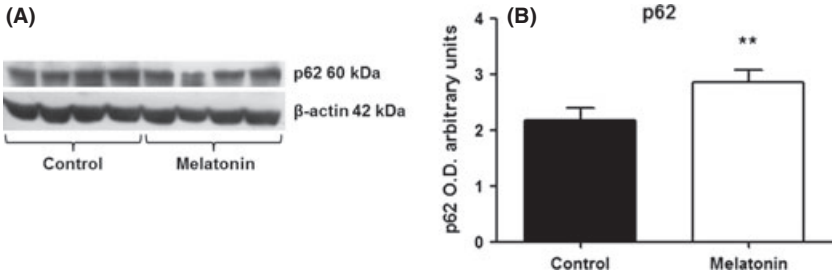

Fig. 6. (A) Western blot analysis of p62 using 100 mg of protein from the livers of ob/ob mice. (B) Bar chart showing the semi-quantitative optical density (arbitrary units of blot bands) normalised to β-actin. The data are expressed as the means ± S.D., calculated from at least three separate experiments performed in triplicate. $^{**}P < 0.01$.

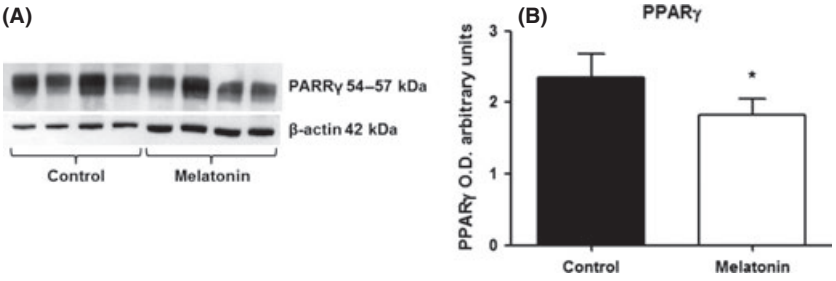

Fig. 7. (A) Western blot analysis of PPAR γ using 50 mg of protein from the livers of ob/ob mice. (B) Bar chart showing the semi-quantitative optical density (arbitrary units of blot bands) normalised to β-actin. The data are expressed as the means ± S.D., calculated from at least three separate experiments performed in triplicate. $^{*}P < 0.05$.

of non-shivering thermogenesis and the recruitment of brown fat tissue in small mammals [34]. In addition, melatonin regulates many other aspects of body weight and adiposity, such as glucose uptake [60], serum lipid profile, blood pressure, or inflammation [58]. Hence, it is necessary to examine the potential regulation of obesity mechanisms by melatonin.

The essential role of ROS as second messengers, which trigger a large number of processes, including autophagy, must also be considered [61]. A rise in ROS levels activates autophagy as a defence mechanism to prevent cellular damage. Lavallard and colleagues [40] describe the activation of ROS-mediated autophagy through several mechanisms: the inhibition of mTOR (mammalian target of rapamycin) [62], the up-regulation of Beclin1 expression [63], and the conversion of LC3-I into LC3-II [64].

Table 1. Body weight changes of ob/ob mice

	Baseline	Sacrifice	Δweight
Control (n = 4)	37.08 ± 2.61	37.95 ± 2.04	0.86 ± 1.17
Melatonin (n = 4)	38.40 ± 1.36	35.99 ± 2.57	−2.41 ± 1.54*

Effect of melatonin and vehicle treatment on body weight changes from baseline to the end of the study. The data are expressed as the means ± S.D. $^{*}P < 0.05$, Control Δweight versus Melatonin Δweight.

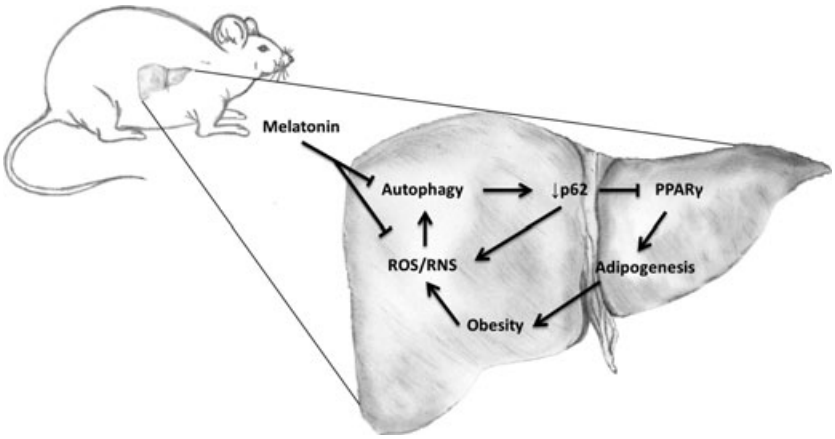

Fig. 8. Melatonin administration reduced oxidative stress and autophagy levels in the liver of ob/ob mice, leading to the accumulation of p62, responsible for inactivating of the adipogenic gene PPARγ, and a decrease in body weight.

The immunoblot analysis of LAMP2A as a CMA marker showed non-significant differences after melatonin treatment. An examination of the oxidative status revealed that melatonin treatment in obese mice reduced oxidative damage; however, the melatonin-treated obese mice maintained a certain level of oxidative stress. The reduced stress might, however, activate CMA, as this autophagic mechanism is typically activated in response to mild ROS production. An assessment of macroautophagy markers showed that melatonin treatment reduced autophagy, reflected as reduced levels of Beclin1 expression compared with the untreated animals. Nevertheless, a higher LC3-II/LC3-I ratio was observed in the melatonin-treated group. Notably, the results of the autophagic flux study must be interpreted with caution. Although the conversion of soluble LC3-I to lipid-bound LC3-II is typically associated with autophagosome formation, this process does not necessarily result in complete autophagy [65]. Increased LC3-II levels might reflect the increased conversion of LC3-I into LC3-II and indicate the reduced degradation of this protein through the inhibition of autophagic activity [66].

Sequestosome1/p62 is a selective substrate for autophagy, which binds to ubiquitinated protein aggregates, marking these proteins for autophagic degradation [55]. p62 is also a marker for autophagic flux [67]. Thus, when p62 binds to LC3, this protein becomes internalised into the autophagosome [55]. Many studies have shown that, when autophagy is impaired, p62 is accumulated along with ubiquitinated aggregates [55, 67, 68], leading to increased oxidative stress [69]. The results of the p62 western blotting analysis showed that melatonin-treated animals presented significantly higher levels of p62 compared with the untreated group. This data suggests that melatonin treatment downregulates autophagy in the livers of ob/ob mice.

p62 has also been implicated in various signal transduction pathways associated with obesity, such as the control of energy homeostasis and adipogenesis [70]. Thus, p62-knockout mice showed alterations in energy expenditure and increased PPARγ mRNA levels, resulting in an increase in adipogenesis and the development of obesity and insulin and leptin resistance [71]. These results suggest that p62 acts as a negative regulator of PPARγ [71], the ligand-activated transcription factor and master regulator of the genes involved in lipogenic pathways and adipocyte differentiation [72].

The results obtained in the present study are consistent with the results of Dr. Rodriguez, as PPARγ exhibited antagonic effects toward p62 in both groups, significantly associated with decreased body weight in obese animals after melatonin treatment. This improvement in body weight has previously been demonstrated in obese Boscat male rabbits after daily treatments with 1 mg/kg melatonin for 4 wk [48].

The reduced PPARγ levels observed in the melatonin-treated group are consistent with in vitro studies, showing of the association of melatonin treatment with the suppression PPARγ expression during the early stages of adipogenesis [47, 73]. These data imply that melatonin could act as a direct inhibitor of adipocyte differentiation, showing potential as a therapeutic agent for adipogenesis.

In the present study, we were not only able to describe the beneficial effects of reducing the body weight of obese animals under melatonin treatment, but we also documented the mechanisms modulated by melatonin induced this effect. Based on our results, melatonin reduces autophagy processes through reducing ROS levels, characteristic of obesity through scavenging free radicals, and stimulating antioxidant enzymatic activity. This reduced autophagic activity implicates p62 accumulation in the down regulation of adipogenic pathways, accompanied by an eventual reduction in the body weight (Fig. 8). Melatonin modulates several physiological processes involved in obesity as a potential treatment for this pathology [33, 34, 48]; however, to our knowledge, this study provides the first evidence of an association between the regulation of obesity-related adipogenesis and the modulation of autophagic activity through melatonin.

Acknowledgements

We thank to Dr. de Gonzalo-Calvo and Mme. Garcia-Macia for helping in study design and Mr. de Luxán-Meléndez for assistant in developing figures. We are members of the INPROTEOLYS and INEUROPA network. This work was supported by: FISS-06-RD06/0013/0011 and FISS-06-RD06/0013/0028; BFU2010-20919 and FEDER funds. B.de L-D is FICYT pre-doctoral fellow from the

Gobierno del Principado de Asturias. Financial support from the University of Oviedo is also acknowledged.

Author contributions

Concept and design: B.de L-D and A. C-M. Data acquisition: B.de L-D, J.R-G and J.J.S. Data analysis: Y.P, A.R-G and I.R. Manuscript writer: B.de L-D. Data interpretation and manuscript revisions: B.de L-D and A.C-M. Statistical expertise: B.de L-D and B.C.

References

1. World Health Organization (WHO). Obesity and Overweight. WHO, London, UK, 2013; pp. 311. http://www.who.int/mediacentre/factsheets/fs311/en/
2. Speakman J, Hambly C, Mitchell S et al. Animal models of obesity. Obes Rev 2007; **8**(Suppl 1):55–61.
3. Zhang Y, Proenca R, Maffei M et al. Positional cloning of the mouse obese gene and its human homologue. Nature 1994; **372**:425–432.
4. Tartaglia LA, Dembski M, Weng X et al. Identification and expression cloning of a leptin receptor, OB-R. Cell 1995; **83**:1263–1271.
5. Fellmann L, Nascimento AR, Tibirica E et al. Murine models for pharmacological studies of the metabolic syndrome. Pharmacol Ther 2013; **137**:331–340.
6. Vincent HK, Innes KE, Vincent KR. Oxidative stress and potential interventions to reduce oxidative stress in overweight and obesity. Diabetes Obes Metab 2007; **9**:813–839.
7. Vincent HK, Taylor AG. Biomarkers and potential mechanisms of obesity-induced oxidant stress in humans. Int J Obes (Lond) 2006; **30**:400–418.
8. Aronson D, Rayfield EJ. How hyperglycemia promotes atherosclerosis: molecular mechanisms. Cardiovasc Diabetol 2002; **1**:1.
9. Vincent HK, Morgan JW, Vincent KR. Obesity exacerbates oxidative stress levels after acute exercise. Med Sci Sports Exerc 2004; **36**:772–779.
10. Beltowski J, Wojcicka G, Gorny D et al. The effect of dietary-induced obesity on lipid peroxidation, antioxidant enzymes and total plasma antioxidant capacity. J Physiol Pharmacol 2000; **51**:883–896.
11. Vincent HK, Powers SK, Dirks AJ et al. Mechanism for obesity-induced increase in myocardial lipid peroxidation. Int J Obes Relat Metab Disord 2001; **25**:378–388.
12. Ohrvall M, Tengblad S, Vessby B. Lower tocopherol serum levels in subjects with abdominal adiposity. J Intern Med 1993; **234**:53–60.
13. Wallstrom P, Wirfalt E, Lahmann PH et al. Serum concentrations of beta-carotene and alpha-tocopherol are associated with diet, smoking, and general and central adiposity. Am J Clin Nutr 2001; **73**:777–785.
14. Davi G, Guagnano MT, Ciabattoni G et al. Platelet activation in obese women: role of inflammation and oxidant stress. JAMA 2002; **288**:2008–2014.
15. Fernandez-Real JM, Broch M, Vendrell J et al. Insulin resistance, inflammation, and serum fatty acid composition. Diabetes Care 2003; **26**:1362–1368.
16. Saito I, Yonemasu K, Inami F. Association of body mass index, body fat, and weight gain with inflammation markers among rural residents in Japan. Circ J 2003; **67**:323–329.
17. Egan BM, Greene EL, Goodfriend TL. Insulin resistance and cardiovascular disease. Am J Hypertens 2001; **14**:116S–125S.
18. Wheatcroft SB, Williams IL, Shah AM et al. Pathophysiological implications of insulin resistance on vascular endothelial function. Diabet Med 2003; **20**:255–268.
19. Bouloumie A, Marumo T, Lafontan M et al. Leptin induces oxidative stress in human endothelial cells. FASEB J 1999; **13**:1231–1238.
20. Sainz N, Rodriguez A, Catalan V et al. Leptin administration downregulates the increased expression levels of genes related to oxidative stress and inflammation in the skeletal muscle of ob/ob mice. Mediators Inflamm 2010; **2010**: 784343.
21. Reiter RJ, Acuna-Castroviejo D, Tan DX et al. Free radical-mediated molecular damage. Mechanisms for the protective actions of melatonin in the central nervous system. Ann N Y Acad Sci 2001; **939**:200–215.
22. De Matos Cavalcante AG, De Bruin PF, De Bruin VM et al. Melatonin reduces lung oxidative stress in patients with chronic obstructive pulmonary disease: a randomized, double-blind, placebo-controlled study. J Pineal Res 2012; **53**:238–244.
23. Galano A, Tan DX, Reiter RJ. On the free radical scavenging activities of melatonin's metabolites, AFMK and AMK. J Pineal Res 2013; **54**:245–257.
24. Stehle JH, Saade A, Rawashdeh O et al. A survey of molecular details in the human pineal gland in the light of phylogeny, structure, function and chronobiological diseases. J Pineal Res 2011; **51**:17–43.
25. Reiter RJ, Tan DX, Rosales-Corral S et al. The universal nature, unequal distribution and antioxidant functions of melatonin and its derivatives. Mini Rev Med Chem 2013; **13**:373–384.
26. Venegas C, Garcia JA, Escames G et al. Extrapineal melatonin: analysis of its subcellular distribution and daily fluctuations. J Pineal Res 2012; **52**:217–227.
27. Reiter RJ, Tan DX, Mayo JC et al. Melatonin as an antioxidant: biochemical mechanisms and pathophysiological implications in humans. Acta Biochim Pol 2003; **50**:1129–1146.
28. Rodriguez C, Mayo JC, Sainz RM et al. Regulation of antioxidant enzymes: a significant role for melatonin. J Pineal Res 2004; **36**:1–9.
29. Reiter RJ, Tan DX, Fuentes-Broto L. Melatonin: a multitasking molecule. Prog Brain Res 2010; **181**:127–151.
30. Carrillo-Vico A, Guerrero JM, Lardone PJ et al. A review of the multiple actions of melatonin on the immune system. Endocrine 2005; **27**:189–200.
31. Witt-Enderby PA, Radio NM, Doctor JS et al. Therapeutic treatments potentially mediated by melatonin receptors: potential clinical uses in the prevention of osteoporosis, cancer and as an adjuvant therapy. J Pineal Res 2006; **41**:297–305.
32. Hardeland R, Madrid JA, Tan DX et al. Melatonin, the circadian multioscillator system and health: the need for detailed analyses of peripheral melatonin signaling. J Pineal Res 2012; **52**:139–166.
33. Prunet-Marcassus B, Desbazeille M, Bros A et al. Melatonin reduces body weight gain in Sprague Dawley rats with diet-induced obesity. Endocrinology 2003; **144**:5347–5352.
34. Tan DX, Manchester LC, Fuentes-Broto L et al. Significance and application of melatonin in the regulation of brown adipose tissue metabolism: relation to human obesity. Obes Rev 2011; **12**:167–188.

35. Agil A, Rosado I, Ruiz R et al. Melatonin improves glucose homeostasis in young Zucker diabetic fatty rats. J Pineal Res 2012; **52**:203–210.
36. Barrett P, Bolborea M. Molecular pathways involved in seasonal body weight and reproductive responses governed by melatonin. J Pineal Res 2012; **52**:376–388.
37. Leja-Szpak A, Jaworek J, Pierzchalski P et al. Melatonin induces pro-apoptotic signaling pathway in human pancreatic carcinoma cells (PANC-1). J Pineal Res 2010; **49**:248–255.
38. Kim CH, Kim KH, Yoo YM. Melatonin protects against apoptotic and autophagic cell death in C2C12 murine myoblast cells. J Pineal Res 2011; **50**:241–249.
39. Coto-Montes A, Boga JA, Rosales-Corral S et al. Role of melatonin in the regulation of autophagy and mitophagy: a review. Mol Cell Endocrinol 2012; **361**:12–23.
40. Lavallard VJ, Meijer AJ, Codogno P et al. Autophagy, signaling and obesity. Pharmacol Res 2012; **66**:513–525.
41. Rodriguez A, Gomez-Ambrosi J, Catalan V et al. The ghrelin O-acyltransferase-ghrelin system reduces TNF-alpha-induced apoptosis and autophagy in human visceral adipocytes. Diabetologia 2012; **55**:3038–3050.
42. Rautou PE, Mansouri A, Lebrec D et al. Autophagy in liver diseases. J Hepatol 2010; **53**:1123–1134.
43. Zhang Y, Goldman S, Baerga R et al. Adipose-specific deletion of autophagy-related gene 7 (atg7) in mice reveals a role in adipogenesis. Proc Natl Acad Sci USA 2009; **106**:19860–19865.
44. Zhang Y, Zeng X, Jin S. Autophagy in adipose tissue biology. Pharmacol Res 2012; **66**:505–512.
45. Goldman S, Zhang Y, Jin S. Autophagy and adipogenesis: implications in obesity and type II diabetes. Autophagy 2010; **6**:179–181.
46. Younce CW, Kolattukudy PE. MCP-1 causes cardiomyoblast death via autophagy resulting from ER stress caused by oxidative stress generated by inducing a novel zinc-finger protein, MCPIP. Biochem J 2010; **426**:43–53.
47. Zhang L, Su P, Xu C et al. Melatonin inhibits adipogenesis and enhances osteogenesis of human mesenchymal stem cells by suppressing PPARgamma expression and enhancing Runx2 expression. J Pineal Res 2010; **49**:364–372.
48. Hussein MR, Ahmed OG, Hassan AF et al. Intake of melatonin is associated with amelioration of physiological changes, both metabolic and morphological pathologies associated with obesity: an animal model. Int J Exp Pathol 2007; **88**:19–29.
49. Bradford MM. A rapid and sensitive method for the quantitation of microgram quantities of protein utilizing the principle of protein-dye binding. Anal Biochem 1976; **72**:248–254.
50. Levine RL, Garland D, Oliver CN et al. Determination of carbonyl content in oxidatively modified proteins. Methods Enzymol 1990; **186**:464–478.
51. Coto-Montes A, Hardeland R. Antioxidative effects of melatonin in Drosophila melanogaster: antagonization of damage induced by the inhibition of catalase. J Pineal Res 1999; **27**:154–158.
52. Lubinsky S, Bewley GC. Genetics of catalase in *Drosophila melanogaster*: rates of synthesis and degradation of the enzyme in flies aneuploid and euploid for the structural gene. Genetics 1979; **91**:723–742.
53. Martin JP Jr, Dailey M, Sugarman E. Negative and positive assays of superoxide dismutase based on hematoxylin autoxidation. Arch Biochem Biophys 1987; **255**:329–336.
54. Rubinsztein DC, Cuervo AM, Ravikumar B et al. In search of an "autophagomometer". Autophagy 2009; **5**:585–589.
55. Komatsu M. Potential role of p62 in tumor development. Autophagy 2011; **7**:1088–1090.
56. Ros Perez M, Medina-Gomez G. Obesity, adipogenesis and insulin resistance. Endocrinol Nutr 2011; **58**:360–369.
57. Nunn AV, Bell J, Barter P. The integration of lipid-sensing and anti-inflammatory effects: how the PPARs play a role in metabolic balance. Nucl Recept 2007; **5**:1.
58. Kozirog M, Poliwczak AR, Duchnowicz P et al. Melatonin treatment improves blood pressure, lipid profile, and parameters of oxidative stress in patients with metabolic syndrome. J Pineal Res 2011; **50**:261–266.
59. Reiter RJ, Garcia JJ, Pie J. Oxidative toxicity in models of neurodegeneration: responses to melatonin. Restor Neurol Neurosci 1998; **12**:135–142.
60. Lima FB, Machado UF, Bartol I et al. Pinealectomy causes glucose intolerance and decreases adipose cell responsiveness to insulin in rats. Am J Physiol 1998; **275**:E934–E941.
61. Valko M, Leibfritz D, Moncol J et al. Free radicals and antioxidants in normal physiological functions and human disease. Int J Biochem Cell Biol 2007; **39**:44–84.
62. Alexander A, Cai SL, Kim J et al. ATM signals to TSC2 in the cytoplasm to regulate mTORC1 in response to ROS. Proc Natl Acad Sci USA 2010; **107**:4153–4158.
63. Chen Y, McMillan-Ward E, Kong J et al. Oxidative stress induces autophagic cell death independent of apoptosis in transformed and cancer cells. Cell Death Differ 2008; **15**:171–182.
64. Scherz-Shouval R, Shvets E, Fass E et al. Reactive oxygen species are essential for autophagy and specifically regulate the activity of Atg4. EMBO J 2007; **26**:1749–1760.
65. Gimenez-Xavier P, Francisco R, Platini F et al. LC3-I conversion to LC3-II does not necessarily result in complete autophagy. Int J Mol Med 2008; **22**:781–785.
66. Skop V, Cahova M, Papackova Z et al. Autophagy-lysosomal pathway is involved in lipid degradation in rat liver. Physiol Res 2012; **61**:287–297.
67. Mizushima N, Yoshimori T. How to interpret LC3 immunoblotting. Autophagy 2007; **3**:542–545.
68. Aghajan M, Li N, Karin M. Obesity, autophagy and the pathogenesis of liver and pancreatic cancers. J Gastroenterol Hepatol 2012; **27**(Suppl 2):10–14.
69. Mathew R, Karp CM, Beaudoin B et al. Autophagy suppresses tumorigenesis through elimination of p62. Cell 2009; **137**:1062–1075.
70. Lee SJ, Pfluger PT, Kim JY et al. A functional role for the p62-ERK1 axis in the control of energy homeostasis and adipogenesis. EMBO Rep 2010; **11**:226–232.
71. Rodriguez A, Duran A, Selloum M et al. Mature-onset obesity and insulin resistance in mice deficient in the signaling adapter p62. Cell Metab 2006; **3**:211–222.
72. Videla LA, Pettinelli P. Misregulation of PPAR functioning and its pathogenic consequences associated with nonalcoholic fatty liver disease in human obesity. PPAR Res 2012; **2012**:107434.
73. Alonso-Vale MI, Peres SB, Vernochet C et al. Adipocyte differentiation is inhibited by melatonin through the regulation of C/EBPbeta transcriptional activity. J Pineal Res 2009; **47**:221–227.